

University of Alberta

**Structural Characterization of Serine/Threonine Protein
Phosphatase Inhibition: Understanding Natural Product Binding
and Their Use in the Design of New Immunosuppressants**

by

Jason T. Maynes



A thesis submitted to the Faculty of Graduate Studies and Research in partial fulfillment of the requirements for the degree of Doctor of Philosophy

Department of Biochemistry

Edmonton, Alberta, Canada
Fall 2006



Library and
Archives Canada

Bibliothèque et
Archives Canada

Published Heritage
Branch

Direction du
Patrimoine de l'édition

395 Wellington Street
Ottawa ON K1A 0N4
Canada

395, rue Wellington
Ottawa ON K1A 0N4
Canada

Your file *Votre référence*
ISBN: 978-0-494-23080-0
Our file *Notre référence*
ISBN: 978-0-494-23080-0

NOTICE:

The author has granted a non-exclusive license allowing Library and Archives Canada to reproduce, publish, archive, preserve, conserve, communicate to the public by telecommunication or on the Internet, loan, distribute and sell theses worldwide, for commercial or non-commercial purposes, in microform, paper, electronic and/or any other formats.

The author retains copyright ownership and moral rights in this thesis. Neither the thesis nor substantial extracts from it may be printed or otherwise reproduced without the author's permission.

AVIS:

L'auteur a accordé une licence non exclusive permettant à la Bibliothèque et Archives Canada de reproduire, publier, archiver, sauvegarder, conserver, transmettre au public par télécommunication ou par l'Internet, prêter, distribuer et vendre des thèses partout dans le monde, à des fins commerciales ou autres, sur support microforme, papier, électronique et/ou autres formats.

L'auteur conserve la propriété du droit d'auteur et des droits moraux qui protègent cette thèse. Ni la thèse ni des extraits substantiels de celle-ci ne doivent être imprimés ou autrement reproduits sans son autorisation.

In compliance with the Canadian Privacy Act some supporting forms may have been removed from this thesis.

Conformément à la loi canadienne sur la protection de la vie privée, quelques formulaires secondaires ont été enlevés de cette thèse.

While these forms may be included in the document page count, their removal does not represent any loss of content from the thesis.

Bien que ces formulaires aient inclus dans la pagination, il n'y aura aucun contenu manquant.


Canada

Abstract

The control of cellular activities and modification of protein activity is partially mediated by reversible protein phosphorylation. The Protein Phosphatase P (PPP) family of protein phosphatases is the major class of enzymes that removes the phosphate from Ser/Thr residues.

The best understood inhibitors of the PPP family are the natural product inhibitors, which have vastly different binding affinities for the different family members, despite strong structural similarity between the proteins. The X-ray crystallographic structure of a PP-1:natural product toxin complex indicates that structural changes in the active site region may be responsible. This was the main question that we attempted to answer with our structural studies.

The X-ray crystallographic structure of PP-1 complexed with the natural product toxin okadaic acid reveals a binding mode similar to that observed previously. The inhibitor interacts with residues of the protein adjacent to the active site: the β 12- β 13 loop and the hydrophobic groove. The enzyme-free and enzyme-bound structures of the inhibitor are identical, indicating an entropic energy contribution to binding.

The X-ray crystallographic structure of PP-1 complexed with another natural product toxin, motuporin, illustrated a slightly different method of binding. The solution NMR and enzyme-bound structures of motuporin differ significantly, indicating a minor reliance on entropic energy.

The X-ray crystallographic structure of a microcystin bound to PP-1 clarifies the role of β 12- β 13 loop conformation in determining PPP selectivity. The modified

microcystin cannot covalently react with the enzyme. The structure revealed that the microcystin bound in a similar mode to the enzyme but did not cause β 12- β 13 loop conformational changes, indicating that sequence and not structure determines inhibitor selectivity.

To determine the contribution of primary structure to PPP family selectivity we determined the structure of a chimeric PP-1, where the residues of the β 12- β 13 loop of PP-1 were replaced by the equivalent residues of calcineurin, bound to okadaic acid. This structure showed that okadaic acid bound identically to the chimeric enzyme and wild-type enzymes. Subsequent kinetics highlighted the role of Cys273 in natural product binding, accounting solely for the kinetic difference between the wild-type and chimeric enzymes. The endogenous inhibitors were not dramatically affected, indicating a more sophisticated binding mode.

Acknowledgements

I would like to thank Dr. M.N.G. James for his guidance and support during the period of my PhD work. Without his patience and mentorship, I would not have been able to make the accomplishments that I did, especially when combining clinical and research training. The opportunities that I enjoyed were a direct result of his support, both personal and professional.

I would also like to thank all the members of the James lab. The unique mix of personalities, backgrounds and ethnicities gave me the prospect to further myself not only academically but also culturally and personally.

A significant amount of gratitude is indebted to my collaborator, Dr. Charles Holmes. His input, ideas and enthusiasm made this project successful and exciting.

Finally I would like to thank my family. Without the support of my wife, Jessica, I would not have been able to complete the work that I did in such a short period of time. Ewan is the best stress reliever I could hope for and makes life worth living. I would also like to thank my parents for their never-ending support. They have always done anything I needed to achieve academically and this work is a testament to their success.

Table of Contents

	Pg
Chapter 1: Introduction	
A. Protein phosphatases partially mediate cellular protein function	1
B. The X-ray crystallographic structures of the PPP family reveal similar protein tertiary folds	5
C. The catalytic mechanism of PPP family dephosphorylation	9
D. Members of the PPP family have distinct inhibitory profiles to both exogenous and endogenous inhibitors	11
E. Structural insights into PPP family inhibition	19
F. Research Overview	29
Chapter 2: The inhibitor mechanism of the tumor promoter okadaic acid is revealed by its crystal structure bound to protein phosphatase-1	
A. Introduction	31
B. Experimental Procedures	
B.1 Protein purification and crystallization	39
B.2 Data collection, structure determination and refinement	39
B.3 Deposited coordinates	40
B.4 Publication	40
B.5 Contribution to this work	41
C. Results and Discussion	
C.1 General description of the PP-1:okadaic acid structure	44

C.2 Inhibitor binding to PP-1	45
C.3 Crucial PP-1:OA interactions	47
C.4 Comparison between the free and enzyme bound structures of OA	51
C.5 Comparison of the PP-1:OA complex to other PPP family structures	52
D. Conclusions	56
Chapter 3: Elucidation of the role of the PP-1 β12-β13 loop in natural product inhibitor binding and specificity: The crystal structure of two novel natural products bound to PP-1	
A. Introduction	61
B. Experimental Procedures	
B.1 Protein and toxin purification and crystallization	67
B.2 Data collection, structure determination and refinement	67
B.3 Coordinates	70
B.4 Publication	70
B.5 Contribution to this work	71
C. Results and Discussion	
C.1 X-ray crystal structure of motuporin (nodularin-V) bound to PP-1	73
C.2 Interactions between MOT and the β 12- β 13 loop	78
C.3 Structure of MCLA-2H bound to PP-1	78

C.4 Toxin interactions with the β 12- β 13 loop region	79
C.5 Comparison of toxin-bound PP-1 structures	81
D. Conclusions	88
Chapter 4: Elucidating the role of the β12-β13 loop of the PPP family of protein phosphatases in the selectivity of natural product toxin binding	
A. Introduction	90
B. Experimental Procedures	
B.1 Expression, purification and kinetic analysis of recombinant PP-1	96
B.2 Crystallization of the chimeric PP-1:OA complex	96
B.3 Data collection, structure determination and refinement	98
B.4 Coordinates	98
B.5 Publication	98
B.6 Contribution to this work	99
C. Results and discussion	
C.1 X-ray crystal structure of the PP-1-CAN chimera complex with okadaic acid	101
C.2 Interactions of OA with the chimeric β 12- β 13 loop region	103
C.3 Kinetic analysis of the wild-type PP-1 and chimeric PP-1	104
D. Conclusion	116

Chapter 5:	Summary	
	A. Natural product inhibitor binding to the PPP family members is not dependent on protein structural changes	119
	B. The primary sequence of PPP family members determines inhibitor binding	120
	C. The natural product inhibitors utilize similar functional groups to interact with the PPP family but rely on different sources of binding energy	122
References		125

List of Tables

Table		Pg
1.1	The families of protein phosphatases	2
1.2	Proteins interacting with PP-1 and their control mechanisms	6
2.1	Inhibitory potencies of okadaic acid and selected derivatives	32
2.2	Data collection and refinement statistics for PP-1:OA complex	42
2.3	Comparison of PPP family structures	46
3.1	Data collection and refinement statistics for the PP-1:MOT and PP-1:MCLA-2H crystallographic complexes	72
4.1	Effect of mutagenesis in the β 12- β 13 loop region on the inhibition by natural product toxins	93
4.2	Data collection and refinement statistics for the chimeric PP-1:OA crystallographic complex	100
4.3	Kinetic values for the inhibition of wtPP-1 and chimeric PP-1	109

List of Figures

Figure		Pg
1.1	Primary sequence alignment of PPP family members	4
1.2	Role of PP-1 in glycogen metabolism and insulin signaling	8
1.3	X-ray crystal structure of the PP-1:tungstate complex	10
1.4	X-ray crystal structure of the PP-1:MCLR complex	12
1.5	X-ray crystal structure of the complex of CAN, calcineurin B and the autoinhibitory C-terminal tail	14
1.6	X-ray crystal structure of the CAN:FK506 and CAN:CsA complexes	16
1.7	X-ray crystal structure of the PP-1:calyculin complex	18
1.8	X-ray crystal structure of the PP-1:MYPT-1 complex	20
1.9	Alignment of the X-ray crystal structures of the PPP family of protein phosphatases	22
1.10	Surface topology and electrostatic potential of PP-1 with MCLR and calyculin bound	24
1.11	Proposed catalytic mechanism of phosphorolysis for the PPP family	25
1.12	Natural product inhibitors of the PPP family of protein phosphatases	28
2.1	Small molecule X-ray crystal structure of okadaic acid	35
2.2	Ribbon representation of the crystal structure of the PP-1:OA complex	38
2.3	Representative electron density from the PP-1:OA crystal complex	43
2.4	Active site contacts present in the PP-1:OA complex X-ray crystal structure	48

2.5	Alignment of the small molecule and enzyme-bound X-ray crystal structures of okadaic acid	53
2.5	Alignment of PPP family member structures with the structure of the PP-1:OA complex	55
3.1	Chemical structure of MCLR, MOT and nodularin-R	62
3.2	NMR solution structure of MOT and nodularin-R	65
3.3	Observed X-ray diffraction patterns from the PP-1:MOT and PP-1:MCLA-2H complexes	68
3.4	Representative electron density from the PP-1:MOT and PP-1:MCLA X-ray crystal complexes	69
3.5	Ribbon representation of the PP-1:MOT X-ray crystal complex	75
3.6	Active site contacts present in the PP-1:MOT complex	77
3.7	Superposition of the determined structures of motuporin and nodularin-R	80
3.8	Active site contacts in the PP-1:MCLA-2H X-ray crystal complex	82
3.9	Alignment of the PP-1:MOT, PP-1:MCLA-2H and PP-1:MCLR structures	84
3.10	Comparison of the active site residue and toxin locations for PP-1:MCLR, PP-1:MCLA-2H and PP-1:MOT	86
4.1	Sequence alignment of the β 12- β 13/L7 loop regions from PP-1, PP-2A and CAN	91
4.2	Representative electron density from the chimeric PP-1:OA X-ray crystal complex	97

4.3	Ribbon representation of the chimeric PP-1:OA X-ray crystal structure	102
4.4	Alignment of the chimeric PP-1:OA structure with other PP-1:toxin complexes	105
4.5	Active site contacts in the chimeric PP-1:OA X-ray crystal complex	106
4.6	Electron density in the β 12- β 13 loop for the wtPP-1:OA and chimeric PP-1:OA X-ray crystal complexes	108
4.7	Inhibitory profiles of OA against wtPP-1 and chimeric PP-1	113
4.8	Inhibitory profiles of MCLR against wtPP-1 and chimeric PP-1	114
4.9	Inhibitory profiles of inhibitor-2 against wtPP-1 and chimeric PP-1	115

List of Abbreviations

Å	Angstrom
Adda	3-amino-9-methoxy-2,6,8-trimethyl-10-phenyl- deca-4,6-dienoic acid
ALS	Advanced Light Source, Berkeley, California
CAN	calcineurin/protein phosphatase-2B
CsA	cyclosporine A, neoral
DARPP-32	dopamine and cAMP regulated phosphoprotein of 32
kDa	
FK506	tacrolimus, Prograf
Gga	γ -linked D-glutamic acid
I-1	endogenous protein phosphatase inhibitor-1
I-2	endogenous protein phosphatase inhibitor-2
Masp	D-methyl aspartic acid
Mdb	<i>N</i> -methyldehydrobutyrine
MOT	motuporin
N/D	not determined
Nmda	<i>N</i> -methyldehydroalanine
NMR	nuclear magnetic resonance spectroscopy
MCLA-2H	dihydromicrocystin-LA
OA	okadaic acid
PDB	Protein Data Bank
PKC	protein kinase C

PP-1	protein phosphatase-1
PPM	protein phosphatase M family
PPP	protein phosphatase P family
PTP	protein tyrosine phosphatase
rmsd	root mean square distance
SAR	structure activity relationship
TNF- α	tumor necrosis factor- α
TPA	12-O-tetradecanoylphorbol-13-acetate
TPR	tetratricopeptide repeat

Chapter 1

Introduction and Background

A. Protein phosphatases partially mediate cellular protein function

The interaction of an organism, or more fundamentally a cell, with its external environment is intrinsic to its survival, development, evolution and fecundity. In part, the cell's response to stimuli and modification of its processes is mediated by protein phosphorylation. This task is performed by two types of proteins, the protein kinases that covalently link a phosphate group to a serine, threonine or tyrosine of the target protein, and protein phosphatases, whose function it is to remove the same phosphate group. Modification of cellular protein activity can be by phosphorylation or by dephosphorylation, either modification may cause an allosteric change in the protein, affect protein-protein interactions or directly change the active site of the protein. Approximately 30% of the cellular proteins are subject to reversible protein phosphorylation with the cell possessing about 2000 kinase and 1000 phosphatase genes.¹ Cellular processes that are modified directly by protein phosphorylation include glycogen metabolism, cell cycle control, cellular metabolism, cytoskeletal arrangements and cellular transport and secretion.

The protein phosphatases are divided into three distinct families (Table 1.1). The Protein Phosphatase P (PPP) and Protein Phosphatase M (PPM) families encode Ser/Thr phosphatases, whereas the Protein Tyrosine Phosphatase (PTP) family encodes protein tyrosine phosphatases and dual specificity phosphatases. Specificity, both in terms of enzymatic activity and in terms of subcellular localization, is imparted by separate regulatory subunits for all families (Table 1.2).

Table 1.1 The families of protein phosphatases (adapted from¹)

Family	Family Members
Protein Phosphatase P (PPP) Family	<p>PP-1 PP-2A PP-2B (calcineurin) Novel Members: PPP-1, PPP2A, PPP5</p>
Protein Phosphatase M (PPM) Family	<p>PP2C <i>Arabidopsis</i> ABI1 <i>Arabidopsis</i> KAPP-1 Pyruvate dehydrogenase phosphatase <i>Bacillus subtilis</i> SpoIIE phosphatase</p>
Protein Tyrosine Phosphatase (PTP) Family	<p><i>Tyrosine specific cytosolic, non-receptor forms:</i> PTP1B, SHP-1, SHP-2 <i>Tyrosine specific receptor-like, transmembrane forms:</i> CD45, RPTPμ, RPTPα <i>Dual-specificity:</i> CDC25, Kinase-associated phosphatase, MAP kinase phosphatase-1</p>

The PPP family of protein phosphatases accounts for the majority of the cell's Ser/Thr protein phosphatase activity.¹ Within this family, a similar core catalytic subunit is shared among protein phosphatase-1 (PP-1), protein phosphatase-2A (PP-2A) and protein phosphatase-2B (PP-2B, also called calcineurin (CAN)), with approximately 80% sequence similarity (Fig. 1.1). The main differentiation between the proteins occurs in the N- and C-terminal regions and in the diverse array of regulatory subunits that are used to form target-specific protein phosphatase complexes.

The physiological role of the PPP family is vast and involves numerous, seemingly unrelated processes. For example, insulin signaling causes the activation of PP-1 by phosphorylation of its glycogen-targeting regulatory subunit where the same insulin signal causes inactivation of PP-2A by tyrosine phosphorylation of its catalytic subunit (Fig. 1.2).^{2,3} Polymorphisms of the PP-1 glycogen-targeting subunit have been associated with some forms of diabetes mellitus type II.⁴ It was recently shown that PP-1 was involved in long term potentiation of neurons by partially determining the phosphorylation state of the NMDA and AMPA glutamate receptors.⁵ This may have therapeutic consequences for recovery following injury and tempering the abnormal neuronal activity in hyperresponsive states like chronic pain or drug abuse.⁶ Inhibitors of PP-1 and PP-2A can induce premature cell cycle progression by stimulating hyperphosphorylation of cyclins/cyclin kinases (PP-2A) or Rb protein (PP-1). The phosphatase inhibitors stimulate progression through the cell cycle at an unwonted rate, causing the cell to reach the mitotic stage before the machinery for the process is in place.⁶ The increased phosphorylation state of Rb

PP-1	-----AD-----SIIQRL-----	-18
PP-2A	-----DDKAF-----QW-----	-13
PP-2B	SEPKA DPK-L RVVKA VFP PSHRL TAKEVFDNDGKPR	-44
PP-1	KNV	-63
PP-2A	--	-56
PP-2B		-89
PP-1	* * FLGDY GK	-108
PP-2A	FMGDY DR	-101
PP-2B		-134
PP-1	*	-152
PP-2A	GM	-146
PP-2B	-SE	-178
PP-1	*	-197
PP-2A		-191
PP-2B		-223
PP-1	DKDVLGWGEND-----	-235
PP-2A	D-DRG	-228
PP-2B	LEDFG HFTHTV	-268
PP-1	*	-274
PP-2A	Q-----	-267
PP-2B	N----- QTTGFPS	-313
PP-1	M-----	-290
PP-2A	K-----	-283
PP-2B	MNIRQFNCSPPHYWLPNFMVDVFTWSL PFG	-358
PP-1	-----E-----KK-----	-307
PP-2A	-----P-----RRG-----	-300
PP-2B	EKVTEMLVNVLNI DGFDGATAAARKEVIRNKIRAI	-403
PP-1	-----PV-----PRGM-----	-318
PP-2A	-----R-----DYFL-----	-309
PP-2B	GKMARVFSVLREESESVLTLKG TGML GGGQTLQSAT	-448
PP-1	-----	-322
PP-2A	-----	-322
PP-2B	VEAIEADEA I KGFSPQHKITSF GLDRINERMPPRRDAMP SD	-493

Figure 1.1 Primary sequence alignment of the three main PPP family members, PP-1 (γ isoform), PP-2A (β isoform) and PP-2B/CAN (α isoform). The residues are coloured from no similarity (white) to distant similarity (green) to identity (red). The β 12- β 13 loop is outlined in a box and the six active site metal binding residues are highlighted by blue asterisks above the residues. Alignment of the sequences was performed with the program T-coffee.⁷

protein, Bcl-x1 and BAD associated with phosphatase inhibition are all linked to decreased cellular apoptosis and death. The action of PP-1 and PP-2A in all of these diverse processes is mediated by their targeting and regulatory subunits (Table 1.2).

Calcineurin is characterized and unique by its dependence on calcium ions and related regulation by calmodulin. The most medically relevant role for CAN is in the control of calcium mediated T-cell signaling. The increases in intracellular calcium concentration associated with antigen binding to the T-cell receptor stimulates CAN to remove a phosphate from NFAT-1 (nuclear factor of activated T-cells), which then translocates to the nucleus and induces expression of interleukin-2, an important cytokine in T-cell activation. Failure or inhibition of this process causes suppression of T-cell activation.⁸ Calcineurin is implicated in neuronal function and the calcineurin inhibitor and immunosuppressant FK506 has neuroprotective qualities against NMDA toxicity⁹⁻¹¹ This may even play a role in the immunosuppressant function of FK506 since a small study of 28 post-liver transplant patients showed improved cerebral perfusion in twice as many patients receiving FK506 (in comparison to other immunosuppressants).¹² The main limitation in the medical use of inhibitors of CAN is due to their nephrotoxicity. This is most likely secondary to inhibition of the calcineurin-mediated regulation of the Na⁺-K⁺ ATPase in renal tissue.¹³

B. The X-ray crystallographic structures of the PPP family reveal similar protein tertiary folds

Prior to beginning our studies, there were five available PPP family structures. These included three structures of PP-1: PP-1 with the phosphate mimic

Table 1.2 Proteins interacting with PP-1 and their control mechanisms

Protein	IC ₅₀	RVXF Motif	Function	Control Mechanism
NIPP-1 ¹⁴	10 pM	200-RVTF-203	Nuclear local., inhibition, ?spliceosome assembly	pSer199(PKA) and pSer204(casein kinase-2) dissociates from PP-1
Inhibitor-1	1 nM with pThr35 (PP-2A IC ₅₀ = 25 μM) ¹⁵ , 1 nM for Thr35Glu ¹⁵ , 9.5 nM with pSer67 ¹⁶ , 40 nM for Mn ²⁺ -dependant PP-1 ¹⁷ ,	9-KIQF-12	Cardiac contractility, regulation of learning and memory ¹⁸	pThr35 (PKA) activates, also binds PP-1 when not phosphor, pSer67 (neuronal cdc2-like PK) activates indep.of pThr35 ¹⁶ , dephos by CAN ¹⁵ , alternative splice products ¹⁹
Inhibitor-2	3 nM ²⁰	144-KLHY-147 ²¹	Cell cycle regulation, centrosome dissociation, ?chaperone	pThr72 (MAPK/ cdk2/ cdk5/GSK-3 ²²) inactivates without dissociating from PP-1, "IKGI" motif binds unknown site ^{23,24} , nuclear localization seq.
Inhibitor-4	0.2 nM ²⁵		?Nuclear localization, causes inactivation of PP-1:G _M complex ²⁵	pThr73 (GSK-3 only) causes dissociation ²⁵ , "IKGI" motif as I-2 ²⁵
DARPP-32	2 nM (pDARPP-32), 1 μM (dephosphor or with Glu substitute at Thr34) ^{26,27}	8-KIQF-13	?dopamine regulated neuronal stimulation ²⁶	pThr34 (cAMP dependant PK) activates, pSer137/pSer189 (casein kinase-1) ²⁷ , pSer137 inhibits dephos by CAN ²⁸
PNUTS (R111)	0.1 nM (GST fusion) ²⁹	397-KVTW-401 ²⁹	Nuclear local. and inhibition, targeting to RNA complexes	Thr398 (PKA) promoted dissociation from PP-1 ²⁹
MYPT-1		35-KVKF-38	Dephosphorylate myosin ³⁰	
Neurabin ³¹	2 nM (as GST fusion)	457-KIKF-460		Ser461 (PKA) causes dissociation from PP-1 ³²
G _M ³¹	20 nM (PP-1β) > 2 μM (PP-1γ) (both GST fusion)	65-RVSF-68	Targets to glycogen and sarcoplasmic reticulum	pSer67(PKA) causes dissociation and inactivation of PP-1
M ₁₁₀		35-KVKF-38	Targets to myosin	
PHI-1 ³³	2 nM (pPHI-1), 100 nM (dephosphor.), 30 nM (glycogen/ myosin bound)	27-RVYF-30		pThr57 (PKC) activates
PHI-2 ³³		83-RVYF-86		
p53BP		798-RVKF-801		
Nek-2		383-KVHF-386	Binds in KIQF area, requires I-2 for kinase activity, centrosome dissoc. ³⁴	

tungstate bound into the active site, PP-1 with the cyanobacterial toxin microcystin-LR (MCLR) covalently bound into the active site and a final structure with a peptide from a targeting subunit bound into the targeting groove distal to the active site (Fig.'s 1.3 and 1.4).³⁵⁻³⁷ Two structures were also available for CAN, one apoenzyme complex of CAN with its regulatory subunit (calcineurin B) and the autoinhibitory C-terminal tail bound into the active site and one with the inhibitor FK506 and its binding protein (FK506BP) bound adjacent to the active site area (Fig.'s 1.5 and 1.6).^{38,39} In addition to the structures presented here, four others have been published since, including two structures of the CAN:cyclosporine/cyclophilin complex and two PP-1 structures, one with the inhibitor calyculin and one with the regulatory subunit MYPT-1 present (there are no structures available of PP-2A) (Fig.'s 1.6, 1.7, 1.8).⁴⁰⁻⁴²

These X-ray crystal structures revealed that all the PPP family members possess very similar protein folds, not surprising given their sequence similarity. (Figs. 1.1 and 1.9) (see Table 2.1 for an inclusive list of C_{α} RMSD values). The catalytic domain for both PP-1 and CAN contains a central β -sandwich consisting of two mixed β sheets. This is flanked by an α -helical domain (7 helices) on one side and a mixed domain, consisting of three α -helices and a three-stranded β -sheet, on the other side. The active site lies on one face/edge of the β -sandwich and residues from the β -sandwich provide the binding residues for catalytic metals.

The surface topology of the enzyme shows that the active site area lies at the trifurcation of three surface grooves (Fig. 1.10). The three grooves have distinct chemical characteristics, a groove that is predominantly hydrophobic in character

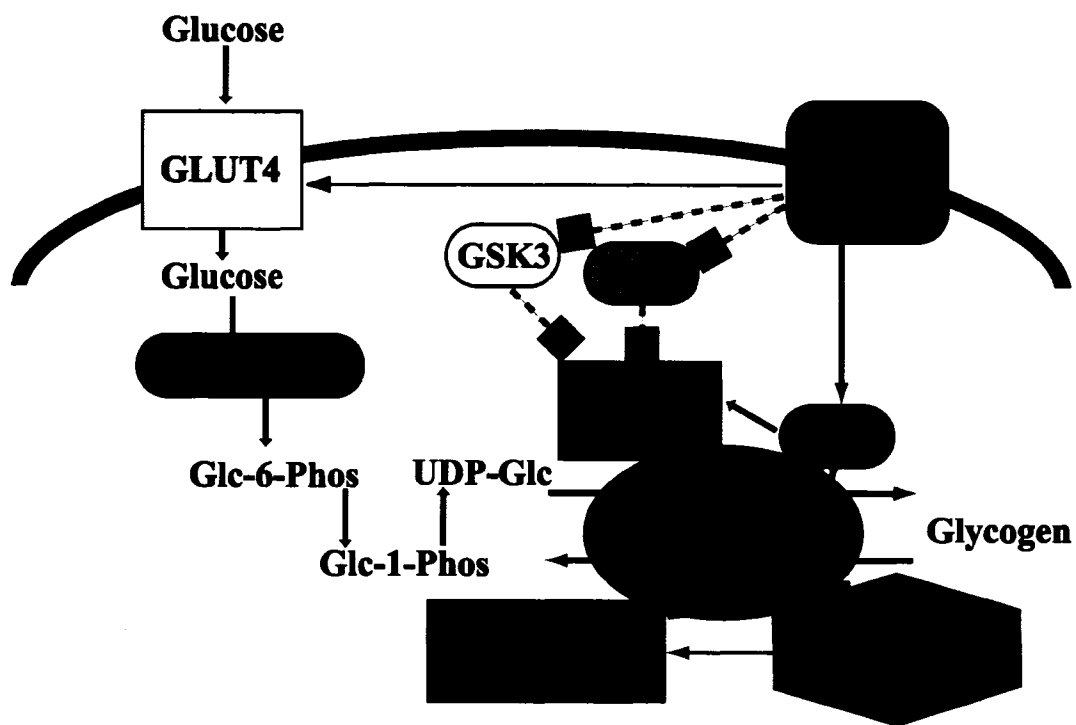


Figure. 1.2 Schematic representation of the role of PP-1 in glycogen metabolism and insulin signaling. Arrow indicate activation where dotted lines with boxes indicate inhibition. GSK-3 = glycogen synthase kinase-3, PKA = protein kinase A, PTG = protein targeting glycogen (PP-1 regulatory subunit).³

(coined the “hydrophobic groove”), a groove with a negative electrostatic potential (coined the “acidic groove”) and a C-terminal groove created by the final β -strand observed in the crystal structures (coined the “C-terminal groove”, not the actual C-terminus of the protein). The physiological role of these grooves, if any, is unknown.

C. The catalytic mechanism of PPP family dephosphorylation

The catalytic mechanism of the PPP family members is postulated to involve a metal activated water molecule for dephosphorylation and the active site of all determined PPP family members contains two metal ions (Fig. 1.11). The physiological identity of the two metals is most likely either iron alone or iron and zinc, numerous studies having failed to conclusively identify them.^{35,43,44} Most of the X-ray crystal structures possess manganese ions added after recombinant protein purification since this stabilizes the protein. The manganese dependant enzyme is slightly different from the iron or zinc containing form, having a broader range of active substrates and being 40 to 50-fold less sensitive to some endogenous inhibitors but with no observable changes in protein structure.¹⁷ The metals adopt an octahedral configuration, using active site waters (or tungstate in the case of the PP-1:tungstate complex) to complete their coordination spheres. The metal coordination residues are conserved among PPP family members (Fig. 1.1). The PPP family catalyses dephosphorylation in a single step using the metals to activate a water or hydroxide ion, without the creation of a phosphoryl-enzyme intermediate (unlike the PTP family). Other active site residues also play an important role in the catalytic mechanism. The two active site arginine residues, Arg96 and Arg221, are



Figure 1.3 X-ray crystal structure of the PP-1:tungstate complex.³⁵ The protein is visualized by its secondary structural elements and colored blue to red, N-terminus to C-terminus. The active site tungstate is shown as sticks.

likely to stabilize the transition state and His125 donates a proton to the leaving group oxygen.¹ Loss of any of these residues dramatically affects the catalytic potential of the enzyme.^{45,46} Adjacent to the active site, a loop between β -strand 12 and β -strand 13 (coined the β 12- β 13 loop) has several residues that lie in proximity to the catalytic residues. None of the loop residues have formal interactions with any catalytic residues or the metals but have been shown to be important for enzyme inhibition.⁴⁷

D. Members of the PPP family have distinct inhibitory profiles to both exogenous and endogenous inhibitors

The most well studied of the PPP family inhibitors are the natural product inhibitors, produced by a variety of organisms and implicated in a number of public health issues like diarrhetic shellfish poisoning (okadaic acid) and toxic blue-green algae blooms in fresh water depositories (the microcystins). The natural product inhibitors, despite their diverse origins, possess common structural characteristics that are postulated to be important in binding to their cognate enzymes and make up a pharmacophore for PPP family inhibition (Fig. 1.12). All the inhibitors have at least one acidic residue, some (as is the case for the microcystin class of inhibitors) possess two acid groups. The exact chemical nature of this acid varies from a carboxylic acid for most of the inhibitors to a phosphate group for the calyculins and related clavosines.⁴⁸ Another common structural element is the presence of a long hydrophobic region. This again can take many forms but usually involves a section of aliphatic or branched chain moieties. In the case of okadaic acid, the hydrophobic region contains a double ring spiroketal element. The final common structural

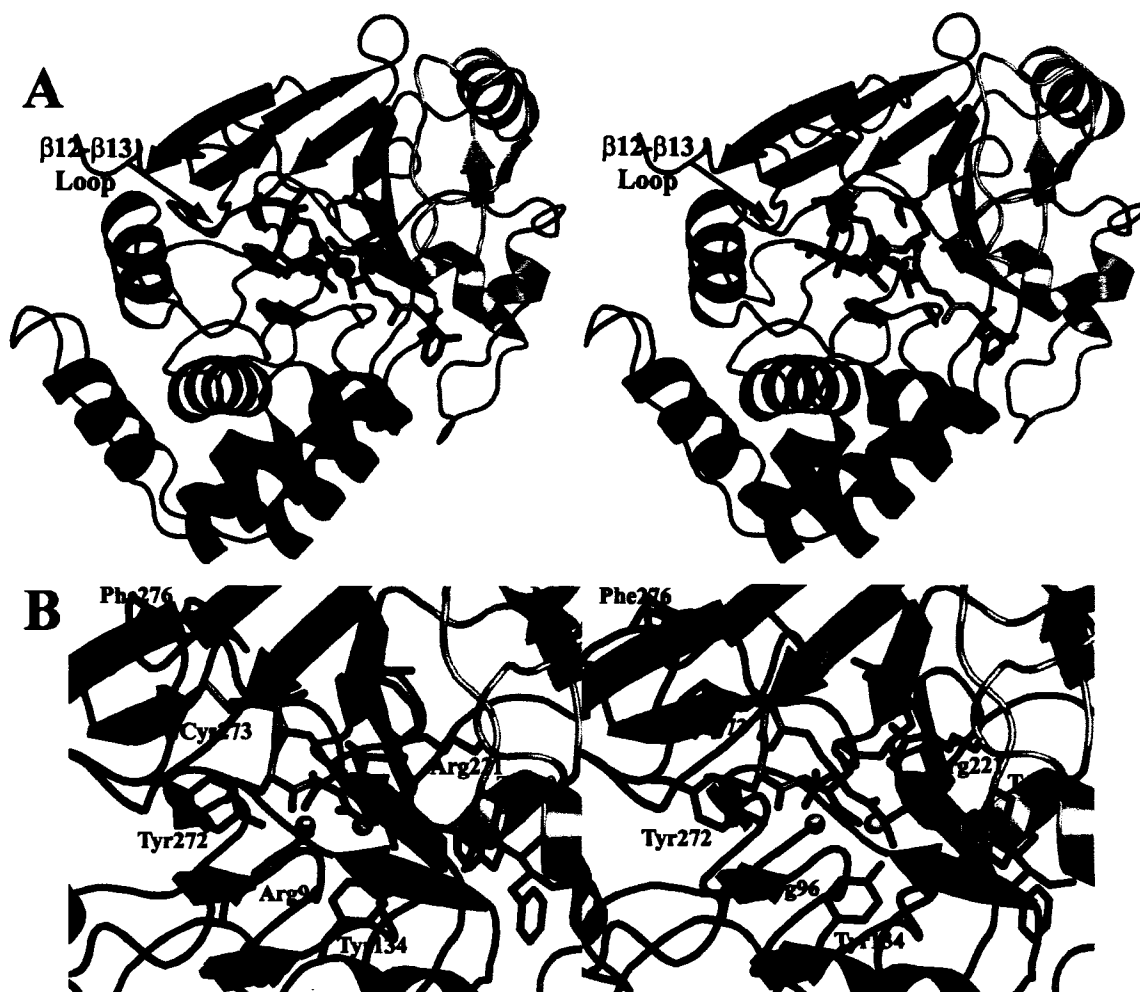


Figure 1.4 X-ray crystal structure of the PP-1:MCLR complex.³⁷ (A) overall protein structure with the protein shown as a secondary structure representation and coloured blue to red, N-terminus to C-terminus. The inhibitor is shown as sticks with the carbon atoms coloured orange. Active site metals are shown as yellow spheres and the $\beta 12$ - $\beta 13$ loop region is labeled. (B) Close-up of the active site area of the PP-1:MCLR complex. The inhibitor is shown as in (A) and important protein residues are shown as sticks and labeled. The covalent bond between the inhibitor and Cys273 of the $\beta 12$ - $\beta 13$ loop is apparent. The interaction between one acid of the inhibitor and Tyr272 is also observed.

characteristic of these inhibitors is the presence of a large macrocyclic ring, usually containing the acidic residue. Exceptions to this rule include the calyculins/clavosines, which do not possess any macrocyclic ring, and okadaic acid, which does not intrinsically possess a covalently closed ring but was shown in its small molecule X-ray crystal structure to form a ring via an intramolecular hydrogen bond.⁴⁹ The importance of each of these regions was made apparent by the first crystal structure of one of these inhibitors bound to PP-1 (see below).³⁷

The natural product inhibitors have profoundly different activities against the various PPP family members, for an unknown reason. To help elucidate the basis for this, many of the natural products have had their structures determined, either by NMR or small molecule crystallography (members of the microcystin family,⁵⁰ nodularin⁵¹ and okadaic acid⁴⁹). The solution NMR structures of the inhibitors showed that the macrocyclic regions were relatively stable but the long hydrophobic regions were, not surprisingly, very mobile. In the absence of applicable X-ray crystal data, docking methods were also employed to determine the probable binding mode of the inhibitors.⁵² These studies showed that the natural product inhibitors most likely used their macrocyclic domains with acidic residues to occupy the active site of the enzyme, the hydrophobic tail regions binding in an adjacent groove. The docking studies did not assist in elucidating the reason for the different binding capacities of the natural product inhibitors to the PPP family members.

Calcineurin is the cellular receptor for the immunosuppressive compounds cyclosporine and FK506 (also called tacrolimus). The binding of these compounds to CAN requires their interaction with an intracellular binding protein, cyclophilin

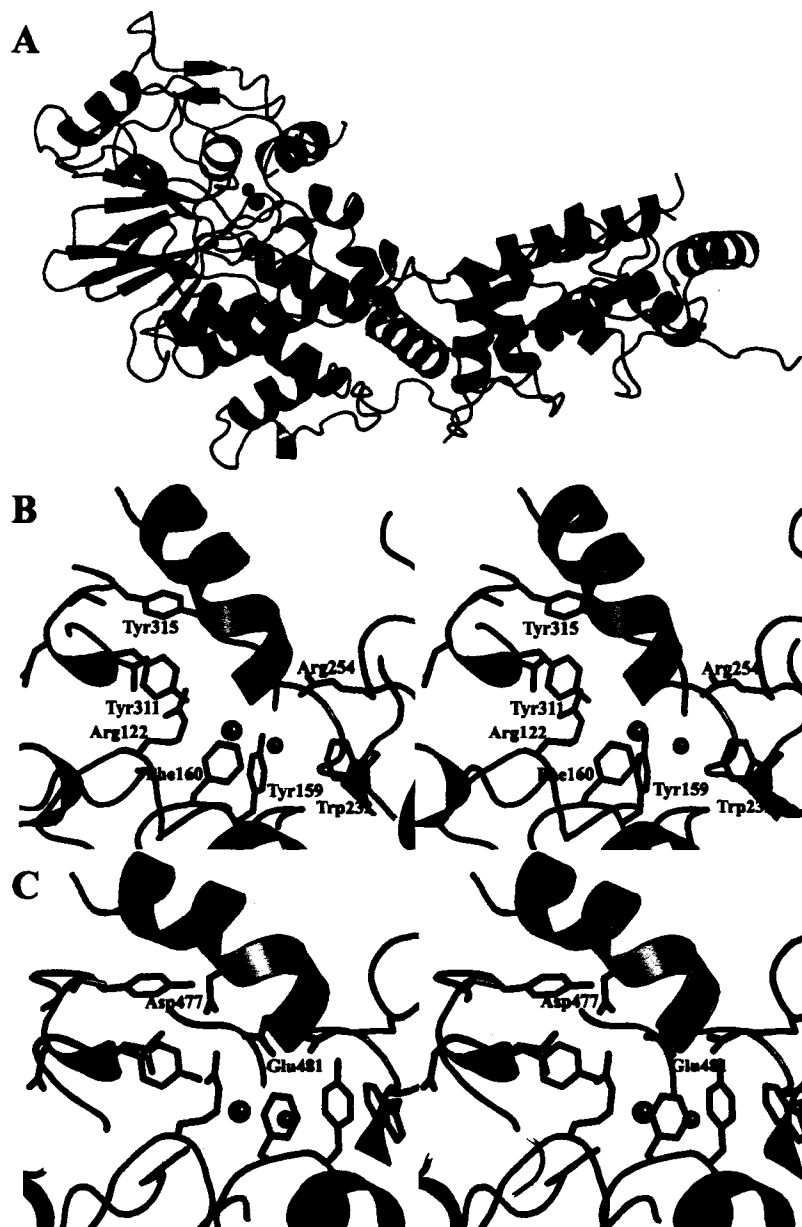


Figure 1.5 X-ray crystal structure of calcineurin.³⁹ (A) the overall structure of the calcineurin catalytic subunit (blue) in complex with its main regulatory subunit, calcineurin B (red). The autoinhibitory C-terminal tail of the protein is shown in orange. The proteins are shown with their secondary structure representations. The catalytic metals are shown as green spheres. Residues 374 to 468 are disordered, leaving no visible linker region between the end of the catalytic core and the C-terminus lying in the active site. (B) Close-up of the active site showing important active site residues and catalytic metals. (C) Similar view as (B) showing the two binding acids, Asp477 and Glu481, of the C-terminal tail.

for cyclosporine and FK506BP for FK506. Both of the binding proteins are cis-trans peptidyl prolyl isomerases and, although they require inhibitor binding before being able to interact with CAN, their protein structure does not change to a noticeable degree upon binding the small molecule inhibitor or the enzyme (Fig. 1.6). Neither cyclosporine nor FK506 are able to directly compete for the active site area but, together with their binding proteins, distally block access to the active site for physiological targets. Small molecules (like *p*-nitrophenol phosphate) are still able to diffuse into the active site and undergo dephosphorylation.^{38,40,41} Physiological analogues of CsA or FK506 have not been found but the drugs are able to dislodge CAN from the ryanodine and IP₃ receptors, which may suggest that these receptors bind in a similar manner.⁵³

The PPP family is auto-regulated by their C-terminal tail regions. Phosphorylation of Thr311 by Cdk-2 causes inhibition of PP-1 and prevents the dephosphorylation of Rb protein, which allows for progression into the S-phase of the cell cycle.⁵⁴ Cell cycle progression may also be stimulated by C-terminal phosphorylation of PP-1 at residues Thr307 and Thr318 by the kinase Nek2.⁵⁵ In a similar manner, the C-terminal tail of PP-2A can be tyrosine phosphorylated, which causes enzyme inhibition.⁵⁶ The C-terminal tail of CAN binds directly into the enzyme's active site, utilizing glutamate and aspartate residues and not requiring phosphorylation. This complex has been captured crystallographically (Fig. 1.5).³⁹

The members of the PPP family are broad specificity phosphatases and lack an apparent mechanism of substrate specificity for their cellular targets. This is resolved by the association of targeting and regulatory subunits to the catalytic

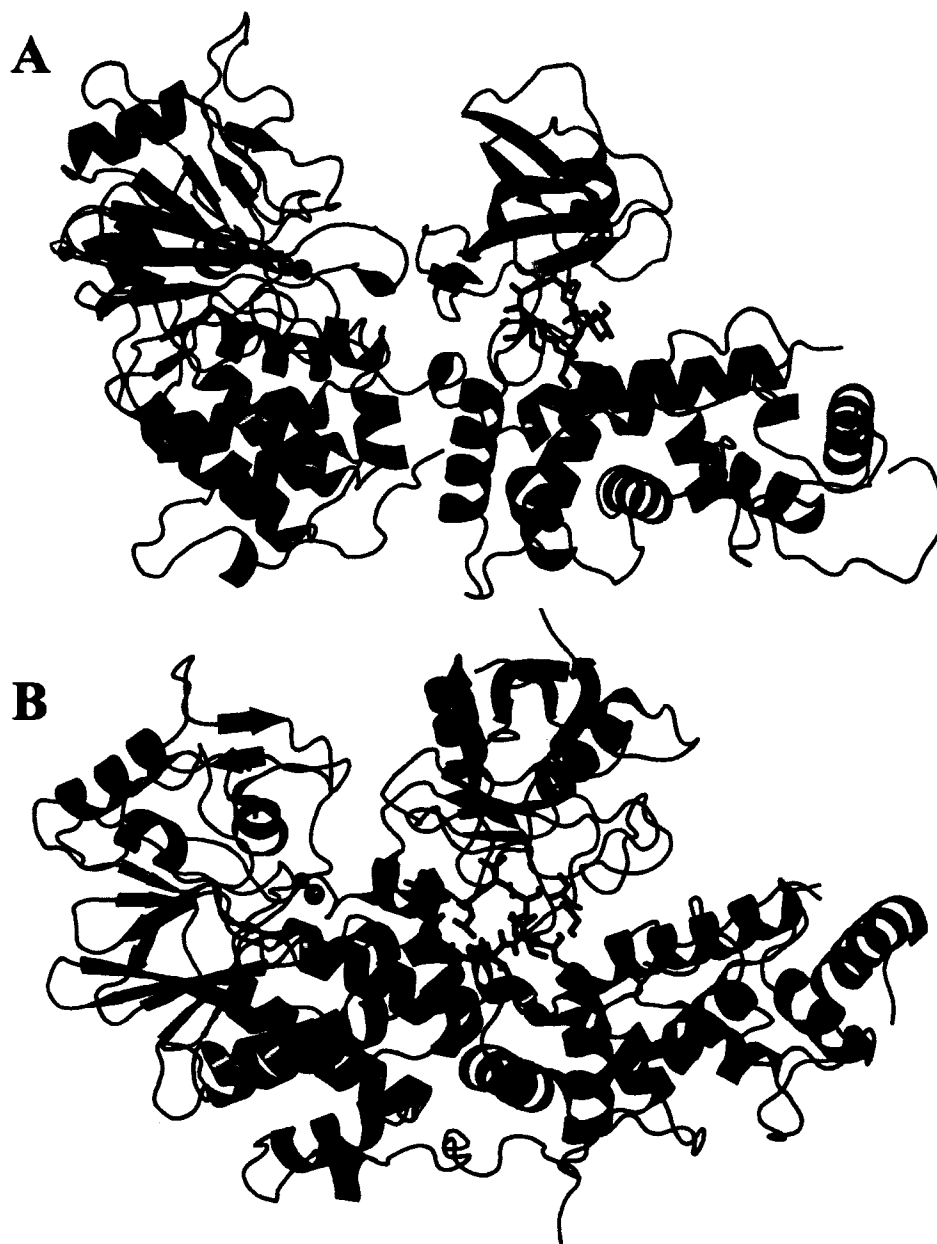


Figure 1.6 Determined X-ray crystal structure of calcineurin bound to immunosuppressive agents. (A) structure of the CAN:FK506BP:FK506 complex.³⁸ The enzymatic core is coloured blue, regulatory calcineurin B subunit coloured red and FK506BP coloured orange. The small molecule inhibitor is shown as sticks. (B) structure of the CAN:cyclophilin:cyclosporine (CsA) complex.⁴¹ Colouring of CAN/calcineurin B is the same as (A), cyclophilin is coloured green and CsA is shown as sticks. Neither FK506 nor CsA bind to the active site, instead binding at the interface between the catalytic subunit and calcineurin B, sterically occluding the active site.

cores, primarily for PP-1 and PP-2A. PP-1 possesses a wide variety of targeting subunits that bind to a site distal to the active site and not only control the intrinsic enzymatic activity but also control the subcellular localization of the protein, creating an importance for the local concentrations of substrates within the cell.⁵⁷ For example, PP-1 is targeted to the fibrils of smooth and skeletal muscle by the M₁₁₀ subunit, which also stimulates its activity towards myosin light chain and reduces its activity against glycogen phosphorylase. The targeting subunits themselves may be subject to regulation by protein phosphorylation as is the case for the G_M subunit, (which targets PP-1 to glycogen in skeletal and smooth muscle) where phosphorylation by protein kinase A leads to dissociation of the subunit from PP-1. The binding of the targeting subunits to PP-1 is mutually exclusive and is mediated through interaction with the coined “RVXF” (also called “KIQF”) motif, after the consensus sequence for the residues that bind this region (the actual consensus sequence for the region is [RK]-X₀₋₁-[VI]-{P}-[FW] where {P} means that proline cannot take that position).^{23,36,58} The X-ray crystal structure of a minimal binding portion of the G_M targeting subunit bound into this area was solved (but not deposited into the Protein Data Bank).³⁶ The binding region on PP-1 is primarily hydrophobic and the peptide from the G_M subunit bound in an extended conformation.³⁶ Three of the binding residues adopt a β -strand conformation and incorporate as a sixth strand in one of the enzyme’s β -sheets. The hydrophobic interactions between the peptide and the enzyme seem to predominate as mutation of the hydrophobic residues in the peptide either reduces or abolishes the peptide’s binding ability. Similar binding sequences are found in the regulatory proteins



Figure 1.7 X-ray crystal structure of the PP-1:calyculin structure.⁴² (A) overall structure of the complex with the enzyme shown as its secondary structure representation and coloured blue to red, N-terminus to C-terminus. The active site metals are shown as yellow spheres. The inhibitor is shown as sticks with the carbon atoms coloured orange. The $\beta 12$ - $\beta 13$ loop is labeled. (B) Active site region of the PP-1:calyculin complex showing important active site residues, including Tyr272 of the $\beta 12$ - $\beta 13$ loop that binds the phosphate of the inhibitor. The inhibitor is shown as in (A) and the phosphate residue is labeled.

inhibitor-1, DARPP-32, NIPP-1, p53BP2 and RNA splicing factor, among others (Table 2.2).¹ Since the binding region for the targeting subunits is not in the active site (although some may possess active site binding regions as well), they do not competitively block the natural product inhibitors (Fig. 1.8). Reports show that PP-1 can also be inhibited by phosphatidic acid with an IC₅₀ of 15 nM.⁵⁹ The mechanism of inhibition by this lipid is unclear but the enzyme kinetics followed a noncompetitive profile. Both the phosphate and the fatty acid portions of phosphatidic acid were vital to its inhibitory function but the biological relevance of this is unknown. Given the similarity between the hydrophobic moiety of the natural product inhibitors and phosphatidic acid, the possibility exists for coincident binding modes.

E. Structural insights into PPP family inhibition

Of the determined PPP family X-ray crystallographic structures, two contain exogenous, natural product inhibitors, namely calyculin and MCLR. These structures illustrate an exception to the broad structural similarity discussed above (Figs. 1.4, 1.7 and 1.9). The PP-1:MCLR structure showed that the inhibitor bound into the active site area and occupied one of the surface grooves of the protein, the hydrophobic groove, with its long hydrophobic tail region. The microcystins possess two acidic residues and MCLR uses these two regions to bind active site residues (primarily Arg96, Arg221 and Tyr134) and metal-bound waters, but not the metals themselves (Fig. 1.4). In addition, the inhibitor has extensive interactions with the β 12- β 13 loop region of the protein, an area shown to be important in inhibitor binding (primarily Tyr272) but not in enzyme catalysis.^{45,46,60,61} The

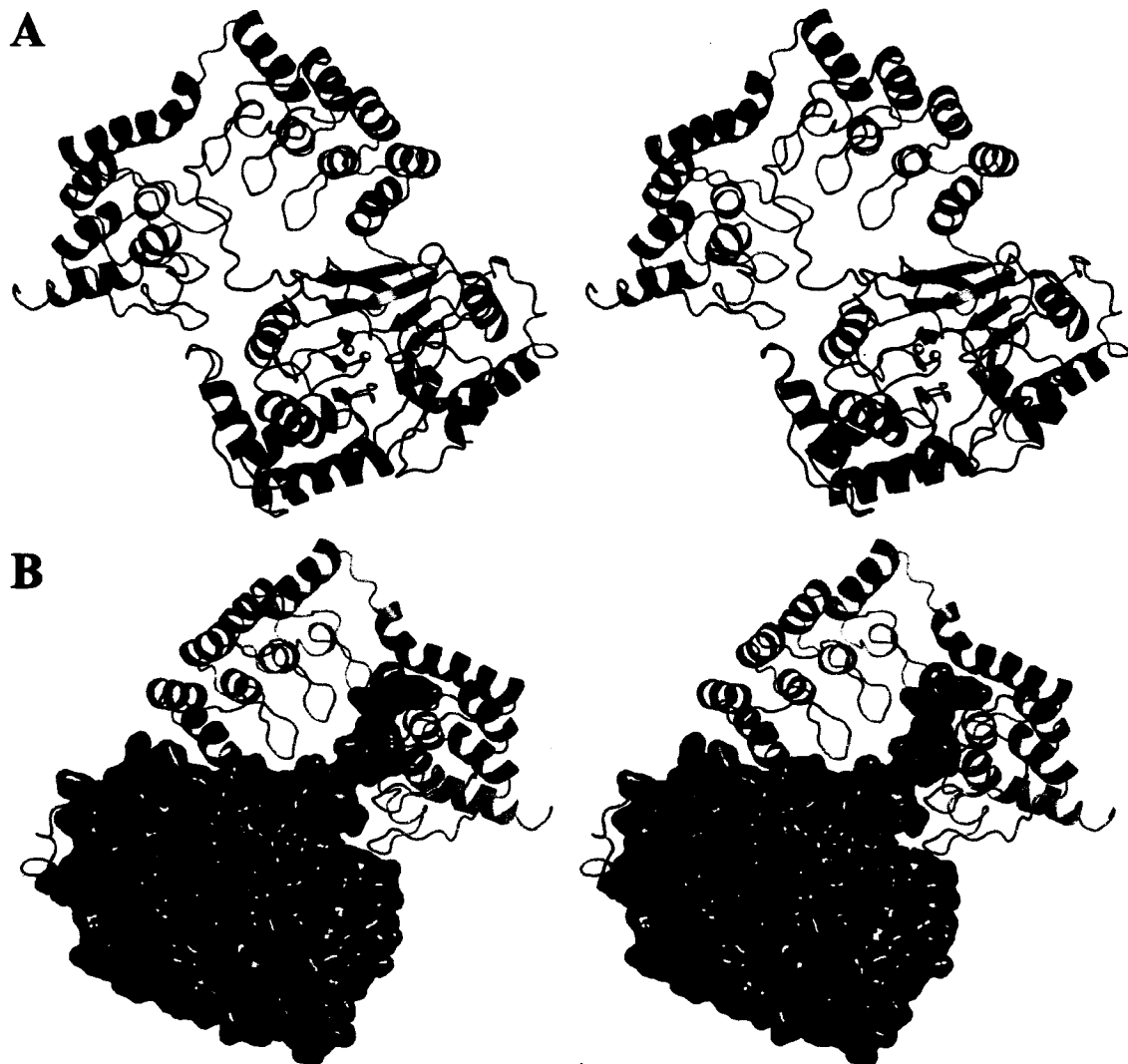


Figure 1.8 X-ray crystal structure of the PP-1:MYPT-1 complex.³⁰ (A) The enzymatic subunit of the protein is coloured blue with the β 12- β 13 loop region coloured red. The active site metals are shown as yellow spheres. The MYPT-1 binding protein is coloured green. The C-terminus of PP-1, usually disordered in crystallographic structures, is anchored and ordered by the ankyrin repeats of MYPT-1. The N-terminus of MYPT-1 wraps around the protein and binds in the distal hydrophobic groove region. (B) The complex as in (A) rotated 180 degrees around the vertical axis. The catalytic subunit is now shown as a surface representation, coloured blue. The RVXF binding domain (coloured orange) is shown bound into the RVXF groove on PP-1 and is between the ankyrin repeat region and the N-terminal hydrophobic region of the binding protein.

importance of the β 12- β 13 is true for both the natural product inhibitors and the endogenous protein inhibitors like DARPP-32 and inhibitor-1. Of particular interest in the PP-1:MCLR structure was the presence of a covalent bond between the inhibitor and the β 12- β 13 loop of the enzyme, occurring between the dehydroalanine residue of MCLR and Cys273 (via a Michael addition reaction) (Fig. 1.4). The inhibitor remained bound into the active site despite the tethering of the covalent linkage. Subsequent kinetic studies have show that this interaction is temporally displaced from the initial enzyme inhibition so the role of the covalent reaction remains in doubt.⁶²

The X-ray crystal structure of the PP-1:calyculin complex shows that the inhibitor binds in a very similar manner to that of MCLR, occupying the active site and the hydrophobic groove regions (Fig. 1.7). Calyculin possesses a phosphate group, which it uses to bind into the active site area in a similar manner to the acids of MCLR. A notable difference is the lack of a covalent reaction between calyculin and the enzyme's β 12- β 13 loop region. Calyculin does not have a residue that is capable of covalently reacting with Cys273, or any other loop residue. Consequently, the β 12- β 13 loop takes on a significantly different conformation than that observed in the PP-1:MCLR complex (Figs. 1.7 and 1.9), casting uncertainty on the importance of β 12- β 13 loop conformation in natural product (or other) inhibitor binding and selectivity.

The X-ray crystal structure of a complex of a portion of the regulatory subunit MYPT-1 bound to PP-1 was solved and revealed how the enzyme is regulated by the endogenous protein (Fig. 1.8).³⁰ This complex is part of a larger

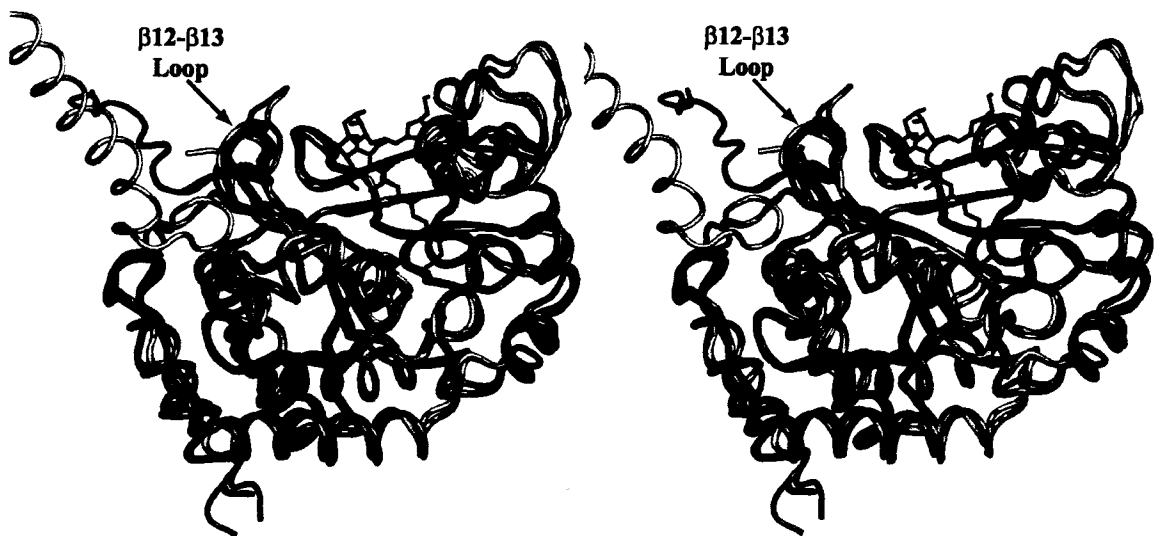


Figure 1.9 Alignment of the available X-ray crystal structures the PPP family of phosphatases. All proteins are shown as backbone C_α traces and calyculin from the PP-1:calyculin complex is shown as sticks. The β12-β13 (PP-1) or L7 (CAN) loop is labeled. The coloured scheme is PP-1:tungstate³⁵ orange, PP-1:calyculin⁴² dark blue, PP-1:MYPT-1³⁰ is red, PP-1:MCLR³⁷ is light blue, CAN:FK506BP:FK506³⁸ and CAN³⁹ yellow. One of the C-terminal extensions of CAN is shown for comparison (usually binds calcineurin B) and the ordered C-terminus of the PP-1:MYPT-1 complex is also shown (usually bound to the ankyrin repeat domain of MYPT-1). The β12-β13 loop region is labeled and the proteins are seen to align well in this region, with the exception of the PP-1:MCLR complex (light blue).

complex that dephosphorylates myosin and includes PP-1, the MYPT-1 targeting subunit and M20, a 20 kDa protein of unknown function. The MYPT-1 subunit interacts with multiple domains of the phosphatase including the RVXF binding motif, an N-terminal region that wraps around the protein and interacts at the terminal part of the hydrophobic groove and an ankyrin repeat region that clamps onto the C-terminus of PP-1, an area of the phosphatase that is disordered in other X-ray crystal structures. This functions to dramatically change the shape and charge distribution of the active site area, which the authors postulate is important to myosin binding and specificity. The anykyrin repeats create a large acidic surface that places the β 12- β 13 loop at the base and prominently displays it. Sequence variations between PP-1 isoforms tend to cluster in the C-terminal region and this may confer targeting subunit specificity. The N-terminal region extends the hydrophobic groove and both this N-terminal extension and the C-terminal ankyrin repeat domain are required for effective targeting and increased enzyme activity toward myosin. There are no allosteric consequences of the MYPT-1 subunit binding to the catalytic domain. The mechanism by which this protein activates the phosphatase is most likely a combination of the targeting subunit bringing the enzyme into proximity with its substrate and an increased affinity for myosin secondary to the electrostatic changes in the active site area.

Another model of PPP family endogenous inhibition was revealed by the structure of PP-5 with its tetratricopeptide (TPR) regulatory domain bound in an inhibited state.⁶³ The PP-5 phosphatase is unique in that the phosphatase and the regulatory TPR domain are produced as a single polypeptide, the TPR domain N-

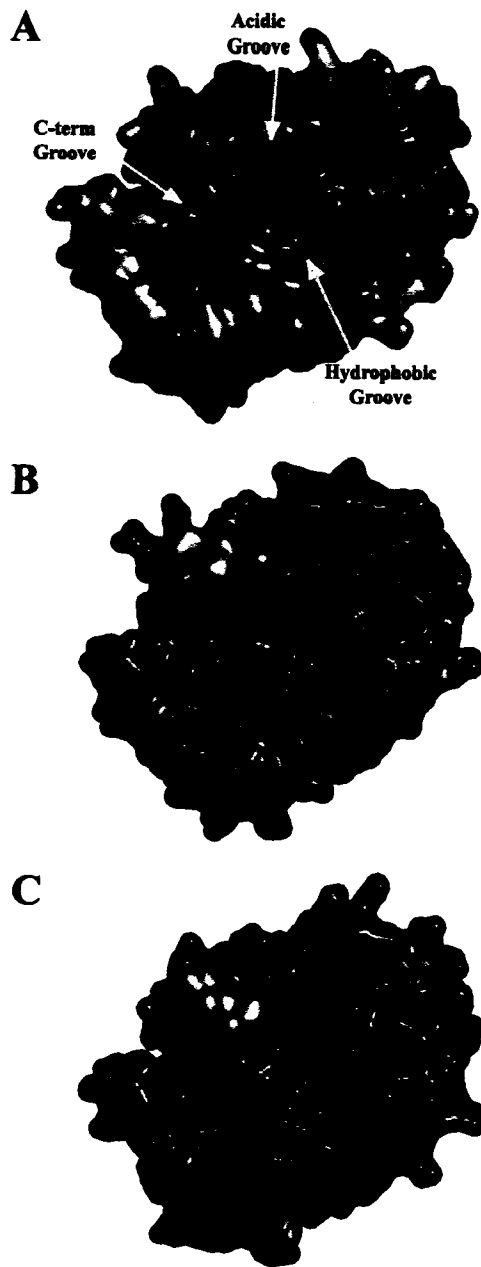


Figure 1.10 Surface representations of PP-1 (A) Electrostatic potential map of PP-1⁴² with the three grooves of the protein labeled. Red areas represent acidic areas, blue areas basic and white areas hydrophobic. The catalytic metals are shown as green spheres. (B) molecular surface of the PP-1:MCLR complex.³⁷ The β 12- β 13 is coloured yellow and Cys273 is coloured orange. The inhibitor is shown as sticks (C) molecular surface of the PP-1:calyculin structure.⁴² The β 12- β 13 loop is coloured yellow and Cys273 is coloured orange. The inhibitor is shown as ball and sticks. The movement of the β 12- β 13 loop in the PP-1:MCLR complex, and its effect on the molecular surface, can be seen easily.

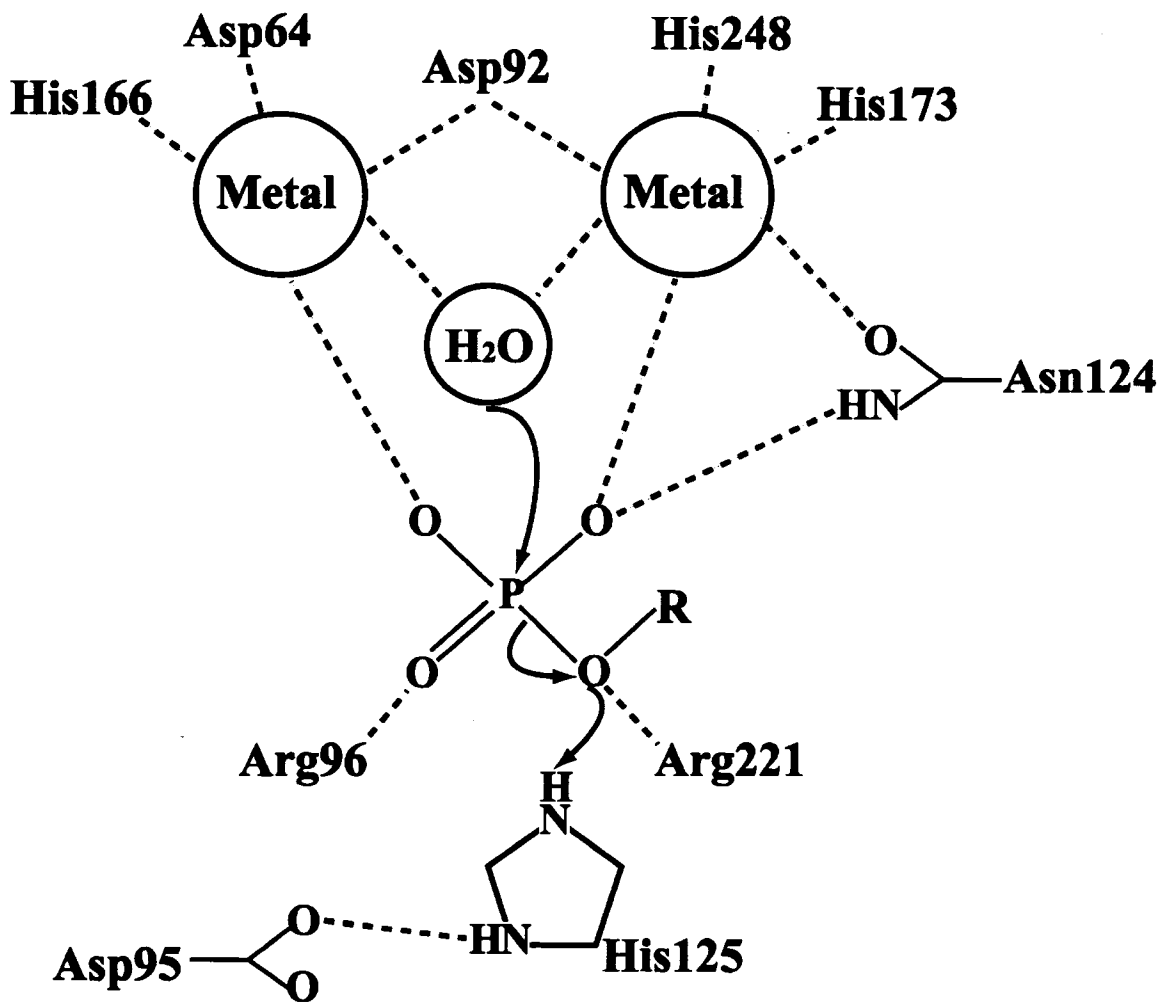


Figure 1.11 Proposed catalytic mechanism for the PPP family of protein phosphatases.³⁵
 All covalent bonds are shown with solid lines, potential interactions with dashed lines
 and catalytic electron transfers with red arrows.

terminal to the enzyme. This enzyme has proven of importance in its association with DNA-protein kinase and ataxia telangiectasia mutated, implying a role in DNA repair.^{64,65} In this structure, the TPR domain occupies a site immediately over the active site and anchors the C-terminus of the enzyme and the equivalent to the β 12- β 13 loop over one side of the active site region. The only area of the catalytic site left uncovered is the hydrophobic groove region. The main interactions are between Glu76 of the TPR domain and Tyr451 (Tyr272 in PP-1) and Arg275 (Arg96 in PP-1). This is reminiscent of the autoinhibitory C-terminal tail of CAN binding into the active site of CAN using glutamate and aspartate as the main binding residues.³⁸ The TPR-phosphatase interface includes the residues of TPR that also bind Hsp90. By binding at this site, Hsp90 can dislocate TPR from the active site and activate the enzyme. In a similar manner, polyunsaturated fatty acids can activate the enzyme by stabilizing an alternate conformation (reduction of the α -helical content) of the TPR domain and removing its binding and inhibitory effect on the catalytic subunit.⁶³

One of the available structures of CAN reveals the catalytic domain in complex with one of its regulatory subunits, calcineurin B (Fig. 1.6). Calcineurin B is a highly conserved protein, initially identified as an EF-hand protein that binds calcium ions. Its dumbbell structure is similar to that of calmodulin and it binds 4 ions of calcium, one with high affinity and three with a lower binding affinity.⁶⁶ The N-terminus of calcineurin B is myristoylated on a glycine residue but does not serve a membrane anchoring or enzyme activity role. The modification may be involved in stabilization of the protein structure since removal of the myristoylation causes disordering of the N-terminal region of calcineurin B.^{67,68} This regulatory protein

has regions that interact with both the immunophilin and the small molecule inhibitor in the FK506BP/FK506 and the cyclophilin/cyclosporine complexes. Since the structure of the catalytic domain of CAN is very similar to that of other PPP phosphatases, it is not clear why the activity of the enzyme is very minimal without binding calcineurin B.⁶⁶ There are currently no structures available of CAN with its other regulatory subunit bound, calmodulin. The binding region for calmodulin is within the catalytic subunit and addition of equimolar amounts of calmodulin increases the activity of the CAN catalytic subunit (in the presence of calcineurin B) by 20-fold, strictly by increasing the V_{max} .⁶⁶ This activation is believed to be secondary to the displacement of the autoinhibitory C-terminal domain of CAN from the active site.⁶⁶

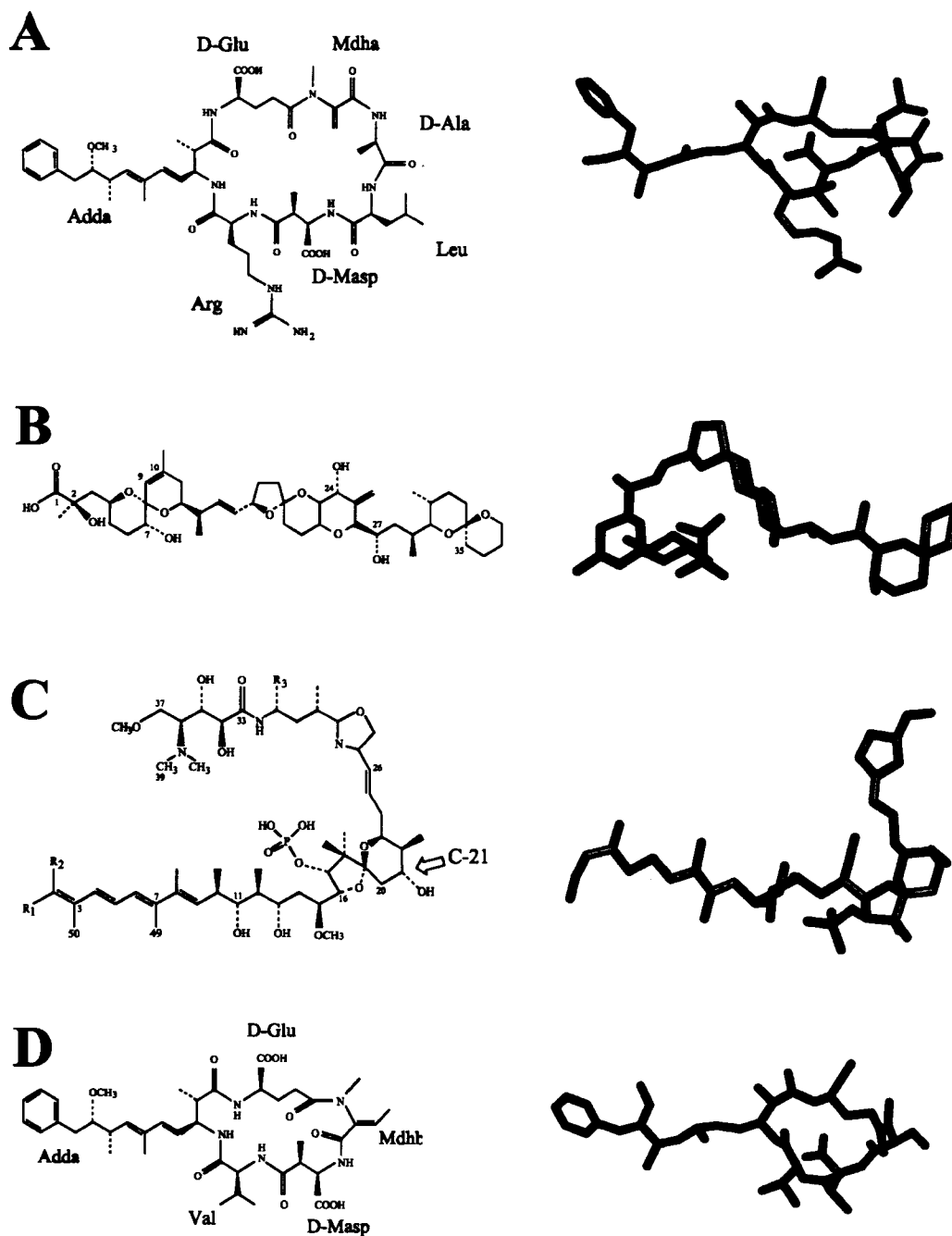


Figure 1.12 Natural product inhibitors of the PPP Ser/Thr Phosphatases, shown with their chemical and three-dimensional structures. (A) microcystin-LR (MCLR)⁵⁰, (B) okadaic acid⁴⁹, (C) calyculin (from the protein:inhibitor complex)⁴² and (D) motuporin⁵⁰.

F. Research overview

As illustrated above, there are several issues regarding PPP phosphatase family activity and inhibition which lend themselves to interpretation and possible resolution by structural biology. The interest in these topics is primarily from three domains. The first is in terms of understanding the diverse processes that are controlled by PPP family members. There is very little information regarding how the broad-specificity PPP family members are able to be targeted and controlled within the cell so that only certain metabolic processes are affected at certain times. The second interest in this topic is an extension of the first. Since the PPP family controls a broad variety of processes, including cellular proliferation, they are potential anti-neoplastic targets. Potential therapeutics in this area, the most well known being fostriecin, have not proven to be beneficial because of unacceptable side effects. By better understanding the mechanisms of enzyme inhibition, the potential exists for the generation of new pharmaceuticals. The final area of interest is in terms of immunosuppression. As mentioned earlier, two PPP family inhibitors (FK506 and CsA) are routinely used in a clinical setting but their efficacy is limited by their toxicity. The overall goal of this research has been to establish the structural basis and intricacies of PPP family inhibition in hopes of addressing the points mentioned above. Specific research projects attempting to fulfill these objectives are outlined below:

Chapter 2: This chapter describes the X-ray crystallographic structure of the PP-1:okadaic acid complex. At the time of publication, this was only the second PP-1:natural product toxin complex available. Okadaic acid has important public health

and biomedical research applications. This structure helps to elucidate the mechanism of natural product inhibition and reveals distinct differences between the enzyme conformation in this structure and in the PP-1:MCLR complex.

Chapter 3: This chapter presents two X-ray crystallographic structures of PP-1 and natural product toxins. The first is the complex between PP-1 and motuporin, another novel natural product inhibitor. This inhibitor has unique features that contribute new information to the mechanism of PPP family inhibition. The second complex is between PP-1 and a modified microcystin (dihydromicrocystin-LA) that does not contain a dehydroalanine residue and thus cannot form a covalent complex with PP-1. This structure serves to clarify the role of covalent modification and protein conformation in PPP family inhibition.

Chapter 4: This chapter describes the unique X-ray crystallographic structure between a chimeric PP-1, having its β 12- β 13 loop residues replaced by the equivalent residues from CAN, and okadaic acid. To assist in crystallographic structure interpretation, the inhibition kinetics were determined for the chimeric protein and several point mutants with natural product and endogenous inhibitors. This structure helps to understand why CAN has significantly different inhibitory profiles for most inhibitors, compared to other PPP family members.

Chapter 5: Summary

Chapter 2

The inhibitory mechanism of the tumor-promoter okadaic acid is revealed by its crystal structure bound to protein phosphatase-1

A. Introduction

Okadaic acid is a marine natural product toxin that is produced by a dinoflagellate (genera *Dinophysis* and *Prorocentrum*) but can be purified from the dinoflagellate-consuming sponge *Halichondria okadai*, which commonly lives near the Pacific coast of Japan. The toxin was first successfully isolated in 1981.⁴⁹ Initial interest in the toxin was from the perspective of seafood poisoning and the related threat to the fishing industry and, indeed, okadaic acid and its congeners are the cause of diarrhetic shellfish poisoning. Although initial isolation was from the Japanese sponge listed above, the toxin-associated disease is present in other regions of the world, especially northwestern Europe.⁶⁹

Okadaic acid was first identified as a possible tumor-promoter after studies performed on mouse ear showed that the compound could induce neoplastic growth but did not interact with the phorbol ester receptors like the TPA-type tumor promoters.^{70,71} This meant that okadaic acid did not specifically induce activation of protein kinase C and therefore acted by a new tumor-promoting mechanism. The identification of okadaic acid as a protein phosphatase inhibitor occurred shortly afterwards.⁷² This new pathway of tumor promotion was coined the "okadaic acid pathway" and several other structurally distinct compounds that induce tumorigenesis by phosphatase inhibition have been discovered since. Despite the

Table 2.1 Inhibitory potencies of okadaic acid and selected derivatives ⁷³⁻⁷⁶			
	PP-1 (K _i)	PP-2A (K _i)	PP-2B (IC ₅₀)
(1) Okadaic Acid	145 nM	0.03 nM	>10 mM
(2) Nor-okadanone	>> 10 000 nM	>> 100 nM	N/D
(3) OA methyl ester	> 10 000 nM	>> 100 nM	N/D
(4) OA-glycine amide (glycookadaic acid)	N/D	N/D but shown kinetically to have 51% activity of native OA	N/D
(5) 2-deoxy OA	870 nM	0.9 nM	N/D
(6) 7-deoxy OA	220 nM	0.07 nM	N/D
(7) 27-dehydro OA	6200 nM	7.3 nM	N/D
(8) OA C ₁ -C ₁₄ fragment	N/D	~0.04 nM ⁷³	N/D
(9) OA C ₁₅ -C ₃₈ fragment	> 10 000 nM ^{74,75}	~0.03 nM ⁷³ / >100 nM ^{74,75}	N/D
(10) OA tetramethyl ether	N/D	N/D but shown kinetically to have 2% activity of native OA	N/D

different mechanism of action from the TPA class of tumor promoters, the end result is quite similar (hyperphosphorylation of cellular proteins) and both classes of compounds induce similar clonal expansions.⁷⁷ In addition, both the TPA and okadaic acid classes of tumor promoters induce expression of TNF- α in a dose-dependant manner, a possible mechanism by which these compounds can further promote protein phosphorylation in the cell independent of their effects on PKC and protein phosphatases.⁷⁷

Okadaic acid is most specific for PP-2A (IC_{50} = 0.2-1 nM) but also inhibits PP-1 with significant potency (IC_{50} = 20 nM)⁷⁴ (Table 2.1). Other PPP family members are similarly inhibited including PP-4, PP-5 and PP-6.⁶⁹ The unrelated PP-3 is not inhibited by okadaic acid. Calcineurin is inhibited to a significantly smaller degree (IC_{50} > 10 mM).⁷⁴

The small molecule X-ray crystal structure of okadaic acid was determined as its *O*-bromobenzyl ester derivative (Fig. 2.1).⁴⁹ The toxin's general composition is that of a polyether with a 38 carbon backbone and spiroketal ring systems. The molecule possesses a noticeable difference in polarity between its extreme ends. Okadaic acid has a carboxylic acid and an alcohol within a spatially restricted region, whereas at the opposite end of the molecule, hydrophobic rings and methyl groups dominate. From this initial structure, it seemed likely that these features would play an integral role in the molecule's function. While the primary structure of the toxin itself is quite linear, the small molecule crystal structure revealed that an intramolecular hydrogen bond was present (between the carboxylic acid moiety and the hydroxyl group on C₂₄). This created a macrocycle, excluding only the hydrophobic end of

the molecule from the cyclic structure. Shortly thereafter a multitude of structure-activity studies emerged that attempted to determine the salient features of okadaic acid. These studies showed that the acidic moiety of OA was especially important for its inhibitory activity (Table 2.1). Removal of the entire acidic region, as in nor-okadanone, or esterification of the acid, as in the OA-methyl ester derivative, essentially ablated the inhibitory activity (compounds #2 and #3, Table 2.1).⁷³ This result could also be attributed to disruption of the internal structure of the inhibitor since the acid is involved in formation of the macrocyclic ring. Replacement of the acid with an N-linked glycine (glycookadaic acid, extension of the acid by two atoms, compound #4, Table 2.1) halved the inhibitory potency of OA, suggesting that spatial relationships are important since this chemical modification would significantly alter the topology of the inhibitor but maintain the same binding properties present in the acid. Removal of the C₂-hydroxyl adjacent to the acidic group also has effects on inhibitory potency but not as profoundly as the removal of the carboxylic acid (compound #5, Table 2.1). The other moiety involved in the macrocycle, the C₂₄-hydroxyl, has not been selectively changed but removal of all alcohols (by creating four methyl ethers in the tetramethyl ether derivative, compound #10, Table 2.1) essentially ablates the toxin's activity. Separation of OA into two fragments by ozonolysis at the C₁₄-C₁₅ double bond produces varying results (compounds #8 and #9, Table 2.1). Nishiwaki *et. al.* (1990) were able to achieve significant inhibition of PP-2A with either the acidic or hydrophobic portions of the inhibitor, although neither was as effective as the entire molecule. In contrast, two studies from Takai *et. al.* showed that minimal inhibition of PP-1 or

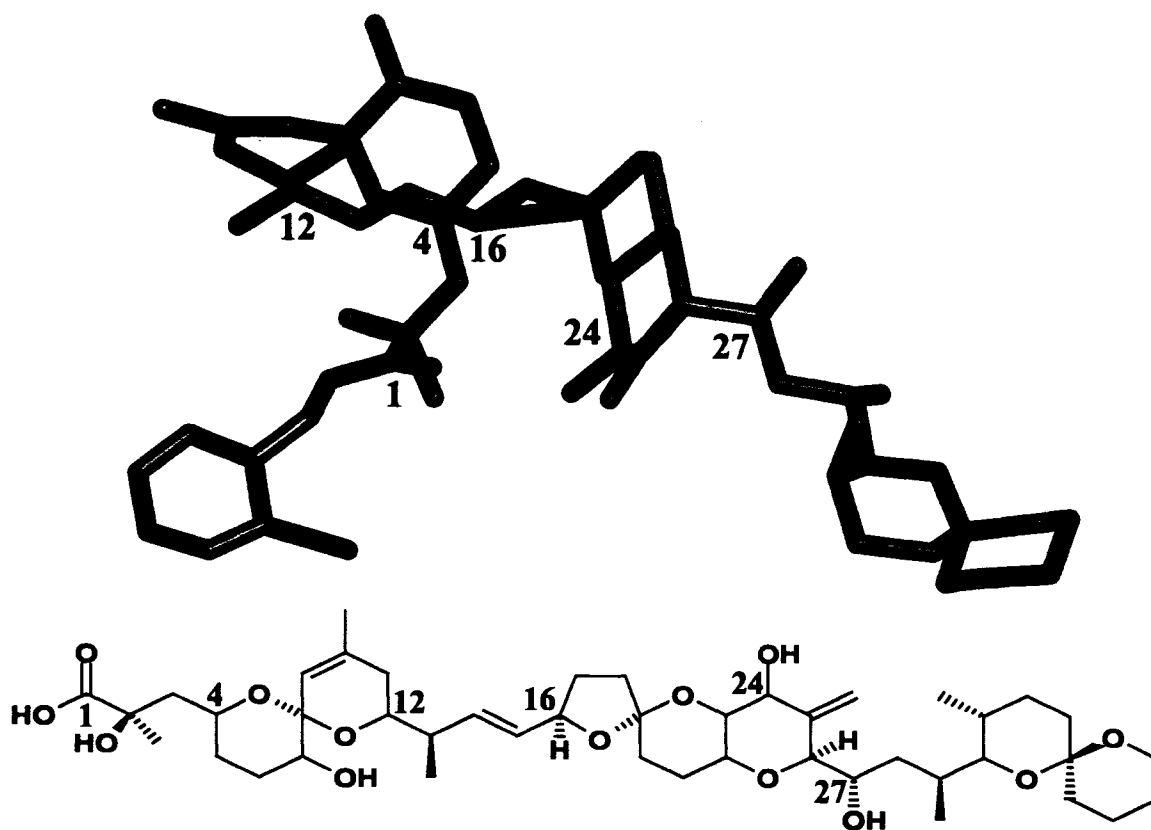


Figure 2.1 X-ray crystal structure of the *O*-bromobenzyl ester derivative of okadaic acid.⁴⁹ The derivative substructure is coloured blue. The chemical structure is shown below for reference.

PP-2A was possible with the hydrophobic half of okadaic acid alone.^{74,75} They did not perform studies on the acidic portion of the molecule.

Based on the numerous SAR and chemical modification studies that were performed, a pharmacophore model of okadaic acid activity was developed.⁷⁸ This model included four important areas: (1) the acidic moiety, (2) the hydrophobic tail region, (3) the C₇ alcohol (although the kinetic data did not support this, Table 2.1) and (4) the C₂₄ alcohol.

Shortly after the publication of this pharmacophore model, the first four structures of the PPP family of phosphatases became available.^{35,37-39} From these structures, models of okadaic acid binding were proposed. Gupta *et. al.* (1997) proposed important interactions between the inhibitor and Arg96, Arg221, Glu275 and with the hydrophobic groove of the protein.⁷⁹ Kinetic studies have promoted the importance of the β 12- β 13 loop and some of the models attempted to rationalize this information.^{45,46,80} Gauss *et. al.* (1997) proposed interactions between the toxin and the β 12- β 13 loop residues Tyr272 and Phe276, both interactions consisting of hydrophobic contacts.⁸¹ These models remained unverified in the absence of an X-ray crystal structure.

This chapter describes the determination of the three-dimensional crystal structure of okadaic acid bound to the catalytic subunit of protein phosphatase-1. This crystal structure shows the bifunctional nature of the binding of okadaic acid to PP-1, reveals the rationale for the kinetic data discussed above and shows that previously hypothesized models for okadaic acid binding were only partially correct. The information provided allows for future structure-based refinements of the

okadaic acid structure that may provide a phosphatase-specific inhibitor of clinical value.

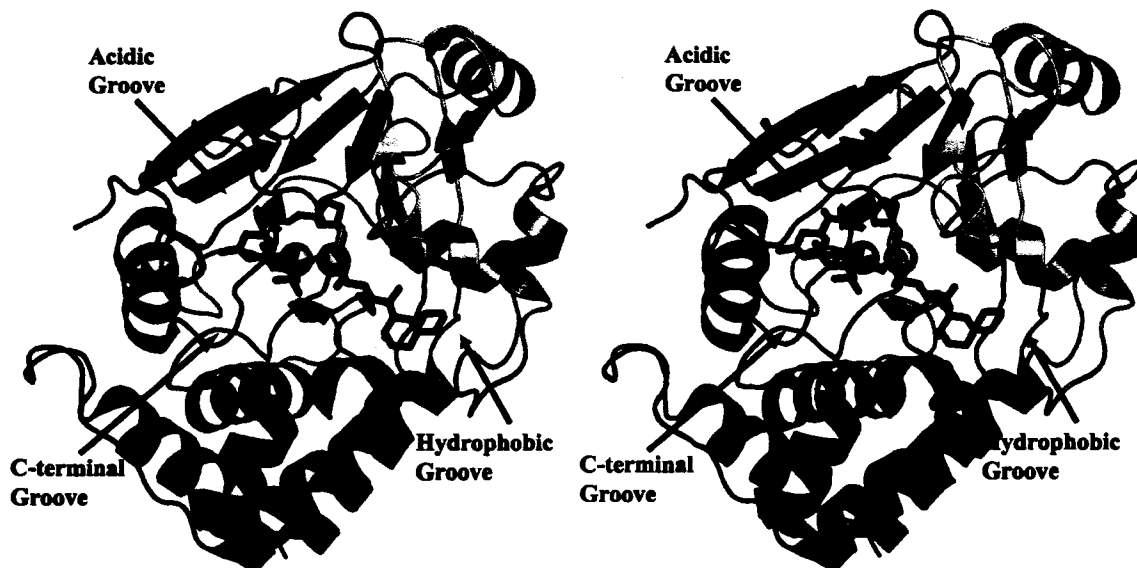


Figure 2.2 Ribbon representation of the X-ray crystal structure of the PP-1:OA complex. OA is shown as sticks with colouring by atom: carbon is grey and oxygen is red. The enzyme is coloured blue to red from N- to C-terminus. The three surface grooves of the protein are labeled. Two active site manganese metals are shown as yellow spheres.

B. Experimental Procedures

B.1 Protein purification and crystallization

The catalytic subunit of protein phosphatase-1 (γ isoform) was purified as described previously.⁶² Okadaic acid was purified from *Prorocentrum lima*⁶². Prior to crystallization, the protein was dialyzed against a solution containing manganese, which is known to stabilize and activate the enzyme⁶¹. Crystals were obtained by the hanging drop vapour diffusion method at room temperature. The protein and inhibitor were mixed in a 1:2 molar ratio, with the final protein concentration being 1.4 mM. The protein: inhibitor complex was then mixed with an equivalent volume of mother liquor. The mother liquor consisted of 2M lithium sulphate, 100 mM Tris (pH=8.0), 2% polyethylene glycol 400 and 10 mM β -mercaptoethanol. Crystal formation occurred over the course of several weeks. The complex crystallized in the tetragonal space group P4₂2₁2 with the cell dimensions $a = b = 99.18 \text{ \AA}$, $c = 67.19 \text{ \AA}$, $\alpha = \beta = \gamma = 90^\circ$. This equates to a Matthew's coefficient of $2.6 \text{ \AA}^3/\text{Da}$ with a solvent content of 52%.

B.2 Data collection, structure determination and refinement

Data collection took place under cryopreservation via a liquid nitrogen stream at 100° K. The crystals were placed in a solution containing 75% mother liquor and 25% glycerol for 3-4 seconds before being flash frozen in the liquid nitrogen stream. Data were collected on a Rigaku RU-H3R rotating anode generator with a RAXIS-IV++ image plate detector. On this instrumentation, an initial data set was collected to 2.9Å. The data were processed with the HKL suite of programs⁸². An initial structure was solved by molecular replacement with the program

AMoRe⁸³, using the protein structure (without inhibitor) from the previously determined PP-1:MCLR complex (PDB accession code 1FJM) as the search model. Electron density for both the protein and inhibitor were clear from the initial map generated from the molecular replacement solution (Figs. 2.2 and 2.3). Another data set to 1.9Å resolution was collected on the same instrumentation described above. The initial molecular replacement solution was used as a search model for molecular replacement for the second higher resolution data set. Okadaic acid was fit to the difference electron density using the previously determined free crystal structure⁸⁴. The protein:inhibitor model was subjected to rigid body refinement in the program CNS prior to manual manipulation and fitting in the program Xtalview^{85,86}. The model was subjected to iterative rounds of macromolecular refinement using the program CNS with a maximum likelihood target. The final model consisted of residues 6-299 of the protein and the entire okadaic acid inhibitor. The model was validated using the programs WHATCHECK⁸⁷ and PROCHECK^{87,88}, which showed that 98% of residues were in the allowed regions of the Ramachandran plot. The overall complex had a G-factor of 0.24. The crystallographic statistics are shown in Table 2.2.

B.3 Deposited Coordinates

The atomic coordinates and structure factors have been deposited in the PDB with accession code 1JK7.

B.4 Publication

This work was first published in the *Journal of Biological Chemistry* in 2001.⁸⁹

B.5 Contributions to this work

Of the work presented in this chapter, the author completed protein crystal harvesting, freezing and screening, data collection, integration and scaling and structure solution, refinement and validation. The author also completed data deposition in the Protein Data Bank and authored the primary citation for this work. Other contributions include protein purification by H.A. Luu (Lab of C.F.B. Holmes), crystal growth and refinement by Dr. M. Cherney and initial structure solution in collaboration between the author and Dr. K. Bateman and Dr. A. Das.

Table 2.2 Data collection and refinement statistics for PP-1:OA complex

Data Collection	
Unit Cell	$a = b = 99.2 \text{ \AA}, c = 62.17 \text{ \AA},$ $\alpha = \beta = \gamma = 90^\circ$
Space Group	P4 ₂ 2 ₁ 2
Wavelength (Å)	1.5418
Resolution (Å) ¹	30-1.9 (1.97-1.90)
Total Number of Reflections	434 544
Number of Unique Reflections	24 439
Completeness (%) ¹	97.6 (95.4)
Redundancy ¹	5.46 (5.33)
$\langle I / \sigma(I) \rangle$ ¹	30.0 (4.9)
R_{sym} (%) ^{1,2}	4.3 (35.8)
Mosaicity (°)	0.46
Refinement	
Resolution (Å)	30-1.9
Protein Atoms	2371
Inhibitor Atoms	57
Waters	181
R.m.s. deviations	
Bond length (Å)	0.007
Bond angles (°)	1.523
Average B-factors	
Protein atoms (Å ²)	32
Inhibitor atoms (Å ²)	34
Solvent (Å ²)	44
R_{cryst} (%) ³	19.9
R_{free} (%) ⁴	22.4
¹ Data in parentheses correspond to highest resolution shell	
² $R_{\text{sym}} = \sum_{\text{hkl}} \sum_i (I_i(\text{hkl}) - \langle I(\text{hkl}) \rangle) / \sum_{\text{hkl}} \sum_i I_i(\text{hkl})$, where I is the observed intensity, and $\langle I \rangle$ is the average intensity obtained from multiple observations of symmetry related reflections	
³ $R_{\text{cryst}} = \sum F_o - F_c / \sum F_o $, where $ F_o $ and $ F_c $ are the observed and calculated structure factor amplitudes respectively	
⁴ R_{free} was calculated as for R_{cryst} with 5% of the data omitted from structural refinement	



Figure 2.3 Representative electron density from the PP-1:OA complex solved to 1.9 Å. The electron density map shown is a σ_A -weighted omit map, contoured at 1σ , where the OA molecule was omitted during map generation.

C. Results and Discussion

C.1 General description of PP-1:Okadaic Acid structure

The tertiary structural configuration of the PP-1:OA complex includes three domains; a central β -sandwich, a flanking 6-member α -helical domain and a mixed domain composed of a three-member β -sheet and three α -helices (Fig. 2.2). The active site is at one edge of the β -sandwich and active site residues are found on random coil segments that join strands of the sandwich. The topology and surface characteristics of the enzymes includes features noted in previous PPP family structures. The active site region lies at the trifurcation of three surface grooves: the hydrophobic groove, the acidic groove and the C-terminal groove (Fig 2.2). The hydrophobic and acidic regions are evident when analyzing the electrostatic surface potential of the enzyme, as is the active site, which is predominantly acidic to facilitate catalytic metal binding. There are two metals found in the acidic active site of the enzyme. These were modeled as manganese ions because of the dialysis of the protein preparation as described in the methods section above, manganese was known to bind into the PP-1 active site³⁵ and the coordination geometries observed were possible for divalent manganese. On the opposite side of the enzyme from the active site lies the targeting subunit binding site (KIQF binding region). There are no changes noted in this region from previous structures and no substances were found bound to this site in the PP-1:OA complex.

The protein structure observed is very similar to other PPP family structures determined prior and since this investigation (Table 2.3). Most striking is the similarity between the various PP-1 structures bound to structurally diverse

inhibitors. Of the eight published and unpublished structures of PP-1:toxin/tungstate complexes, the largest C α RMSD between any two structures is 0.66 Å. The only exception to this similarity occurs in the β 12- β 13 loop region, where the PP-1:MCLR differs from all the other structures, including the PP-1:OA complex. This is the subject of the next chapter and will be discussed in detail there.

C.2 Inhibitor Binding to PP-1

Okadaic acid contains several regions that possess distinct chemical properties and requires similarly characterized regions of the enzyme with which to interact. A majority of the OA hydrophobic tail is comprised of the double ring spiroketal moiety. The tail remains primarily in an extended conformation and binds in this fashion into the hydrophobic groove of the phosphatase, interacting mostly with Trp206 and Ile130 (Fig. 2.4). Other hydrophobic interactions occur between the C₄ to C₁₆ region of OA (a region that contains two six-membered rings) and residues Phe276 and Val250. The remaining interactions between the inhibitor and the enzyme are hydrogen bonds. The acidic motif that is conserved in all known PP-1 inhibitors creates the most important of these interactions, forming a hydrogen bond with Tyr272 of the β 12- β 13 loop. In addition to this interaction with the acidic moiety, Tyr272 forms a hydrogen bonding interaction with the C₂-hydroxyl group, present adjacent to the OA acidic moiety. Further hydrogen bonding interactions are present between Arg96 and the C₂-hydroxyl group and between Arg221 and the C₂₄-hydroxyl functional group. While OA does not directly interact with the catalytic metals, the acidic group of OA does interact with a water molecule that bridges to one of the active site metals. Despite the acidic group of OA being in proximity to a

Table 2.3 Comparison of PPP family structures

PDB ID	1FJM	1S70	1JK7	1IT6	2BCD	JTM1	2BDX	BAR1	1AUI	1TCO	1M63	1MF8
1FJM	-	0.5	0.6	0.4	0.5	0.5	0.5	0.5	1.0	0.97	0.99	1.0
1S70	-	-	0.6	0.5	0.5	0.5	0.5	0.5	1.1	1.0	1.0	1.0
1JK7	-	-	-	0.5	0.3	0.5	0.3	0.7	1.0	1.1	1.0	1.0
1IT6	-	-	-	-	0.5	0.4	0.4	0.5	1.0	1.0	1.0	1.1
2BCD	-	-	-	-	-	0.5	0.2	0.6	1.1	1.1	1.0	1.0
JTM1*	-	-	-	-	-	-	0.5	0.5	1.0	1.0	1.0	1.1
2BDX	-	-	-	-	-	-	-	0.5	1.0	1.0	1.0	1.0
BAR1*	-	-	-	-	-	-	-	-	1.0	1.0	1.0	1.0
1AUI	-	-	-	-	-	-	-	-	-	0.5	0.7	0.5
1TCO	-	-	-	-	-	-	-	-	-	-	0.5	0.5
1M63	-	-	-	-	-	-	-	-	-	-	-	0.5
1MF8	-	-	-	-	-	-	-	-	-	-	-	-

Legend for Complexes: 1FJM (PP-1:MCLR)³⁷, 1S70 (PP-1:myosin phosphatase targeting subunit)³⁰, 1JK7 (PP-1:OA)⁸⁹, 1IT6 (PP-1:calyculin)⁴², 2BCD (PP-1:motuporin), JTM1 (PP-1:clavosine), 2BDX (PP-1:MCLA:2H), BAR1 (PP-1:tungstate)³⁵, 1AUI (CAN)³⁹, 1TCO (CAN:FK506)³⁸, 1M63 (CAN:CsA)⁴¹, 1MF8 (CAN:CsA)⁴⁰

*These structures have not been submitted to the PDB

metal-bound water, it is unlikely that this complex represents a substrate or transition-state complex since the proposed catalytic mechanism involves His125 donating a proton to the leaving group and the N^ε of His125 (from which the hydrogen would be provided) is 4.8Å from the acidic carbon of OA.¹

C.3 Crucial PP-1:OA Interactions

The small-molecule structures of the natural product Ser/Thr protein phosphatase inhibitors depict the structural diversity that exists but also illustrate several structural elements that may have convergently evolved. One such element that appears to be important in the PP-1:OA structure is the long hydrophobic moiety of OA. As mentioned previously, all the natural product inhibitors contain a hydrophobic tail region, each toxin-producing organism choosing its own variation. In the PP-1:OA structure, the double ring spiroketal region of OA binds into the similarly characterized hydrophobic groove of PP-1. While there does not appear to be a consistent method of hydrophobic tail pattern recognition between the PP-1:MCLR and the PP-1:OA structures, Ile130 and Trp206 lie in close proximity (< 4 Å, Fig. 2.4) to the inhibitors in both structures and Ile133 is slightly farther away (4.4 Å), contributing to the character of the hydrophobic groove. Mutational analysis is unable to unequivocally confirm the importance of Trp206 in hydrophobic binding since this residue also appears to be important for the alignment of metal binding residues and mutation to a similarly hydrophobic Phe residue drastically alters both the maximal enzyme velocity and the binding constant for phosphorylase a.⁶⁰ Similar results were obtained for Ile130 although why the V_{max} dropped significantly for this mutation was not clear since the residue does not

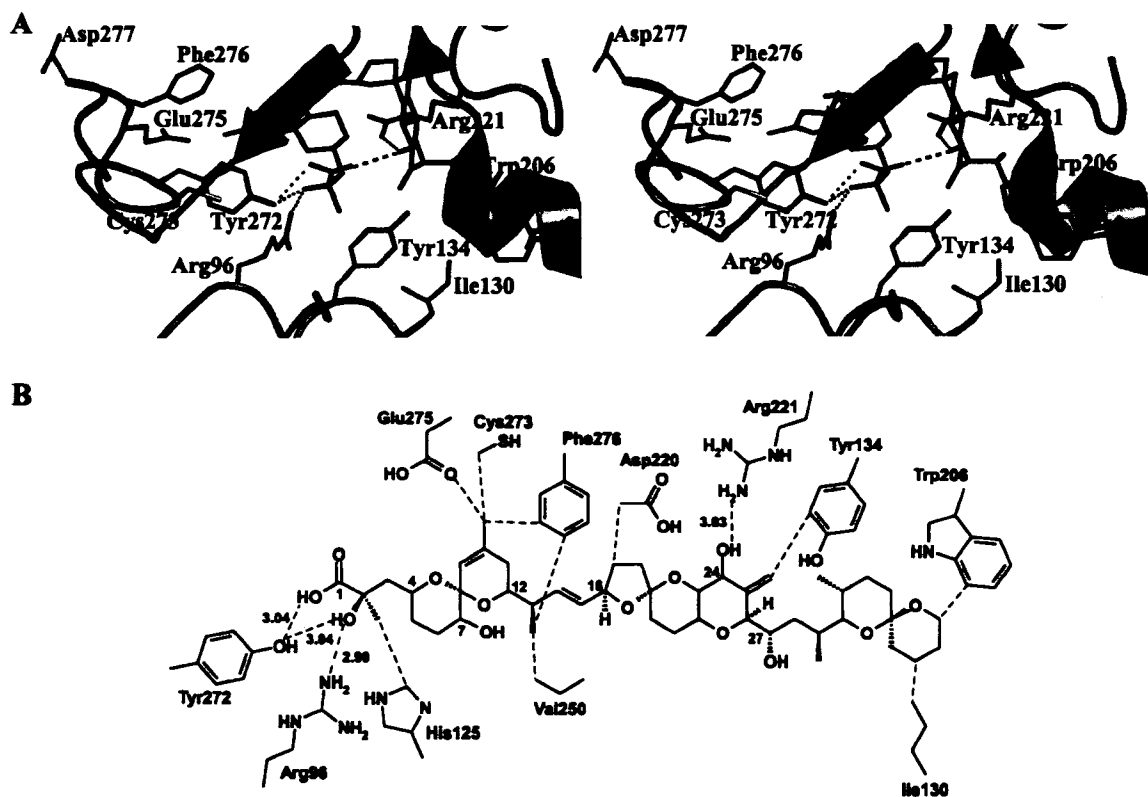


Figure 2.4 Active site orientation and important contacts between PP-1 and OA as observed in the X-ray crystallographic complex. (A) Stereo representation of the active site of the PP-1:OA complex showing important residues as sticks and the remaining protein as a backbone trace including the secondary structure. Hydrogen bonding interactions are shown with dashed lines. OA is shown as sticks and the intramolecular hydrogen bond is shown by a dashed line. (B) Chemical representation of all PP-1 residues within 4.0 Å of the OA molecule. The closest interaction for each residue is shown as a dashed line and if this is a putative hydrogen bond, the distance is given.

play any obvious catalytic role (the authors of the study did not comment on this finding). They did not choose to mutate Ile133. In the absence of reliable kinetic data, it is reasonable to conclude that the character of the hydrophobic groove is created by a combination of these residues and that the presence of this groove is important for OA (and other natural product inhibitor) binding. Additional hydrophobic interactions do occur between OA and PP-1 involving Phe276 and Val250 of the protein with the hydrophobic alkyl segment of OA, proximal to the C₁ acid. These interactions may be coincidental since mutation of Phe276 to Cys would remove a large proportion of the possible hydrophobic interactions but still decreases the K_i 40-fold for okadaic acid (the same mutation marginally increases the K_i for the other natural product inhibitors that the authors tested)⁴⁶. It is possible that the large ring of Phe provides a steric disadvantage to OA binding, which itself occupies a significantly large volume in the active site via its macrocyclic ring structure. Mutation to Cys may relieve the β 12- β 13 loop (on which Phe276 lies) of this unfavourable interaction, while maintaining some of the hydrophobic character. The other two surface grooves proximal to the active site (the acidic and C-terminal grooves) do not form any contacts in the crystal structure and have not been shown to be important kinetically for OA inhibition.

Other residues of the β 12- β 13 do however provide important binding residues for OA. In the PP-1:OA complex, the main interaction between the protein and the inhibitor occurs as a hydrogen bond between Tyr272 and the acidic group of OA. Indeed, removal of either the hydroxyl group of Tyr272 (by mutation to Phe) or the acidic moiety of OA (by esterification or by removal of the alcohol of the acid

(nor-okadanone), see Table 2.1), reduces the inhibitory potential of OA.^{46,73}

Similarly, the orientation and position of the acidic group appears to be important since disruption of the acidic conformation in OA glycine amide (glycookadaic acid, addition of N-linked glycine) reduces inhibition by one-half.⁷³

The remaining residues in the β 12- β 13 loop (after Tyr272 and Phe276) do not appear to play a significant role in OA binding since mutation of these residues does not significantly affect OA inhibition⁴⁶. This is well understood from the PP-1:OA crystal structure since only those two residues are both in a spatial location and have their side chains correctly oriented for potential inhibitor interactions.

In addition to the hydrogen bonding interaction that occurs between Tyr272 and the C₁-acidic group, a hydrogen bond is present between Arg96 and the C₂-hydroxyl group and between Arg221 and the C₂₄-hydroxyl group. Despite the close interactions between Arg96 and the C₂-hydroxyl, removal of the hydroxyl group only increases the K_i value by 7-fold (compound #5, Table 2.1).⁷⁵ The possibility exists that this interaction is an opportune one, occurring only when the inhibitor is bound in the active site of the enzyme and held in place by the interaction with Tyr272. The Arg96 residue was shown to anchor one of the product oxygens in the PP-1:tungstate complex, so it may play a larger role in the recognition of substrates. This can only be confirmed with the solution of a substrate or substrate analog complex.³⁵ The hydrogen bonding interaction between Arg221 and the C₂₄-hydroxyl group is much more important, removal by mutation of Arg221 to Ser confers resistance of PP-1 to OA.⁴⁵ This hydrogen bonding interaction is also the only non-hydrophobic interaction that occurs outside of the active site area and may

serve to help anchor the hydrophobic tail region in the hydrophobic groove of the enzyme.

The two remaining functional groups on OA are two hydroxyl groups, on C₇ and C₂₇. Removal of the C₇-OH group does not change the enzyme inhibition, consistent with the structural data which shows no potential interactions with the enzyme (Table 2.1).⁷³ Direct removal of the C₂₇-hydroxyl group has not been attempted but oxidation to a ketone group (27-dehydro OA, compound #7, Table 2.1) significantly reduces the inhibitory potential of the toxin. There are no potential interactions between PP-1 and the C₂₇-hydroxyl in the X-ray crystal complex but introduction of a sp² hybridized carbon would alter the position of the hydrophobic tail and this might explain the kinetic effects observed.

C.4 Comparison Between the Free and Enzyme Bound Structures of OA

The small molecule crystal structure of a derivatized OA was previously determined⁴⁹. This structure revealed that, despite possessing no intrinsic covalent ring structure, the molecule formed a macrocyclic ring via an intramolecular hydrogen bond between the C₁-acid and the C₂₄-hydroxyl groups. A prior modeling study concluded that OA most likely bound to PP-1 in an extended conformation, unlike the small molecule structure⁹⁰. The crystal structure of the PP-1:OA complex reveals, however, that the inhibitor does indeed maintain its cyclical structure, using the same intramolecular hydrogen-bonding interaction (the two OA structures have an RMSD of 0.7 Å over all 57 non-hydrogen atoms of the inhibitor) (Fig. 2.5). This gives OA a similar three-dimensional topology in comparison to the other marine toxins, most of which possess a covalently-closed macrocyclic substructure (only the

clavosines/calyculin do not have this).⁴⁸ The rationale for the ring structure in OA is most likely two-fold. The macrocyclic structure serves an inhibitory function, occluding the active site area. The macrocycle probably also serves an energetic role. The PP-1:OA complex contains very few hydrogen bonding interactions and no electrostatic interactions. Since the free-crystal structure of OA and the enzyme-bound structure are very similar, the inhibitor has to make minimal structural rearrangements to bind to the enzyme, minimizing the entropic cost of binding and providing a substantial energetic advantage.

C.5 Comparison of the PP-1:OA Complex to Other PPP Family Structures

At the time of our initial publication only four structures of PPP family member protein phosphatases were available. These included CAN with its regulatory subunit and C-terminal tail (1AUI) and with FK506 bound (1TCO) and PP-1 with MCLR (1FJM) and with tungstate in the active site (Egloff *et. al.* (1995), not submitted to PDB). Previously, few conclusions could be drawn regarding active site conformation since the PP-1:MCLR structure contained a significantly altered β 12- β 13 loop conformation (Fig. 2.6). The PP-1:tungstate and PP-1:OA complexes have very similar protein structures (neither having significant movement of the β 12- β 13 loop), possibly because neither of the two ligands were sufficiently similar to a biological substrate to cause active site realignment.

A striking fact when analyzing the PP-1:OA structure is that there are relatively few interactions that occur between the enzyme and the inhibitor (as discussed above, 3 hydrogen bonds and the area of hydrophobic interaction). The size of OA would dictate that a more significant number of chemical interactions

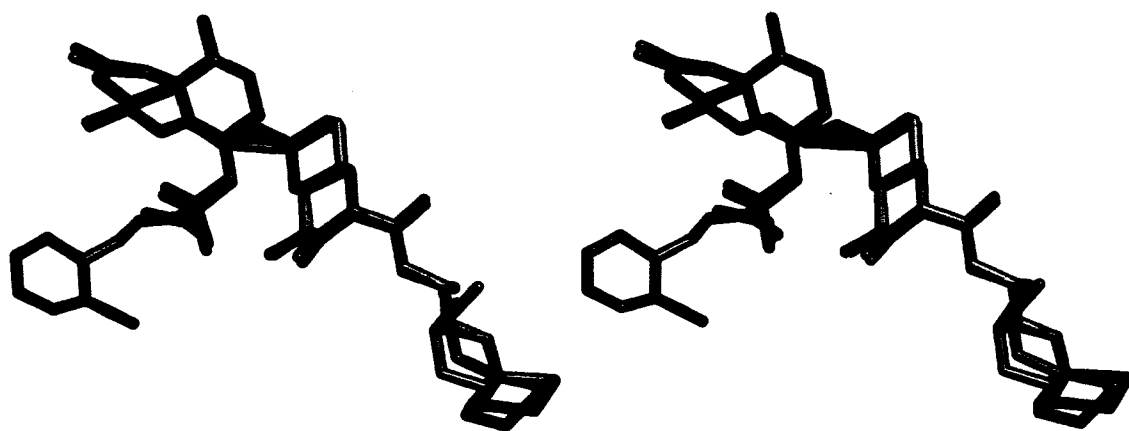


Figure 2.5 Alignment of the two X-ray crystal structures of OA. The inhibitor structure as determined bound to PP-1 is shown as sticks with orange carbons. The unbound *O*-bromobenzyl ester OA derivative structure is shown as sticks with grey carbons.⁴⁹

would be needed for sufficient inhibitory capacity. The microcystins have a slightly different chemical structure that lies in the active site, possessing a second acidic moiety. In the case of the PP-1:MCLR structure, this second acidic group (N-methylaspartate) hydrogen bonds with Arg96 of PP-1. This additional interaction may explain the 100-fold decrease in the inhibitory constant for MCLR in comparison to that of OA. The lack of interactions between PP-1 and OA is compensated for by two factors, the first is the entropic advantage of having similar free and enzyme-bound structures. The small molecule X-ray crystal structure and the enzyme-bound structures of OA only differ by an RMSD of 0.7 Å (57 atoms), compared to the MCLR NMR minimized-average solution structure and enzyme-bound structures that differ by an RMSD of 1.8 Å (55 atoms). This indicates that minimal structural changes and entropic cost are needed for enzyme binding for OA. The second method of compensation is by maximizing hydrophobic interactions, the hydrophobic tail of OA occludes 246 Å² of the protein surface to solvent where MCLR only occludes 207 Å². A similar result is found when comparing the excluded solvent accessible area of OA to other natural product toxins (see chapter 3). Further evidence for the importance of the hydrophobic interactions is that the hydrophobic portion of OA has an average thermal factor only 3 Å² above the average thermal factor for the entire PP-1 molecule in the complex, indicating molecular order and tight binding in this region. This equivalent value is 14 Å² for MCLR, despite being tethered to the protein by a covalent reaction.

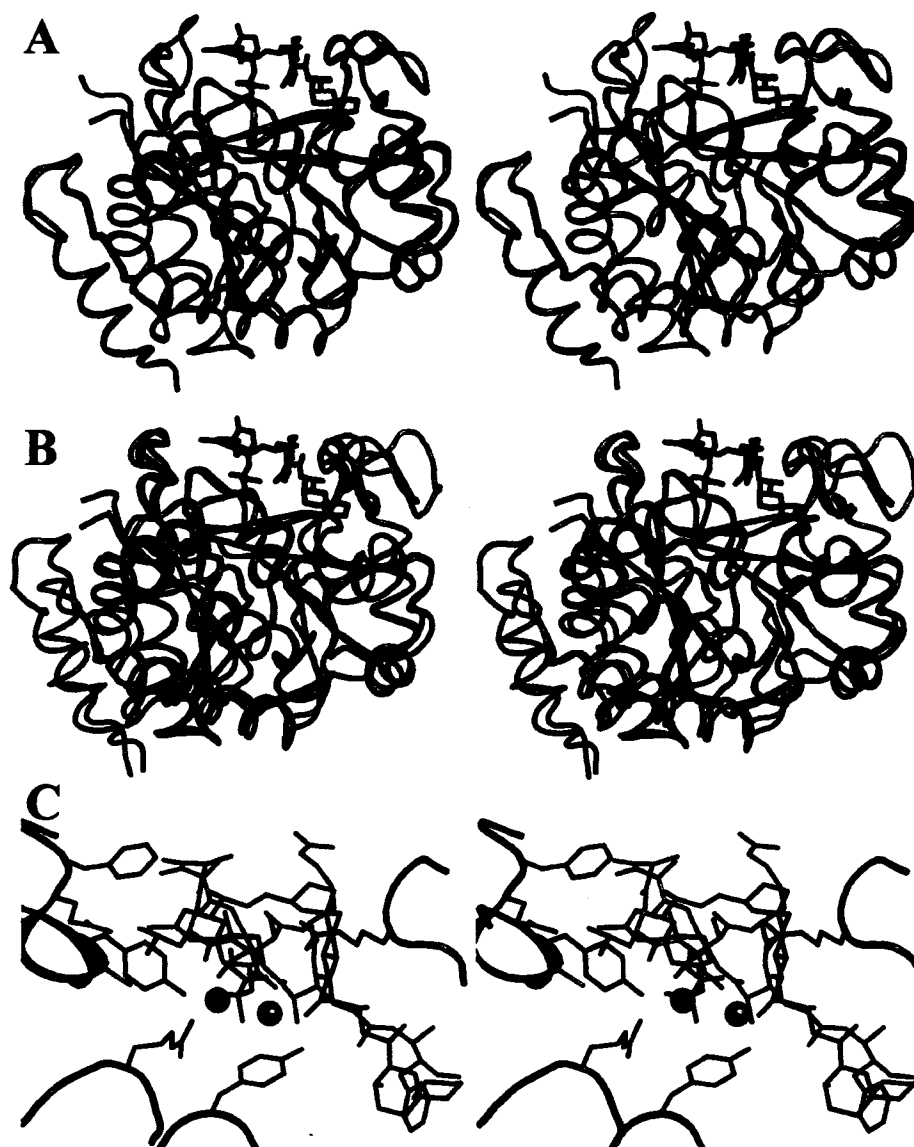


Figure 2.6 Alignment of PPP family members with the PP-1:OA complex. (A) Stereo representation of the alignment of the enzymes from the PP-1:OA (blue) and PP-1:MCLR (orange) X-ray crystal complexes. OA is shown as a stick model for orientation. (B) Stereo representation of the alignment of the phosphatases from the PP-1:OA (blue) and CAN (1AUI) (orange) X-ray crystallographic structures. The C-terminal tail from the active site and the regulatory subunit were removed from CAN. OA is shown as a stick model. (C) Stereo representation of the alignment of OA (blue) and MCLR (orange) in the active site of PP-1. The two protein:inhibitor complexes were aligned using the proteins as a reference frame. The protein from the PP-1:OA complex is shown including its active site metals. All alignments were performed using the program LSQMAN.⁹¹

D. Conclusions

The structure presented here serves to clarify the interactions that are needed for okadaic acid inhibition of PP-1 and begins to elucidate the role of specific protein residues in inhibitor binding and how these interactions change between the members of the PPP family of protein phosphatases. To summarize, the important interactions that occur between PP-1 and OA in the X-ray crystal structure involve the hydrophobic region of the inhibitor with the hydrophobic groove on the protein and three hydrogen bonding interactions between Tyr272 and the C₁-acid, between Arg96 and the C₂-hydroxyl and between Arg221 and the C₂₄-OH.

The interaction that occurs between the OA hydrophobic tail and the similar hydrophobic groove of the phosphatase appears to be very important, compensating for a minimal number of hydrogen-bonding interactions that occur in the active site region. All known natural product inhibitors of PP-1 contain a similar hydrophobic tail but there does not appear to be a common pattern of binding into the hydrophobic groove since each of the three available complexes (MCLR, OA and calyculin) all bind into the groove in slightly different manners. The importance of the hydrophobic groove for substrate binding is unknown since no X-ray crystal structure is available for a PP-1:substrate complex. This is most likely a complicated interaction involving targeting subunits that may change the character of the groove, similar to the way that the MYPT-1 targeting subunit does.³⁰

The interaction between Tyr272 and the inhibitor may be more complex than simple hydrogen bonding since mutation of Tyr272 to a Trp or Phe (i.e. adding/maintaining hydrophobic bulk and removing the hydrogen bonding potential)

only narrowly increases the K_i of the OA.⁴⁶ Mutation of the Tyr to either Ser or Thr, maintaining the hydrogen bonding capacity but removing the hydrophobic nature of the residue, increases the K_i for OA 200 to 250 fold (although the size of the residue also changes substantially in these mutations). Since the structures of these mutant complexes with OA have not been solved, it is difficult to conclude the exact nature of the kinetic results. From the crystal structure of the PP-1:OA complex and the earlier kinetic results mentioned above, it seems likely that the hydrogen bonding interaction between Tyr272 and the C₁-acid is important for enzyme inhibition.

This protein structure is very similar to other available structures of the PPP family, except for the structure of the PP-1:MCLR complex, which differed mostly in the β 12- β 13 loop region. This leaves the question of which structure and β 12- β 13 loop position is most biologically relevant. If loop realignment is important for the biological activity of the natural product toxins, then the PP-1:MCLR complex is considered representative of the *in vivo* structure. This is a distinct possibility since several previous studies had shown the importance of the β 12- β 13 loop in inhibitor recognition and specificity.^{46,47,60,61} However, there are several arguments against physiological movement of the β 12- β 13 loop. The CAN structure that contains the auto-inhibitory C-terminal tail in the active site (structure 1AUI) should induce any physiologically relevant β 12- β 13/L7 loop conformational changes since the C-terminal tail is the inhibitor that most closely resembles a biological substrate (being the only one that is protein based). Although CAN requires a regulatory subunit and calmodulin for activity, neither of these subunits are known or expected to interfere directly with active site residues (no structure of CAN is available with

calmodulin bound). Therefore, the active site and β 12- β 13/L7 loop conformation should be similar between CAN and the physiologically relevant PP-1 structures. Indeed, when comparing these structures it was found that the CAN structure is closest to the PP-1:tungstate and PP-1:OA structures, indicating that the PP-1:MCLR complex may be the outlier. Another indication that β 12- β 13 loop realignment in the PP-1:MCLR structure is unusual is the presence of the additional covalent interaction between Cys273 and the N-methyldehydroalanine residue of MCLR. This interaction may facilitate β 12- β 13 loop movement (by pulling the flexible loop into the active site area after covalent reaction) and was interestingly shown not to be of importance for the inhibitory activity of the microcystin (microcystins without the chemical ability to form the double bond inhibit the PPP family equally well).⁹² Together, this data would suggest that the PP-1:OA structure, and not the PP-1:MCLR structure, is the biologically relevant one. This is supported by our subsequent data and will be discussed in the next chapter.

The structures of PP-1 and CAN are very similar despite the fact that OA does not inhibit CAN (1-2 μ M) as well as PP-1 (10 nM) (Table 2.3, most of the differences between the two structures come from the N- and C-terminal regions and not the enzyme core or active site region) (Fig. 2.6). Since large structural changes in CAN would not be expected with OA binding, the dramatic fall-off in the inhibitory potential is more likely to be a result of primary sequence differences, which occur mostly in the β 12- β 13/L7 loop regions. As mentioned above, the only residues of the β 12- β 13 loop that significantly interact with OA are Tyr272 and Phe276 in PP-1. The Tyr272 residue is identical in CAN but the Phe276 residue is

replaced by another tyrosine. The change to a tyrosine and the proximity of this residue to a largely hydrophobic region of OA (C₄-C₁₂ region) may cause the significant decrease in the inhibitory potential for OA against CAN. There is an additional primary sequence change on the opposite side of the active site where Tyr134 is replaced by a Phe residue. Since OA does not interact with Tyr134 to a significant degree (no hydrogen bonding), this is unlikely to contribute to the inhibitory changes but may affect other natural product inhibitors that do rely on a bonding interaction with Tyr134. The other primary sequence differences in the active site region (Ile133Tyr and Cys273Leu) are not shown in the PP-1:OA complex to provide significant interactions and their role is unclear.

There are no structures available of PP-2A but OA has an enhanced inhibitory potential (and tighter binding) against this enzyme (IC₅₀=0.1 nM PP-2A vs. 10 nM PP-1). The main differences in primary sequence between PP-1 and PP-2A again occur in the β₁₂-β₁₃ loop region where the sequence in PP-1 (274-GEFD-277) is replaced by (267-YRCG-270) in PP-2A. Prior kinetic data showed a 40-fold decrease in the inhibitory constant when Phe276 in PP-1 was changed to a Cys (present in the equivalent position in PP-2A)⁴⁶. This primary sequence difference most likely accounts for the change in binding value, although the exact reason is not clear. Additionally, Gly274 occupies the third position of a type II β-turn and changing this residue to a Tyr in PP-2A may have effects on the active site and β₁₂-β₁₃ loop architecture. Mutation of this residue to a Phe in PP-1 did not effect its OA inhibitory value⁴⁶ so the exact role of this residue is not clear in the absence of a PP-2A crystal structure. This might mean that PP-2A has a different β₁₂-β₁₃ loop

conformation from both PP-1 and CAN.

Chapter 3

Elucidation of the role of the PP-1 β 12- β 13 loop in natural product inhibitor binding and specificity: The crystal structure of two novel natural products bound to PP-1

A. Introduction

The control and inhibition of Ser/Thr protein phosphatases, either by pharmaceuticals or naturally occurring toxins, has many clinical implications including immunosuppression, water quality/toxicity and food poisoning. For these reasons, it is of interest to characterize the interaction that occurs between natural product inhibitors, produced by a variety of organisms, and their PPP phosphatase family receptors. Previous structural data of PPP family members with natural product toxins includes three PP-1:toxin X-ray crystal structures (PP-1:MCLR, PP-1:OA and PP-1:calyculin).^{37,42,89} These structures revealed that the three toxins bound in similar fashions on the surface of the protein, occluding the active site area. The three protein structures were exceptionally similar (C_{α} RMSD 0.4 to 0.6 Å for 290 C_{α} atoms when comparing any of the structures to one another) and all active site residues occupied essentially identical positions in all complexes (Fig. 2.6). The single area of significant difference between the structures was in the β 12- β 13 loop region, where the PP-1:MCLR structure took a conformation significantly different from that in the PP-1:OA or PP-1:calyculin structures. The loop position was also different than that observed in the native PP-1 structure or two available CAN structures (all without natural products bound). This area of the protein was shown in numerous kinetic studies to be of importance in toxin recognition and

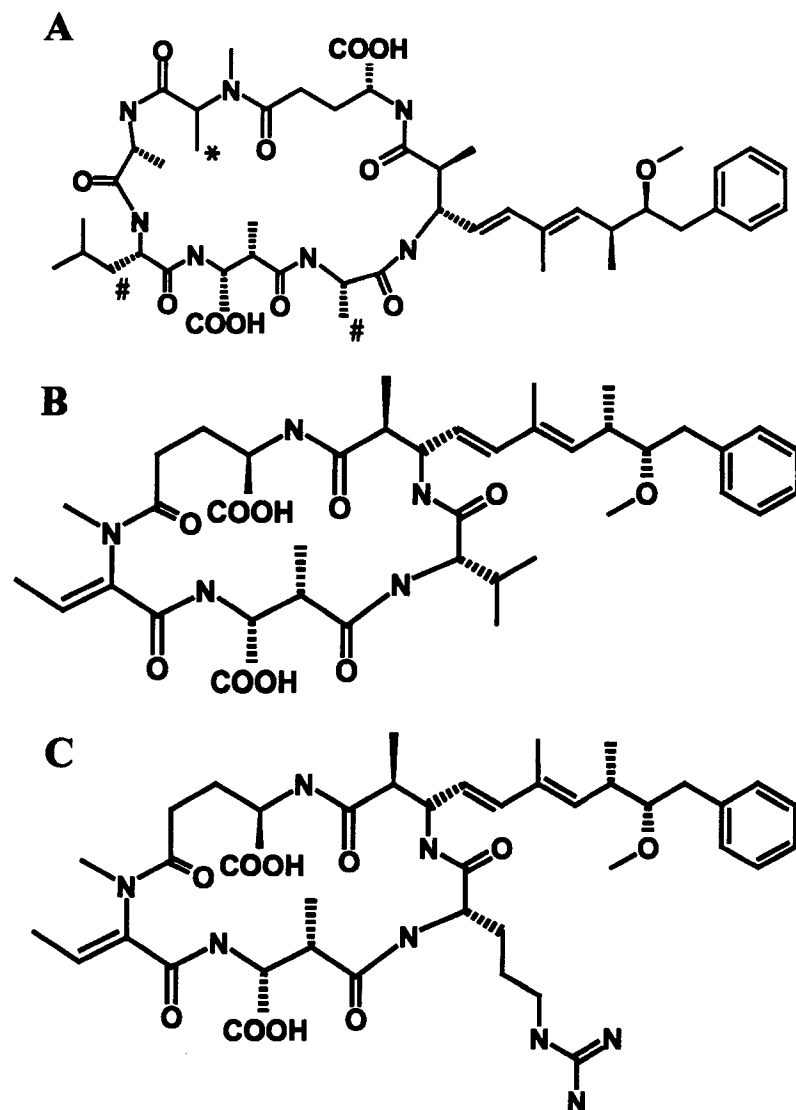


Figure 3.1 Chemical Structures of the Cyanobacterial Toxins (A) structure of dihydromicrocystin-LA(MCLA-2H). #The two sites of modification for the microcystins, in MCLA-2H these sites are Leu and Ala and in MCLR these sites are Leu and Arg. *The site of hydrogenation that removes the N-methyldehydroalanine residue and creates an N-methylalanine residue with no Michael addition properties. (B) Structure of motuporin (nodularin-V). (C) Structure of nodularin-R.

binding.^{46,60,61} A vital residue in this loop, Tyr272, forms hydrogen bonds with OA, MCLR and calyculin and is required for effective inhibition by all toxins. The movement of the β 12- β 13 loop in the PP-1:MCLR structure was the first indication of flexibility in the loop, which may be of importance in toxin inhibitory mechanisms.

The microcystins and nodularins are hepatotoxins that are cyanobacterial metabolites found both in freshwater and in marine environments (Fig. 2.1)⁹³. These toxins are potent tumor-promoters and inhibitors of PP-1 and PP-2A catalytic subunits, producing significant mortality and morbidity in both wildlife and human populations consuming contaminated water supplies.⁹⁴⁻⁹⁸ The members of the microcystin class of inhibitors differ primarily in the identity of two variable amino acid residues. Nodularins are structurally similar natural product inhibitors that only contain one variable amino acid. They inhibit PP-1 and PP-2A with a similar potency to that of the microcystins. Motuporin (MOT) is a member of the nodularin class of inhibitors (also called nodularin-V, for a Val in its variable position) which was first identified from the marine sponge *T. swinhoei*.⁹⁹ The NMR solution structure of two nodularin family inhibitors, MOT and nodularin-R (variable amino acid arginine), have been determined^{50,51}. These structures showed that both adopted a very similar solution structure to that of MCLR (Fig. 3.2).

The X-ray crystal structure of the PP-1:MCLR complex illustrated a few key interactions between the inhibitor and the enzyme. These included interactions with the hydrophobic groove of PP-1 via the long hydrophobic Adda side chain of MCLR, electrostatic interactions between the active site metals and the acidic

moiety of the γ -linked D-glutamic acid and hydrogen bonding interactions between Arg96/Tyr134 and the Masp residue of the toxin (these interactions are described in more detail in Chapter 1). An additional covalent linkage occurs between the N-methyldehydroalanine residue of MCLR and the Cys273 residue present in the β 12- β 13 loop of the phosphatase. This reaction most likely occurs via a Michael addition reaction between the double bond present in the Nmda and the sulphur nucleophile of the cysteine. This reaction was shown to be temporally separated from initial protein inhibition and, therefore, its role in the inhibitory mechanism of MCLR is in doubt.⁶² Important functional differences exist between the microcystins and the nodularins in the way that they interact with the PPP family members. Both classes of inhibitors bind initially in a non-covalent manner, causing enzyme inhibition. The nodularins (including MOT), do not continue on to bind in a covalent manner, even in a delayed reaction.^{62,100} This occurs despite MOT possessing a N-methyldehydrobutyrine residue that could undergo a Michael addition reaction with Cys273, analogous to the Nmda residue of MCLR. There is currently no explanation as to why MOT does not react this way.

The ambiguity in the position of the β 12- β 13 loop led us to investigate further its role using related novel and modified natural product inhibitors. We determined the structure of the PP-1:MOT complex and the structure of PP-1 bound to a modified natural product, dihydromicrocystin-LA (MCLA-2H). This modified microcystin has leucine and alanine as its two variable amino acids but it also has had its double bond chemically removed (by hydrogenation) from the dehydroalanine residue. This ablates the ability of the microcystin to react with

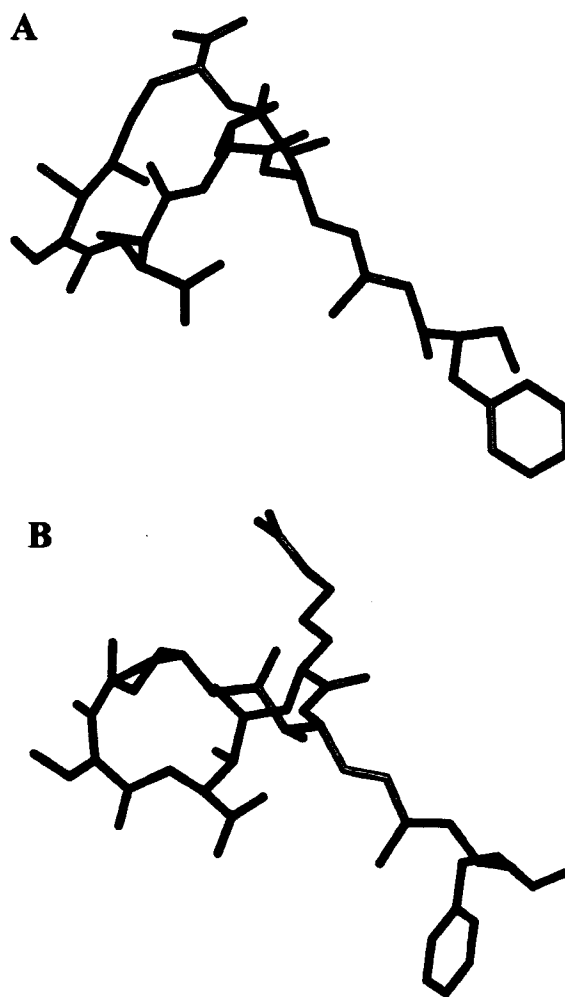


Figure 3.2 Solution (NMR) structures of nodularin toxins (A) minimized-average NMR structure of MOT (nodularin-V)⁵⁰, (B) minimized-average NMR structure of nodularin-R⁵¹.

Cys273 and form a covalent adduct. These two structures allow for investigation of the position of the β 12- β 13 loop and to clarify whether the movement of the loop in the PP-1:MCLR structure is important for inhibition or an irrelevant movement that occurs solely as a result of the covalent linkage.

B. Experimental Procedures

B.1 Protein and toxin purification and crystallization

The catalytic subunit of protein phosphatase-1 (γ isoform) was purified as described previously.⁶² Microcystin-LA was purified from natural blooms of *Microcystis aeruginosa* using procedures described previously.⁶² Motuporin was purified and characterised as described in Desilva *et al.*¹⁰¹ Site specific reduction of MCLA by NaBH₄ was carried out as described in⁶², the final product was fully characterized by high resolution mass spectrometry (FABMS) and ¹H-NMR analysis (data not shown).

Crystals were obtained by co-crystallization using the hanging drop vapor diffusion method at room temperature. For both MOT and MCLA-2H, the enzyme and inhibitor were mixed in a 1:3 molar ratio with the final concentration of protein being 12 mg/ml. The PP-1 inhibitor complexes were then mixed with an equivalent volume of mother liquor that consisted of 2.3 M lithium sulfate, Tris-HCl (100 mM, pH 8.0), polyethylene glycol 400 (2%) and β -mercaptoethanol (10 mM). Both complexes crystallized in the space group P4₂2₁2 with one complex per asymmetric unit. This corresponds to a Matthew's coefficient of 2.53 for both complexes and a solvent content of 51%. The crystal and refinement data for both complexes are given in Table 3.1.

B.2 Data collection, structure determination and refinement

The X-ray diffraction data for both complexes were collected at Beamline 8.3.1 at the Advanced Light Source in Berkeley, California on an ADSC Q210 detector (Fig. 3.3). All data were collected at 1 Å wavelength and were processed

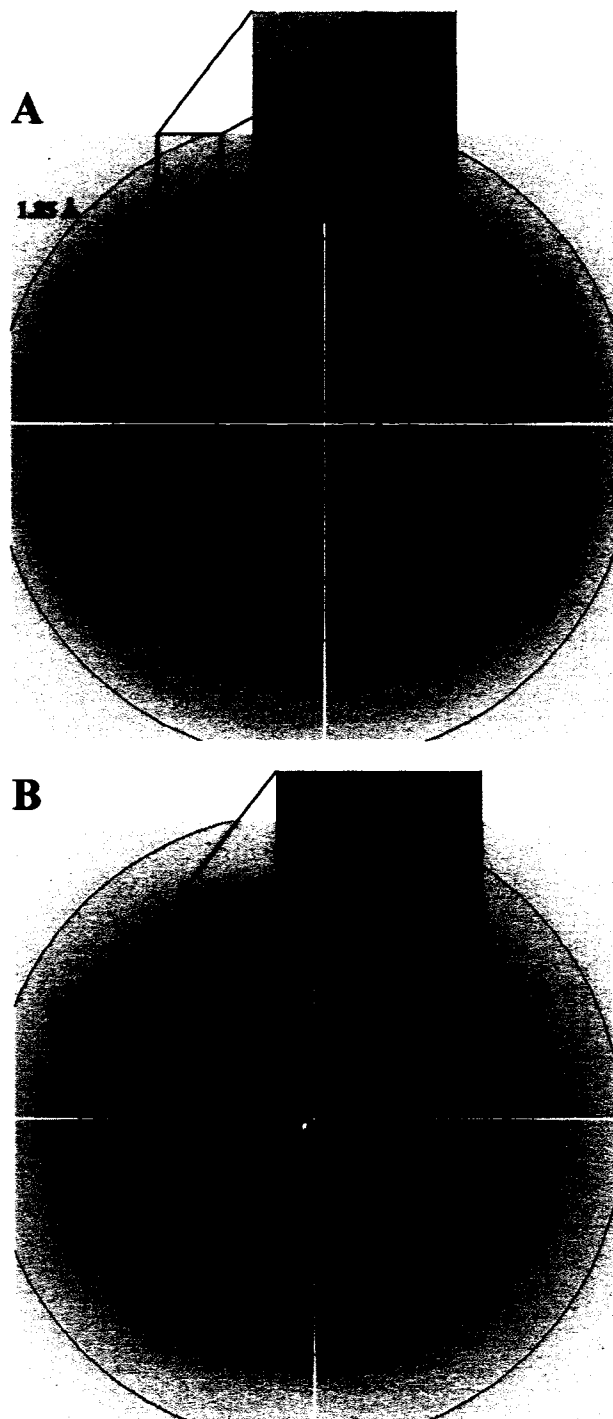


Figure 3.3 Observed X-ray diffraction pattern from (A) a crystal of the PP-1:MOT complex and (B) a crystal of the PP-1:MCLA-2H complex. Both diffraction patterns were collected at the Advanced Light Source.

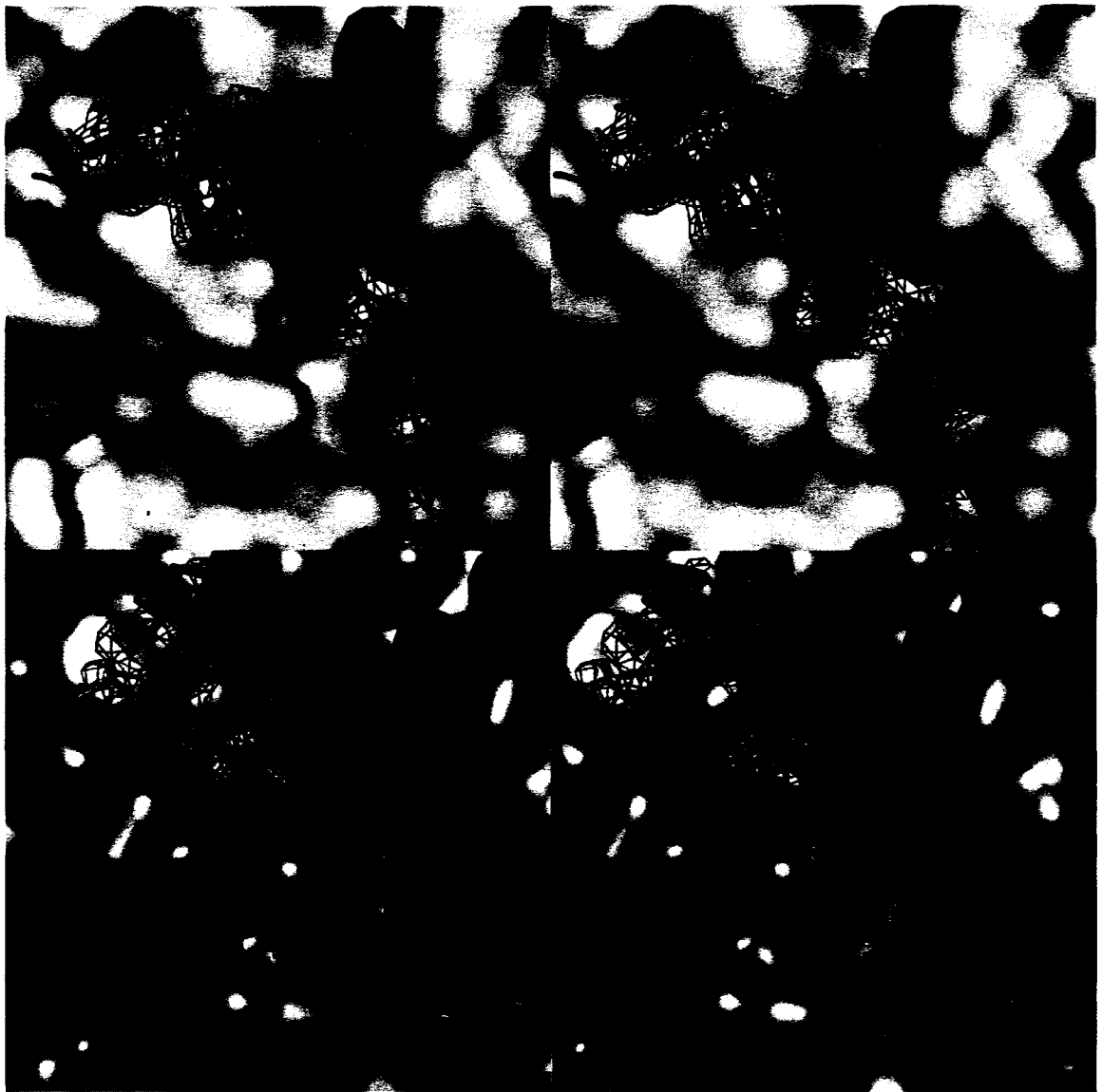


Figure 3.4 (A) Representative electron density from the PP-1:MOT complex solved to 2.1 Å. (B) Representative electron density from the PP-1:MCLA complex solved to 2.1 Å. The electron density map shown is a σ_A -weighted omit map, contoured at 1σ , where the MOT or MCLA molecule was omitted during map generation.

using the programs MOSFLM¹⁰² and SCALA.¹⁰³ Both structures were solved by molecular replacement with the program AMoRe⁸³, using the structure of PP-1 as determined complexed to OA⁸⁹ as the starting model. The electron densities for the protein and bound inhibitors were clear in both instances (Fig. 3.4). The protein-inhibitor model was fitted manually using the program XtalView.⁸⁶ The starting model for MOT came from the NMR structure of the inhibitor⁵⁰ and the starting model for MCLA-2H came from the previous crystal structure of MCLR bound to PP-1.³⁷ The structural models were subjected to iterative rounds of macromolecular refinement using the program REFMAC¹⁰⁴ with a maximum likelihood target. The refinement data are listed in Table 3.1. The final structures consisted of PP-1 residues 6 through 298 and complete inhibitor models for both complexes. The models were checked for validity using the programs WHATCHECK⁸⁸ and PROCHECK.⁸⁷ The final PP-1:MOT structure had 97.3% of residues in traditionally allowed Ramachandran plot regions with a G-factor of -0.2. The final PP-1:MCLA-2H structure had 97.7% of residues in allowed Ramachandran plot regions with a G-factor of -0.1.

B.3 Coordinates

The atomic coordinates and structure factors have been deposited in the Protein Data Bank with accession codes 2BCD (PP-1:MOT) and 2BDX (PP-1:MCLA-2H).

B.4 Publication

This work was first published in the *Journal of Molecular Biology* in 2006.¹⁰⁵

B.5 Contributions to this work

Of the work presented in this chapter, the author partially completed protein preparation and crystallization, fully completed protein crystal harvesting, freezing and screening, data collection, integration and scaling, structure solution, refinement and validation. Other contributions include protein purification by H.A. Luu (Lab of C.F.B. Holmes), inhibitor discovery, purification and chemical modification by D. Williams (Lab of Dr. R.J. Andersen) and crystal growth and refinement by Dr. M. Cherney.

Table 3.1 Data collection and refinement statistics for the PP-1:MOT and PP-1:MCLA-2H crystallographic complexes

	PP-1c:MOT Complex	PP-1c:MCLA-2H Complex
Data Collection		
Unit Cell	$a = b = 101.0 \text{ \AA}$, $c = 63.49 \text{ \AA}$, $\alpha = \beta = \gamma = 90^\circ$	$a = b = 100.0 \text{ \AA}$, $c = 62.9 \text{ \AA}$, $\alpha = \beta = \gamma = 90^\circ$
Space Group	P4 ₂ 2 ₁ 2	P4 ₂ 2 ₁ 2
Wavelength (Å)	1.00	1.00
Resolution (Å) ¹	40-2.1 (2.20-2.10)	40-2.3 (2.42-2.30)
Total Number of Reflections	186190	113187
Number of Unique Reflections	19726	14724
Completeness (%) ¹	99.9 (99.9)	99.9 (99.9)
Redundancy ¹	3.7 (3.8)	7.7 (7.6)
$\langle I / \sigma(I) \rangle$ ¹	13.5 (4.6)	20.4 (6.7)
R _{sym} (%) ^{1,2}	6.5 (29.3)	7.2 (28.7)
Mosaicity (°)	0.37	0.52
Refinement		
Resolution (Å)	40-2.1	40-2.3
Protein Atoms	2350	2338
Inhibitor Atoms	55	65
Waters	73	35
R.m.s. deviations		
Bond length (Å)	0.02	0.013
Bond Angles (°)	1.84	1.57
Average B-factors		
Protein Atoms (Å ²)	26.3	32.7
Inhibitor Atoms (Å ²)	32.3	43.7
Solvent (Å ²)	29.0	30.1
R _{cryst} (%) ³	0.221	0.212
R _{free} (%) ⁴	0.264	0.250

¹Data in parentheses correspond to highest resolution shell

²R_{sym} = $\sum_{hkl} \sum_i (|I_i(hkl)| - \langle I(hkl) \rangle) / \sum_{hkl} \sum_i I_i(hkl)$, where I is the observed intensity, and $\langle I \rangle$ is the average intensity obtained from multiple observations of symmetry related reflections

³R_{cryst} = $\sum (|F_o| - |F_c|) / \sum |F_o|$, where |F_o| and |F_c| are the observed and calculated structure factor amplitudes respectively

⁴R_{free} was calculated as for R_{cryst} with the 5% of the data omitted from structural refinement

C. Results and Discussion

C.1 X-ray Crystal Structure of motuporin (nodularin-V) bound to PP-1

The natural product toxins of the PPP family of protein phosphatases contain three common features: an acidic group (usually a carboxylic acid but this can also be a phosphate), a hydrophobic tail and a large macrocyclic domain (either a covalently closed ring or an intramolecular hydrogen bonding interaction as is the case for OA). Motuporin contains all of these domains (Figs. 3.1 and 3.2) and binds to PP-1 in a similar manner to other natural product toxins with its macrocycle occupying most of the active site region and its hydrophobic tail occupying the hydrophobic groove that is adjacent to the active site (Fig. 3.5 and 3.6). The α -carboxyl moiety from the Gga residue of MOT lies in proximity to the organic acids from other natural product inhibitors. In MOT, this acid binds the active site metals indirectly through bridging water molecules. The hydrophobic region of MOT, consisting of its long Adda tail, primarily interacts with the PP-1 residues Trp206, Val223 and Ile130 in the hydrophobic groove.

The hydrophobic tail of MOT does not interact as strongly with PP-1 as the corresponding segment of OA. This manifests as higher thermal coefficients and poorer electron density for the MOT hydrophobic tail. The thermal coefficients for the atoms in the MOT hydrophobic tail are 5.8 \AA^2 above the average thermal coefficient for the entire inhibitor and 17 \AA^2 above the average thermal factor for the entire protein. The similar calculated values for OA are 1.3 \AA^2 and 3 \AA^2 , indicating tighter binding of OA to the hydrophobic groove area. The hydrophobic tail of OA has five potential hydrophobic interactions within 4 \AA , whereas MOT only has two

potential interactions. In addition, the buried protein surface area that the hydrophobic tail of OA occupies is 246 Å², where MOT occupies only 214 Å². All these factors indicate that hydrophobic tail binding for MOT is most likely less important than for OA.

In contrast to OA, MOT forms a significant number of hydrogen-bonding contacts with PP-1, formed primarily by the two acidic groups present in the inhibitor. The Masp residue has hydrogen-bonding interactions with Tyr134 and Arg96. The interaction with Tyr134 was seen in the PP-1:MCLR structure but not in the PP-1:OA structure, which contains only one acidic group. The hydrogen-bonding interaction between Masp and Arg96 is one of three possible for Arg96, the other interactions being with the acid of the Gga residue and the carbonyl oxygen of the Mdb residue. All of the possible bonding interactions involving Arg96 are via its guanidinium group. A single residue from the β12-β13 loop, Tyr272, bonds to the inhibitor, interacting with the acidic group of the Gga residue. A final hydrogen bonding interaction is present between the guanidinium of Arg221 and the carbonyl of the Adda residue. All five hydrogen bonding interactions have bonding angles between 102° and 153° and three of these bonds are shorter than 2.9 Å (Fig. 3.6).

The inhibitory potential of MOT is very similar to that of MCLR (IC₅₀ < 1 nM with PP-1), both being about 50-fold more potent than OA.⁴⁷ The molecular basis for this difference in inhibition may lie in the number of hydrogen bonds that MOT forms with PP-1. As described above, four areas of the inhibitor (two acids and two carbonyl oxygens) have the ability to form hydrogen bonds with a total of four protein residues (Arg96, Tyr134, Arg221, Try272). These are advantageous in

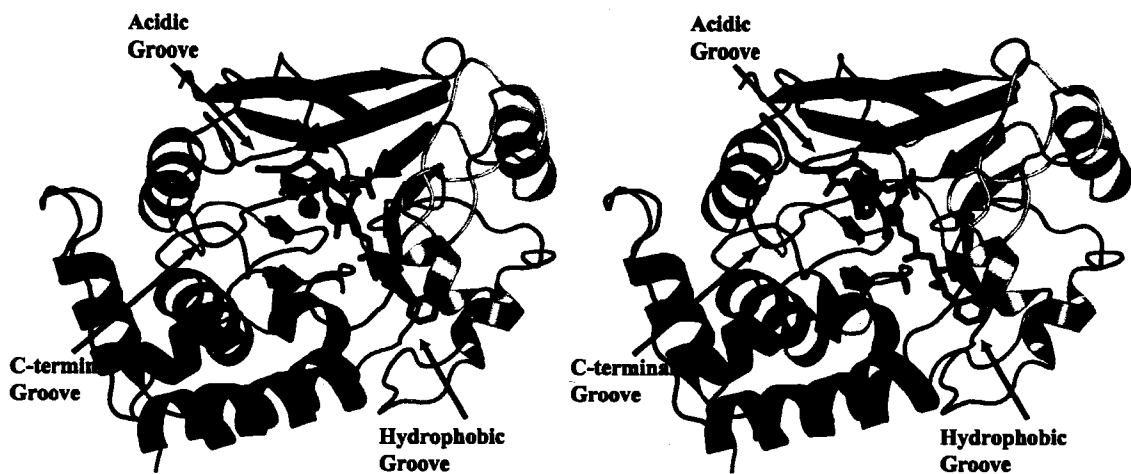


Figure 3.5 Stereo view of the overall structure of the PP-1:MOT complex. MOT is shown as sticks with colouring by atom: carbon is grey, oxygen is red, and nitrogen is blue. The enzyme is displayed as a cartoon representation of its secondary structure and coloured blue to red from N- to C-terminus. The three surface grooves of the protein are labeled. Two active site manganese metals are shown as orange spheres.

comparison to the PP-1:OA interactions in that there are a greater number of hydrogen-bonds and that they involve all geographic locations of the active site. The PP-1:OA hydrogen-bonding interactions are all clustered in a small area. These additional hydrogen bonds could be expected to contribute 8-12 kcal of binding energy.¹⁰⁶ Since there are no equilibrium values available for MOT binding, only inhibitory constants (IC_{50}), it is not possible to correlate the expected benefit of the additional hydrogen bonds with the actual change in binding values.

Inhibitor binding in the PP-1:OA complex appears to rely on three energetic sources: a small number of hydrogen bonds in the active site area, the hydrophobic binding energy associated with the interaction of the hydrophobic tail of OA with the hydrophobic groove of PP-1 and entropic energy contributions since the enzyme-unbound and enzyme-bound structures of OA are structurally similar (RMSD of 0.7 Å over all 57 atoms of the inhibitor) (Fig. 2.5). In comparing the enzyme-bound and the minimized-average solution NMR structure of MOT, this similarity does not exist (RMSD of 1.7 Å over all 55 atoms of the inhibitor) (Fig. 3.7). There is considerable movement and rearrangement of both the ring and hydrophobic tail regions of MOT. Comparing the enzyme-bound structure of MOT to another NMR solution structure of a nodularin, nodularin-R, reveals comparable flexibility in the ring and tail region. The numerous hydrogen bonding opportunities between MOT and PP-1 may allow for maintenance of the inhibitory potential of MOT in the face of this unfavorable entropic situation. A similar number of hydrogen bonds are present between PP-1 and MCLR and the difference between the enzyme-bound and

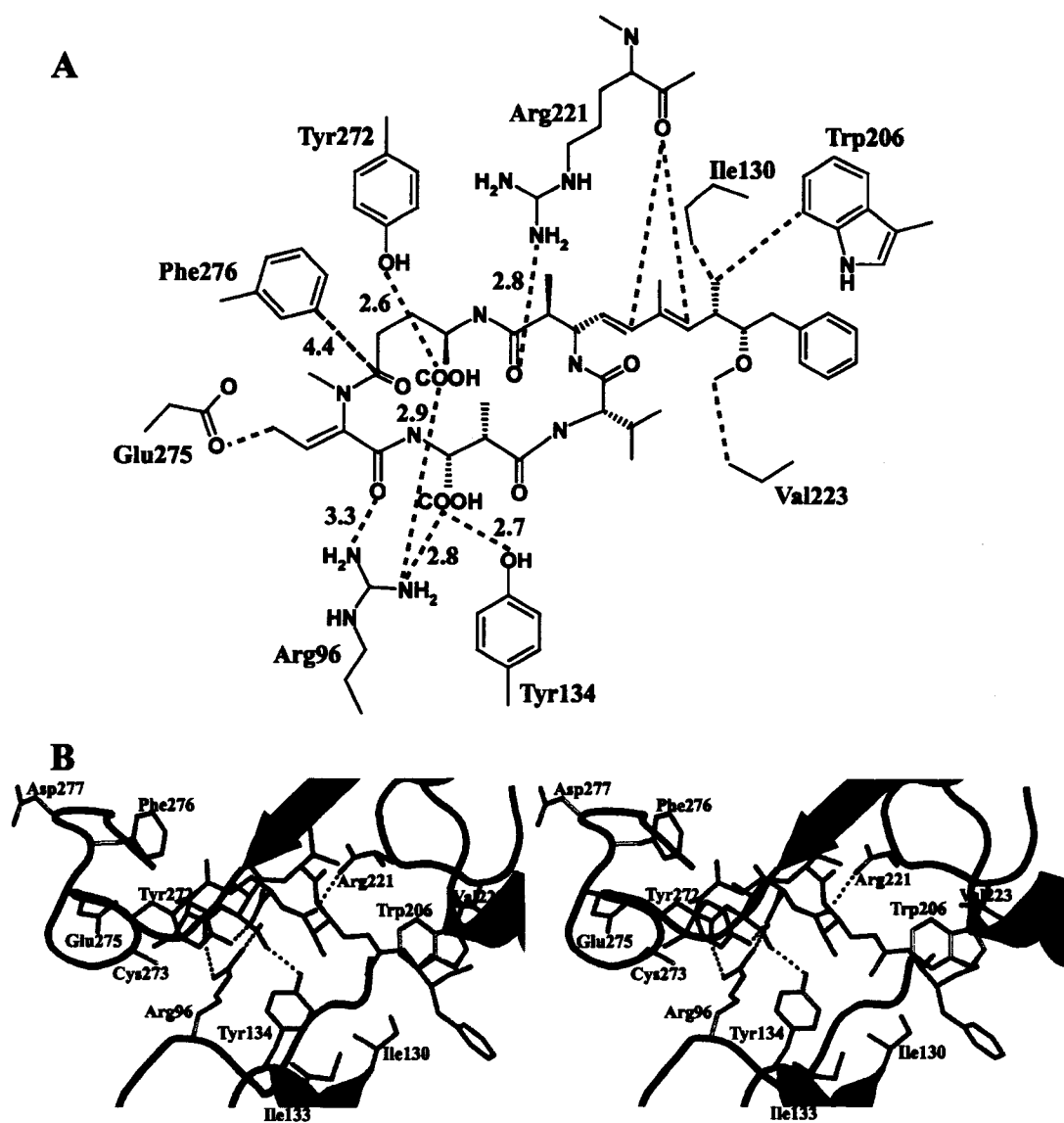


Figure 3.6 Active site contacts observed in the PP-1:MOT X-ray crystal structure. (A) Active site contacts within 4.0 Å of the MOT toxin. The closest interaction for each residue is shown with a dotted line. If a potential hydrogen bond exists, the distance is given. The closest interaction for Phe276 is shown for reference (B) Active site architecture in the PP-1:MOT X-ray crystal complex. MOT is shown as sticks with orange carbons, enzyme residues are shown as sticks with grey carbons. The protein backbone is shown with a ribbon representation. Hydrogen bonding interactions are shown in dotted lines.

the minimized-average solution NMR structure is also quite high at 1.8 Å (over the 73 atoms of MCLR).

C.2 Interactions between MOT and the β 12- β 13 loop

As mentioned above, there is a single hydrogen bond that exists between MOT and the β 12- β 13 loop, involving the phenolic hydroxyl of Tyr272 and the carboxyl group of the Gga residue. There are minimal other interactions between the β 12- β 13 loop and the inhibitor. The *N*-methyldehydrobutyrine residue of MOT does not form a covalent adduct with Cys273, despite possessing a double bond capable of a Michael addition reaction (like the Nmda residue of MCLR in the PP-1:MCLR complex). The distal carbon of the double bond in the Mdb residue is 4.7 Å from the sulphur of Cys273. This lack of proximity to the sulphur nucleophile may disrupt the Burgi-Dunitz angle of approach necessary to obtain a Michael addition covalent reaction.¹⁰⁷ Presumably, the Mdb residue could come close enough to Cys273 for a covalent reaction to occur in the dynamic on/off active site binding that competitive inhibitors exhibit. The other microcystins, including MCLR, most likely covalently react in this manner. While the lack of covalent modification affects the final complex of PP-1 and MOT, it is unlikely to affect MOT's inhibition of the cognate enzyme since the covalent reaction between PP-1 and MLCR was observed to differ temporally from initial enzyme inhibition.⁶²

C.3 Structure of MCLA-2H bound to PP-1

Dihydromicrocystin-LA binds to PP-1 in a very similar manner to its congener MCLR, with the notable exception that it does not form a covalent linkage with Cys273 of the β 12- β 13 loop of the phosphatase (Fig. 3.8). The loop adopts a

significantly different position in the PP-1:MCLA-2H complex when compared to the PP-1:MCLR complex. The distance between the two potential reactants of the Michael addition reaction, Cys273 and the hydrogenated Nmda residue, is 8.2 Å. The other interactions in the active site regions are very similar to that of MOT and MCLR, including hydrogen-bonding interactions with Tyr134, Arg221 and Tyr272. Of notable exception is that MCLA-2H does not interact with Arg96, where in MOT there are interactions between Arg96 and both the Nmda and the Gga residue and in MCLR there are interactions between Arg96 and the Nmda residue. The hydrogen bonding between Arg96 and MCLR may be serendipitous with movement of the β 12- β 13 loop (by slightly reorienting MCLR in the active site) and may not occur without the covalent reaction. There does not appear to be any intrinsic difference between MCLR and MCLA-2H that would cause this difference, the Nmda residue lies 4.0 Å from the Arg96 residue and could form a hydrogen bond with some realignment. The backbone atoms of Arg96 are in identical positions in the PP-1:MCLR, PP-1:MCLA-2H and PP-1:OA structures.

C.4 Toxin interactions with the β 12- β 13 loop region

Both MCLA-2H and MOT interact with the β 12- β 13 loop in a similar manner, hydrogen bonding to the Tyr272 group. Abolition of the hydrogen bonding ability but maintenance of the hydrophobicity of Tyr272 by mutation to a phenylalanine or a tryptophan residue had no effect for either inhibitor, suggesting that hydrogen bonding to the β 12- β 13 loop may not be as important for either inhibitor compared to OA (whose IC_{50} was increased about 50 fold by these mutations). This does not preclude the importance of the carboxylates in the inhibitors which interact with

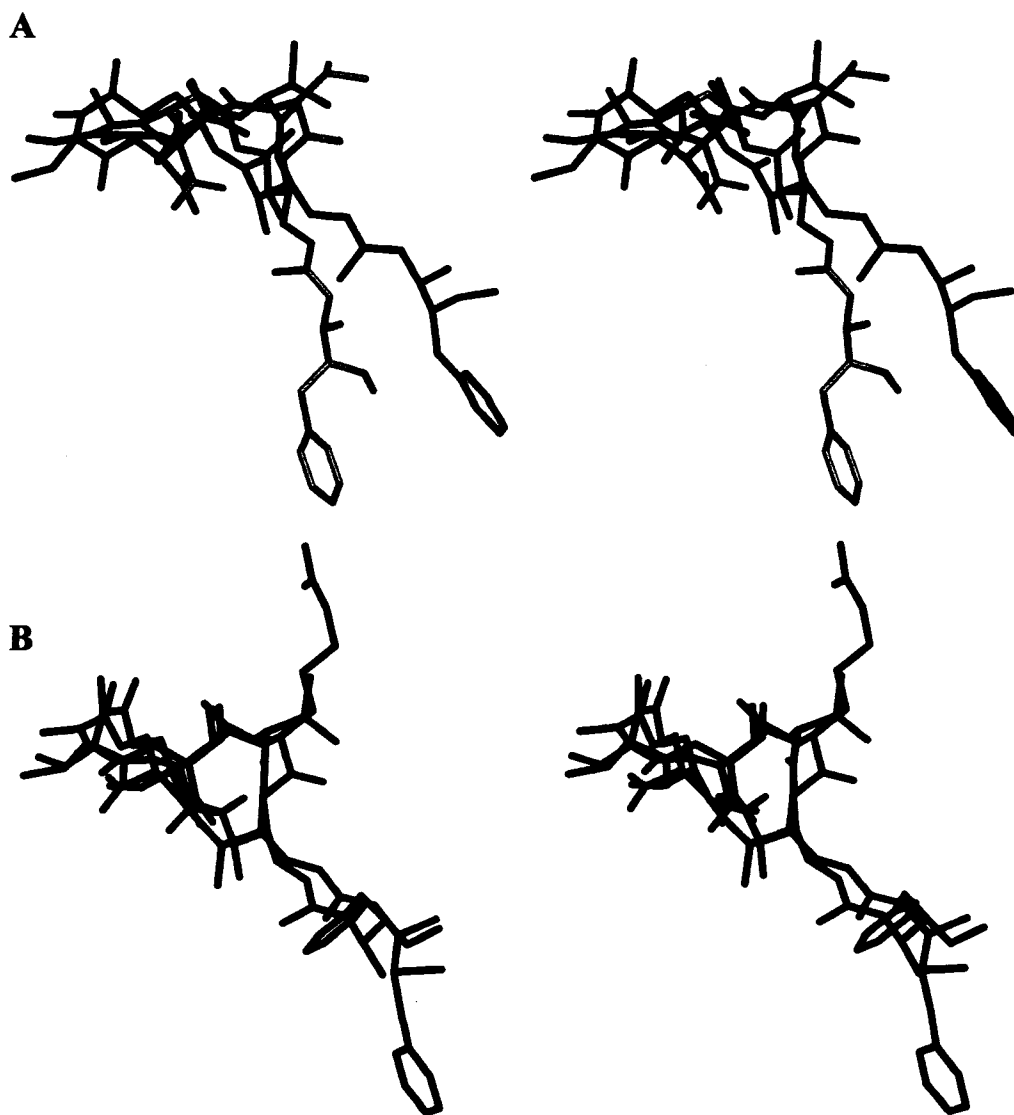


Figure 3.7 Superposition of determined nodularin structures. (A) Alignment of the X-ray crystal structure of MOT bound to PP-1 (green) and minimized-average NMR solution structure (orange).⁵⁰ (B) Alignment of the X-ray crystal structure of MOT bound to PP-1 (green) and minimized-average solution structure of nodularin-R (pink).⁵¹ Orientation of the MOT structures is the same as in Fig. 3.6. Alignment was performed using the program LSQMAN with best global alignment for all atoms.⁹¹ This resulted in the lowest RMSD value compared to aligning only the ring atoms or only the hydrophobic tail atoms.

Tyr272 since they also bind the active site metal ions indirectly via bridging water molecules. Despite this equivalent interaction, previous kinetic data showed that Tyr272 could interact with MOT and the microcystins in different capacities⁴⁶. Replacement of Tyr272 with alanine, serine/threonine, cysteine, glutamate or lysine typically increased the IC₅₀ value of MCLR by 10 to 50 fold, whereas the same mutations for nodularin-R increased the IC₅₀ values by 150 to 250 fold. The tyrosine in the loop region occupies a prominent position, near the catalytic metals (although not implicated in the catalytic mechanism), and at the base of the hinge of the β 12- β 13 loop region. In the previously determined X-ray crystal structure of the PP-1:tungstate complex, Tyr272 does not have a hydrogen bonding partner other than an active site water molecule. The residue may be important for the biological function of the enzyme (since this residue is conserved in all PPP family members) and its role is presumably for the creation of the hydrophobic face of the β 12- β 13 loop and to maintain the loop's position (kinetic analysis has not supported a role for this residue in binding biological substrates). The microcystins have a large covalently closed ring region that lies in the active site and possess a significant number of van der Waals interactions with the loop. Motuporin does not have the capability to have multiple interactions with the loop since its macrocyclic ring region is significantly smaller and does not lie in proximity to the rest of the β 12- β 13 loop. Since MOT has only one interaction with the β 12- β 13 loop, mutations of Tyr272 may affect its binding to a greater degree than that of the microcystins.

C.5 Comparison of toxin-bound PP-1 structures

The overall enzyme structures in both the PP-1:MOT and PP-1:MCLA-2H

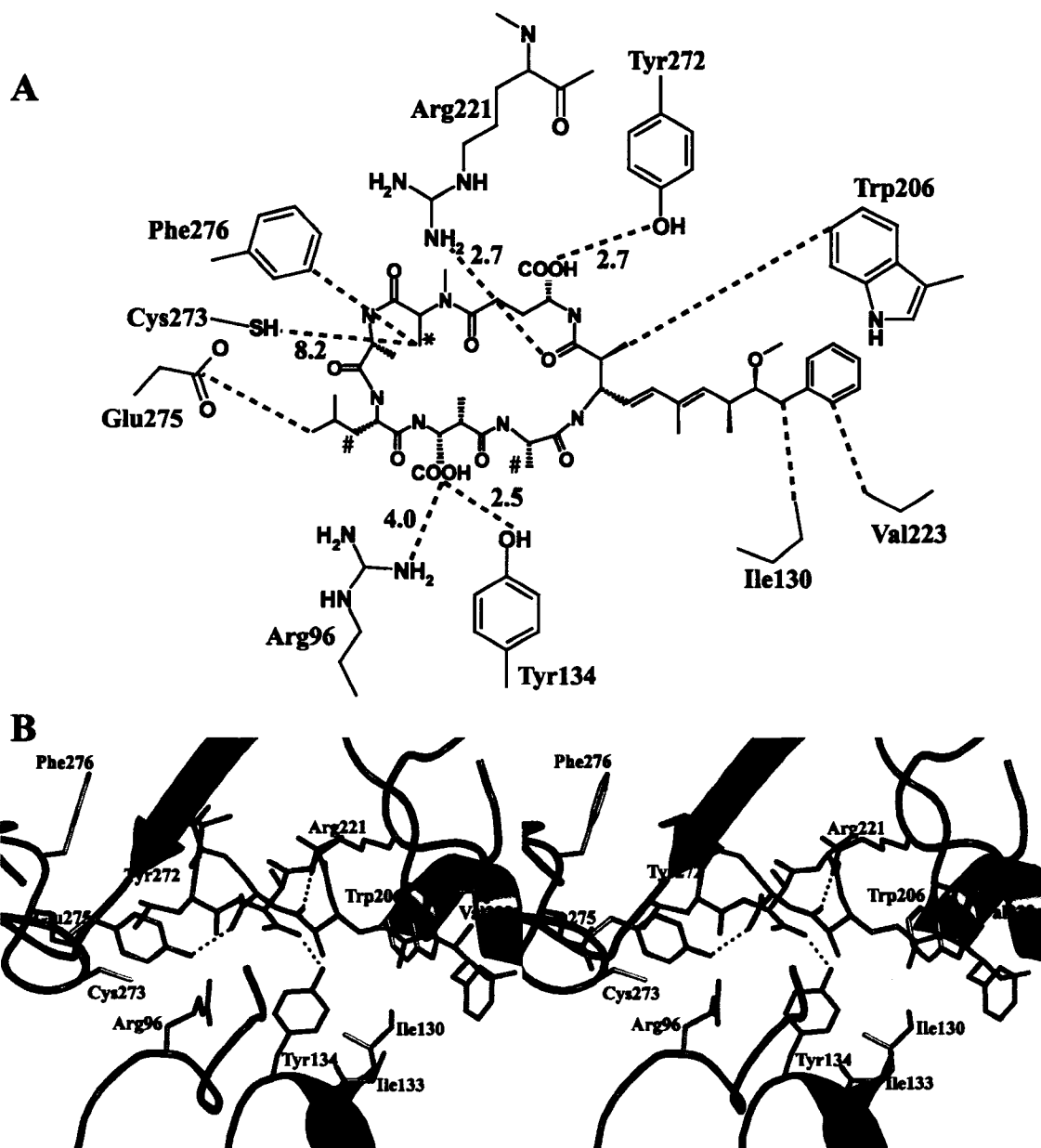


Figure 3.8 Active site contacts present in the X-ray crystal structure of the PP-1:MCLA-2H complex. (A) Contacts present in the active site of the complex, all interactions within 4 Å are shown by a dotted line. The distances are shown for potential hydrogen bonds. (B) Active site architecture in the PP-1:MCLA-2H X-ray crystal complex. The inhibitor is shown as a stick model with orange carbon atoms and protein side chains are shown as stick models with grey carbon atoms. The protein backbone is shown as a ribbon trace. Hydrogen bonds are shown with dotted lines.

complexes are very similar to previous PP-1:toxin complexes (Table 2.3) (Fig. 3.9), including the PP-1:OA and PP-1:MCLR complexes (C_{α} RMSD between any two enzymes in these complexes is ≤ 0.5 Å). While globally very similar, the complexes do differ in the toxin-sensitive $\beta 12$ - $\beta 13$ loop region (Fig. 3.10). As mentioned previously, the PP-1:OA and PP-1:MCLR structures had significant differences in this loop region. Both the PP-1:MOT and PP-1:MCLA-2H have $\beta 12$ - $\beta 13$ loop regions that adopt conformations similar to the conformation in the PP-1:OA complex. The C_{α} RMSD value over residues 270 to 276 of the loop region is 0.1 Å when comparing the PP-1:MOT and PP-1:MCLA-2H complexes. This is in contrast to a C_{α} RMSD of 2.0 Å when comparing the same area of the PP-1:MCLR complex structure to either of the PP-1:MOT or PP-1:MCLA-2H structures.

Because MCLA-2H and MCLR are structurally very similar (except that MCLA-2H does not have the capacity to form a covalent bond with Cys273, the two variable residues in the microcystin do not form any contacts with the protein), the loop rearrangement in the PP-1:MCLR complex can then be attributed exclusively to the covalent enzyme modification by the *N*-methyldehydroalanine residue of the toxin. Previous site-directed mutagenesis data showed that the initial, non-covalent interactions between Cys273 and the microcystins contribute to the initial and rapid enzyme inhibition, before the much slower covalent modification step.^{100,108} Covalent modification of PP-1 is not observed with the microcystins when the enzyme is denatured, indicating that initial inhibition, enzyme:inhibitor interactions and an intact active site are required for the later covalent modification to take place.¹⁰⁹ It was also observed that the Nmda residue of the microcystins was not



Figure 3.9 Comparison of the PP-1:MOT (green), PP-1:MCLA-2H (blue) and PP-1:MCLR (orange) X-ray crystal structures. Motuporin is shown as a stick model and the $\beta 12$ - $\beta 13$ loop is labeled. Alignment was done using the program LSQMAN⁹¹ using the best global fit for all protein C_{α} atoms.

required for initial enzyme inhibition. Microcystins immobilized to Sepharose beads via an aminoethanethiol adduct (abolishing the Nmda double bond) retain PP-1 inhibitory activity.¹¹⁰ Similar removal of the Nmda double bond of MCLR by converting the inhibitor to a microcystin-glutathione conjugate increased the lethal dose in animal models but did not abolish toxicity ($LD_{50}=630 \mu\text{g}/\text{kg}$ for conjugated versus $38 \mu\text{g}/\text{kg}$ for unconjugated).¹¹¹

The covalent reaction does not occur with MOT, despite the fact that the nodularin contains an *N*-methyldehydrobutyrine residue having the capacity to similarly bond with Cys273. This residue does not react with Cys273 for the reason mentioned above, namely that the distance of the double bond in the inhibitor from the sulphur nucleophile of Cys273 probably disrupts the Burgi-Dunitz angle of approach for the Michael addition reaction.¹⁰⁷ This suggests that non-covalent complexes of phosphatases and natural product toxins have the potential to be toxic, the nodularins having a similar toxicity as the microcystins.^{98,112} This is supported by the recent characterization of a dehydrobutyrine containing microcystin variant from *Nostoc sp.*, which does not covalently interact with PP-2A but is as potent and as toxic as MCLR ($LD_{50} = 100 \mu\text{g}/\text{kg}$).¹¹³

Even though MCLA-2H does not bond covalently to Cys273, the residue appears to be important for enzyme inhibition. Previous kinetic analysis illustrated that mutation of the cysteine to either a Leu or a Ser increased the IC_{50} by 10 to 20 fold for the microcystins.¹⁰⁰ Another study showed that, when changing all the residues of the $\beta 12$ - $\beta 13$ loop to the equivalent residues of the L7 loop of CAN, the mutation Cys273Leu had the greatest effect of all changes in the loop.¹¹⁴ An X-ray

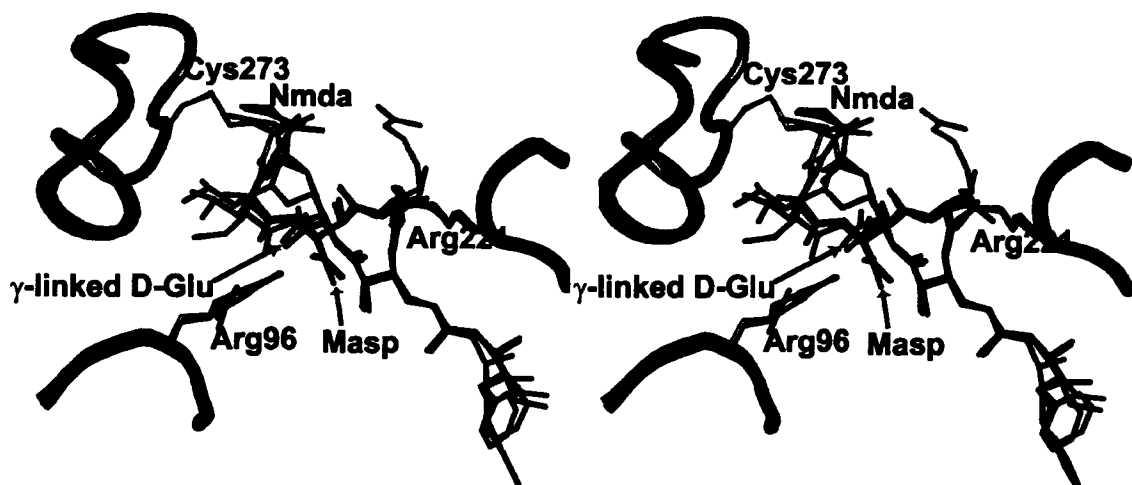


Figure 3.10 Comparison of the active sites of the PP-1:MOT (green), PP-1:MCLA-2H (blue) and PP-1:MCLR (orange) X-ray crystal structures. All three inhibitors are shown in the active site as sticks and colored the same as their respective protein structure. The covalent bond between Nmda in MCLR and Cys273 is shown and the Masp, Nmda and Gga residues are identified.

crystal structure showed that this mutation does not change the overall conformation of the loop. The interactions that make Cys273 a vital residue in initial enzyme inhibition (separate from the covalent modification) are not immediately apparent from the PP-1:MCLA-2H crystal structure. Since Cys273 does not appear to play a vital role in binding to the inhibitor once it occupies the active site, perhaps the cysteine is more important in the dynamic situation that occurs as the inhibitor binds to and releases from the enzyme.

D. Conclusions

The two structures that have been determined here represent the fourth and fifth novel PP-1:toxin structures available. Each of these structures is in some way unique and contributes independent information to the hypothesis that toxin and substrate binding can occur by a multitude of modes. Hydrophobic tail binding is less important for MOT than for OA, shown by the higher average thermal coefficients, poorer electron density for the tail region, smaller solvent excluded area and the reduced number of potential hydrophobic groove interactions. Motuporin has considerably more hydrogen-bonding interactions with the protein (five hydrogen-bonds compared to three for OA), specifically involving the two acidic moieties of the inhibitor. Comparing the enzyme-bound and -unbound structures of MOT and OA further illustrates the differences in energetic contributions, namely the increased reliance of OA on entropic energy for binding to and inhibiting the PPP family. The reliance of OA on hydrophobic binding and entropy may be an evolutionary adaptation to possessing only one acidic group in its macrocyclic ring region. The larger number of hydrogen-bonding interactions may allow MOT to rely less on entropic binding energy and may explain the higher inhibitory potency of MOT versus OA ($IC_{50} = 0.6$ nM for the former and $IC_{50} = 20$ nM for the latter).

In concert with previous kinetic data, the PP-1:MCLA-2H X-ray crystal structure shows that initial interactions occur between the microcystins and the β 12- β 13 loop with the loop in the same position as other PP-1:toxin complexes. This is consistent with the earlier assumption that stoichiometric formation of a covalent complex follows adventitiously after prolonged incubation of enzyme and toxin (the

reason that the reaction is delayed in solution has not been elucidated).^{62,115} The presence of persistent cellular PP-1:MCLR covalent complexes was noted in microcystin-poisoned salmon afflicted by netpen liver disease¹¹⁶, in salt water mussels¹¹⁷ and in microcystin-poisoned trout.¹¹⁸ This illustrates that, although these covalent complexes are not needed for initial enzyme inhibition, they may have a function in the biological role and relevance of the microcystins. This is especially true in regards to the bioavailability of the toxin and its effect in temporally distinct signaling pathways involving the PPP family of phosphatases.^{116,118} Whether the covalent bonding occurs with the inhibitor bound (which would require significant β 12- β 13 loop movement to fold into a proper distance and orientation for reaction) or whether the reaction occurs as the inhibitor cyclically binds and then releases the enzyme is not known. If the latter were true, the binding energy of the inhibitor may compensate for the energy required for the significant loop rearrangement observed in the PP-1:MCLR complex

Chapter 4

Elucidating the role of the β 12- β 13 loop of the PPP family of protein phosphatases in the selectivity of natural product toxin binding

A. Introduction

The PPP family of protein phosphatases share 40% sequence identity and include, among others, the catalytic subunits of PP-1, PP-2A and PP-2B (calcineurin). Structural data are available for both PP-1 and CAN; superimposition of these structures reveals a striking similarity in their catalytic domains, especially in the active site regions (Table. 2.3).^{35,37-41,89} Despite these similarities in both primary and tertiary structure, PP-1 and CAN exhibit distinct differences in their natural product and endogenous inhibitor and substrate specificities. PP-1 is exquisitely sensitive to the endogenous protein inhibitors inhibitor-1 and inhibitor-2, as well as to the exogenous natural product toxins okadaic acid and the microcystin class of inhibitors. Calcineurin is markedly less sensitive to these inhibitors, over 1000-fold for the microcystin class, over 250-fold for OA and is resistant to the endogenous inhibitors-1 and -2.^{80,92,119,120}

In the active site region, most of the primary sequence dissimilarity between PP-1 and CAN is in the β 12- β 13 loop (called the L7 loop in CAN). This area lies adjacent to the active site and has not been implicated in substrate binding or in the enzyme's catalytic mechanism but has been thought to affect inhibitor sensitivity.^{21,121,122} The sequence in the β 12- β 13 loop varies over a five residue stretch including residues 273 to 277 in PP-1, residues 266 to 270 in PP-2A and residues 312 to 316 in CAN (Fig 4.1). The first indication of the importance of this

				274	277
PP-1	254	GYEFFAKRQ-----LVTL	FSAPNYCGEFDN	AGAMMSVDE	
PP-2A	247	GYNWCHDRN-----VVTI	FSAPNYCYRCGN	QAAIMELDD	
CAN (PP-2B)	287	GYRMYRKSQTTGFPSLITI	FSAPNYLDVYNNK	KA AVLKYEN	
				313	316

Figure 4.1 Partial sequence alignment of PP-1, PP-2A and PP-2B (CAN). The β 12- β 13 (L7) loop is outlined with a rectangle, showing the non-conserved regions. The numbering at the top is for PP-1 and the numbering on the bottom is for CAN.

region of the protein in inhibitor specificity was the discovery of an OA-resistant form of PP-2A in Chinese hamster ovary cells that possessed a mutation at Cys269 (corresponding to Phe276 in PP-1 and Tyr315 in CAN).¹²³ The importance of the β 12- β 13/L7 loop region is emphasized by the 10 000-fold inhibitory differences of OA among the PPP family of phosphatases ($IC_{50} = 0.2$ nM for PP-2A, $IC_{50} = 20$ -50 nM for PP-1 and $IC_{50} = 5$ μ M for CAN). Mutagenesis experiments confirmed that differences in the primary structure of the loop region were at least partially responsible for these observations (Table 4.1).^{46,60,61,121,124} These experiments showed the importance of Tyr272 in inhibitor binding, both in its hydrogen-bonding capacity (mutation to Phe or Trp decreases the inhibitor binding) and its hydrophobic bulk (mutation to Ser/Thr/Cys, all with hydrogen bonding capacity but minimal hydrophobic bulk, significantly increase the IC_{50} of the enzyme). The other residue with inhibitor binding consequences was Phe276, where mutation can either decrease (nodularin or MCLR) or increase (OA) inhibitor binding (this is discussed in detail in Chapter 2).

Previous structural studies have also shed light on the nature and importance of the β 12- β 13 loop in PP-1 in the context of inhibitor binding. The distance from the active site metal to the terminal hydroxyl group of Tyr272 was analyzed in four different crystals of the same PP-1:tungstate complex. This distance varied from 3.0 Å to 4.3 Å, suggesting a significant amount of flexibility in the loop region.³⁵ A larger degree of flexibility is noted when comparing the PP-1:MCLR X-ray crystal structure to the structures of complexes of PP-1 with OA, calyculin and tungstate. Although this loop movement is most likely due to a covalent reaction between the

Table 4.1 Effect of mutagenesis in the β 12- β 13 loop region on the inhibition of PP-1 by natural product toxins^{46,47}

<i>Residue</i>	<i>Mutation</i>	<i>Toxin</i>	<i>Change in IC50</i>
Tyr272	Phe	OA	↑ 50-fold
		Nodularin	N/C*
		MCLR	↑ 10-fold
Tyr272	Trp	OA	N/C*
		Nodularin	N/C*
		MCLR	↑ 15-fold
Tyr272	Ala	OA	↑ 200-fold
		Nodularin	↑ 200-fold
		MCLR	↑ 20-fold
Tyr272	Ser	OA	↑ 250-fold
		Nodularin	↑ 200-fold
		MCLR	↑ 75-fold
Tyr272	Thr	OA	↑ 200-fold
		Nodularin	↑ 175-fold
		MCLR	↑ 20-fold
Tyr272	Cys	OA	↑ 200-fold
		Nodularin	↑ 200-fold
		MCLR	↑ 10-fold
Tyr272	Glu	OA	↑ 150-fold
		Nodularin	↑ 200-fold
		MCLR	↑ 20-fold
Tyr272	Lys	OA	↑ 150-fold
		Nodularin	↑ 100-fold
		MCLR	↑ 50-fold
Cys273	Ala	OA/nodularin/MCLR	N/C*
Gly274	Tyr	OA/nodularin/MCLR	N/C*
Glu275	Arg	OA/nodularin/MCLR	N/C*
Phe276	Cys	OA	↓ 40-fold
		Nodularin	↑ 5-fold
		MCLR	N/C*
*No change observed			

inhibitor and the enzyme in the MCLR complex, it still reveals an intrinsic plasticity since the inhibitor remains in the enzyme's active site despite the covalent tethering.¹⁰⁵

Prior to the determination of the X-ray crystal structure of the PP-1:OA complex, it was hypothesized that different conformations and movement of the L7 loop of CAN and the corresponding β 12- β 13 loop of PP-1 were the rationale for resistance of CAN to natural product toxins.^{62,125} However, superposition of the four available CAN structures (PDB ID's 1AUI, 1TCO, 1M63 and 1MF8) and four available PP-1:toxin structures (PDB ID's 2BCD, 2BDX, 1JK7 and 1IT6, the PP-1:MCLR complex was excluded

because loop movement is caused by a covalent reaction) revealed that the L7 loop of CAN and the β 12- β 13 loop of PP-1 superimpose. This is consistent with the conclusion that inhibitor specificity is more a function of the primary sequences than structural changes¹¹⁵ and solidifies the assumption that β 12- β 13 loop movement in the PP-1:MCLR complex is not typical and is secondary to the covalent reaction that occurs. To test this hypothesis and in an attempt to rationalize the varying natural product inhibitor binding to the PPP family of phosphatases, a chimeric mutant of PP-1 and CAN was created in which the β 12- β 13 loop residues 273-CGEFD-277 were replaced by the CAN L7 loop residues 312-LDVYN-316 (therein referred to as chimeric PP-1). In addition, individual point mutants were created where each residue of the L7 CAN loop was placed into the equivalent position of PP-1. The kinetic profile for each mutant was determined with OA, MCLR and inhibitor-2. The X-ray crystal structure of the chimeric mutant with OA bound was also

determined to help rationalize the kinetic results and for comparison to the previous PP-1:OA structure.

B. Experimental Procedures

B.1 Expression, purification and kinetic analysis of recombinant PP-1

Mutants of PP-1c were expressed and purified to homogeneity as previously described.^{48,125}

³²P-labeled phosphorylase a was used as a phosphatase substrate to determine dose response curves with microcystin-LR, okadaic acid, and inhibitor-2. Purified PP-1 stocks were diluted in phosphatase assay buffer (50 mM Tris-HCl, pH 7.0, 0.1 mM EDTA, 1mg/mL BSA, 0.8 mM MnCl₂, and 0.2% β-mercaptoethanol).

Phosphatase was diluted until a 10 μL aliquot of diluted enzyme solution caused 15% ³²P release in a 30 μL assay.^{48,125} Duplicate assays were performed for each toxin and inhibitor protein. Typically, less than 5% variation was seen between duplicates. Microcystin-LR was obtained from Health Canada, okadaic acid from Moana Bioproducts, and recombinant inhibitor-2 was purified from *E. coli*. The loop mutant protein phosphatase-1 exhibited normal activity towards phosphorylase a as a substrate.

B.2 Crystallization of chimeric PP-1:OA complex

Crystals were obtained by the hanging drop vapour diffusion method at room temperature. The enzyme and okadaic acid were mixed in a 1:2 molar ratio with the concentration of protein being approximately 0.4 mM. The PP-1:OA complex was then mixed with an equivalent volume of reservoir solution, which consisted of 2 M lithium sulfate, 100 mM Tris (pH = 8.0), 2% polyethyleneglycol 400 and 10 mM β-mercaptoethanol. The complex crystallized in the space group P4₂2₁2 with cell dimensions a = b = 98.8 Å, c = 62.2 Å, with one complex per asymmetric unit. This

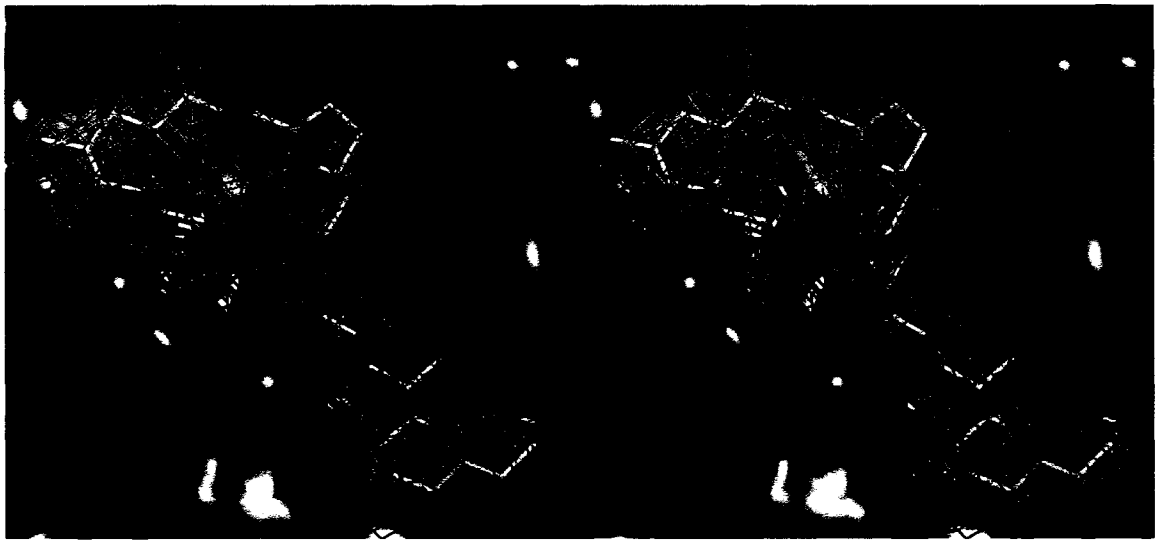


Figure 4.2 Representative electron density from the PP-1-CAN chimeric mutant:OA complex solved to 2.0 Å. The electron density map shown is a σ_A -weighted omit map contoured at 1σ , where the OA molecule was omitted during map generation.

corresponds to a Matthew's coefficient of 2.4 and a solvent content of the crystals of 48%.

B.3 Data collection, structure determination and refinement

A data set to 2.0 Å was collected at 100 K with X-rays (CuK α) generated by a Rigaku RU-H3R rotating anode generator with a Rigaku R-Axis IV++ image plate detector. The data were processed with the HKL suite of programs.⁸² This initial structure was solved by molecular replacement with the program AMoRe⁸³, using the PP-1:OA structure (with OA removed) as the search model (PDB ID 1JK7). Electron density for both the protein and the inhibitor were clear from the initial map generated from the molecular replacement solution (Fig. 4.2). A molecular model of OA was fitted to the difference density using the structure of OA bound to wild-type PP-1 as the starting model. The protein-inhibitor model was subjected to rigid-body refinement in CNS prior to manually fitting the model using the program XtalView^{85,86}. The model was then subjected to iterative rounds of macromolecular refinement using CNS with a maximum likelihood target. The crystallographic and refinement data are listed in Table 4.1. The final model consisted of density for residues 6 through 298 and was checked for validity using WHATCHECK and PROCHECK^{87,88}. PROCHECK showed that 97% of residues were in allowed Ramachandran plot ranges with an overall G factor of 0.2.

B.4 Coordinates

The atomic coordinates and structure factors have been deposited in the PDB with identifier 1U32.

B.5 Publication

This work was first published in the *Journal of Biological Chemistry* in 2004.¹¹⁴

B.6 Contributions to this work

Of the work presented in this chapter, the author partially completed protein preparation and crystallization, fully completed protein crystal harvesting, freezing and screening, data collection, integration and scaling, structure solution, refinement and validation. The author also completed data deposition in the Protein Data Bank and authored the primary citation for this work. Other contributions include protein purification by H.A. Luu (Lab of C.F.B. Holmes), protein mutagenesis and enzyme kinetics by K.R. Perreault (Lab of C.F.B. Holmes) and crystal growth and refinement by Dr. M. Cherney.

Table 4.2 Data collection and refinement statistics for the chimeric PP-1 mutant bound to OA

Data Collection	
Unit Cell	$a = b = 98.8 \text{ \AA}, c = 62.2 \text{ \AA},$ $\alpha = \beta = \gamma = 90^\circ$
Space Group	P4 ₂ 2 ₁ 2
Wavelength (Å)	1.5418
Resolution (Å) ¹	40-2.0 (2.07-2.00)
Total Number of Reflections	321 224
Number of Unique Reflections	21 304
Completeness (%) ¹	99.7 (99.0)
Redundancy ¹	5.83 (5.65)
$\langle I / \sigma(I) \rangle$ ¹	21.1 (5.02)
R _{sym} (%) ^{1,2}	7.6 (36.9)
Mosaicity (°)	0.47
Refinement	
Resolution (Å)	40-2.0
Atoms-protein	2372
Atoms-okadaic acid	57
Waters	89
R.m.s. deviations	
Bond length (Å)	0.006
Bond angles (°)	1.36
Average B-factors	
Protein atoms (Å ²)	27
Okadaic acid (Å ²)	30
Solvent (Å ²)	32
R _{cryst} (%) ³	21.8
R _{free} (%) ⁴	25.5

¹Data in parentheses correspond to highest resolution shell

² $R_{\text{sym}} = \sum_{\text{hkl}} \sum_i (|I_i(\text{hkl}) - \langle I(\text{hkl}) \rangle|) / \sum_{\text{hkl}} \sum_i I_i(\text{hkl})$, where I is the observed intensity, and $\langle I \rangle$ is the average intensity obtained from multiple observations of symmetry related reflections

³ $R_{\text{cryst}} = \sum ||F_o| - |F_c|| / \sum |F_o|$, where $|F_o|$ and $|F_c|$ are the observed and calculated structure factor amplitudes respectively

⁴R_{free} was calculated as for R_{cryst} with 5% of the data omitted from structural refinement

C. Results and Discussion

C.1 X-ray crystal structure of the PP-1-CAN chimera complex with OA

The complex of the PP-1-CAN chimera complex with OA reveals a protein structure that is very similar to other PP-1 structures (Figs. 4.3 and 4.4). Most notably is the similarity between this structure and the previous wild-type PP-1:OA complex (C_{α} RMSD 0.2 Å over 293 backbone carbon atoms).⁸⁹ The other PP-1 structures are also similar, with a C_{α} RMSD values of 0.5 Å when comparing to any of the complexes of PP-1:MCLR, PP-1:tungstate and PP-1:calyculin.

The inhibitor present in this newest complex was also very similar to the OA present in the earlier wild-type PP-1:OA complex (Fig. 4.4 and 4.5). The inhibitor adopts a macrocyclic-like structure via an intramolecular hydrogen bond between the C_1 -carboxylic acid group and the C_{24} -hydroxyl moiety. The inhibitor lies in a similar position on the surface of the enzyme, occupying the active site region primarily with the above mentioned macrocycle and extending into the adjacent hydrophobic groove. All the contacts with phosphatase residues that are present in the wtPP-1:OA complex are also present in the chimeric PP-1:OA complex. This involves the hydrophobic double ring spiroketal moiety of OA binding into the hydrophobic cleft of PP-1 created by residues Ile130, Ile133, Trp206 and Val223. Hydrogen-bonding interactions are present between Tyr272 and the C_1 -acid and C_2 -hydroxyl, Arg221 and the C_{24} -hydroxyl and Arg-96 and an ether oxygen in the backbone of the inhibitor (slightly different than the wtPP-1 complex where a different rotamer of Arg96 is present and it hydrogen-bonds to the C_2 -hydroxyl). The conclusion that

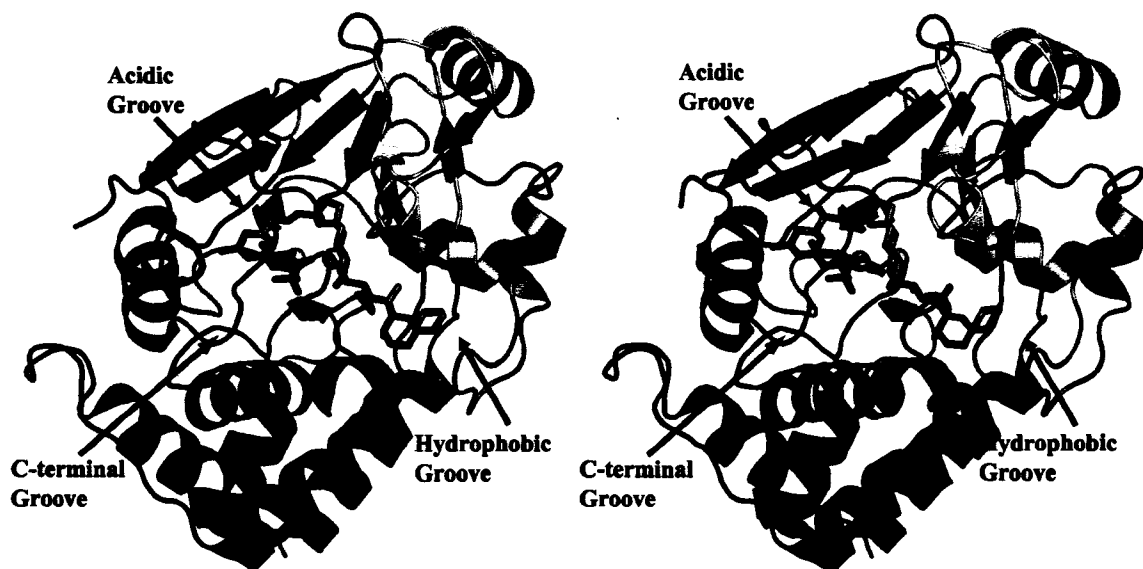


Figure 4.3 Ribbon representation of the X-ray crystal structure of the PP-1-CAN chimera:OA complex. OA is represented by sticks with colouring by atom: carbon is grey and oxygen is red. The enzyme is coloured blue to red from N- to C-terminus. The three surface grooves of the protein are labeled. Two active site manganese metals are shown as yellow spheres.

hydrophobic and entropic energy drives complex formation is supported by this structure since there are very few protein:inhibitor interactions (given the size of the inhibitor, similar to that seen in the wtPP-1:OA complex).⁸⁹

C.2 Interactions of OA with the chimeric β 12- β 13 loop region

The residue changes within the β 12- β 13 loop involve substitution of the amino acid sequence 273-CGEFD-277 from PP-1 with the sequence LDVYN from calcineurin. The orientation of the backbone atoms in the structures of both the wild-type and the loop mutant remains the same, meaning inhibitor specificity must rely on the differences in the amino acid sequences in this region. The residue substitutions do affect the overall charge of the loop region, from -2 in PP-1 to a neutral charge in the chimeric protein. This would not be expected to affect OA binding since the residues that alter the charge are on the face of the β 12- β 13 loop facing away from the active site and, if anything, the lower charge of the CAN loop region would be expected to be beneficial to OA binding, since OA is predominantly hydrophobic in the region contacting the loop. The two most prominent residues that have potential inhibitor interactions are Leu273 and Tyr276 (the equivalent residue to Tyr272 of PP-1 is also a tyrosine in CAN (Tyr311) and therefore the same in the wild-type and chimeric proteins). The leucine lies near a hydrophobic area of OA (C₁₀-methyl), potentially securing a hydrophobic section of the molecule. The equivalent wtPP-1 residue to Tyr276 of the chimeric protein is Phe276, which lies near the same hydrophobic section of OA, again potentially securing this area. The electron density for Phe-276 is very well defined in wild type PP-1; with an average side-chain thermal factor 24 Å² above the average thermal factor for the molecule

(Fig. 4.6). In the loop mutant, the electron density of the side chain of Tyr276 is very poorly defined with an average side chain thermal factor 31 \AA^2 above the average thermal factor for the rest of the molecule (in comparison all four structures of calcineurin have values for the equivalent residue (Tyr315) that are maximally 19 \AA^2 above the average thermal factor for the rest of the enzyme). The tyrosine side chain in this position would not have the potential for hydrophobic interactions that the phenylalanine in wild-type PP-1 possesses (the orientation of the side chain brings the hydroxyl group into proximity with OA, not the flat hydrophobic face, rotation of the side chain would move the hydroxyl but still not allow for hydrophobic interactions). The solvent-accessible surface area excluded by OA interacting with the $\beta 12$ - $\beta 13$ loop residues is 133 \AA^2 for the PP-1:OA complex but only 118 \AA^2 for the chimeric PP-1:OA complex, indicating a larger area of hydrophobic interaction. The conclusion that hydrophobic energy is a predominant force in OA inhibitor binding to the PPP family may involve binding of the hydrophobic tail (that many of the inhibitors contain) and also a hydrophobic binding closer to the active site involving residues in the loop region (residues 273 and 276, or equivalent).

C.3 Kinetic analysis of wild type PP-1 and chimeric PP-1

To investigate the role of the $\beta 12$ - $\beta 13$ /L7 loops in inhibitor selectivity we have examined the inhibitory effects of two natural product inhibitors (OA and MCLR) and one endogenous peptide inhibitor (inhibitor-2) on both the wtPP-1 and the chimeric protein containing the residues from the L7 loop of CAN (Table 4.2). The data for the wtPP-1 were consistent with previously published results.^{46,61} The

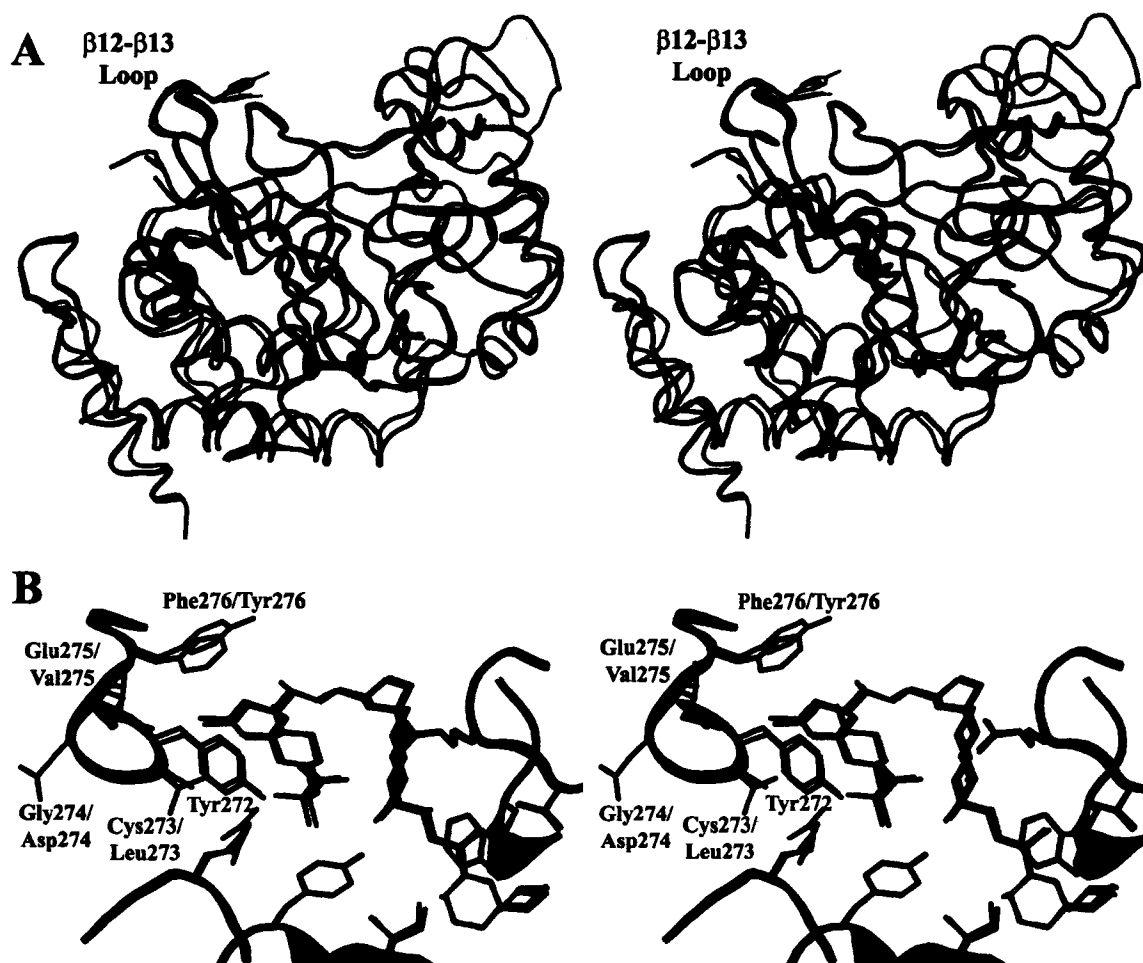


Figure 4.4 Alignment of the chimeric PP-1:OA complex with other PP-1 structures. (A) Alignment of the chimeric PP-1:OA (blue), wtPP-1:OA (red) and calcineurin (1AUI) (orange). The $\beta 12$ - $\beta 13$ /L7 loop is labeled and residue 276 is shown as sticks. (B) Active site alignment of the chimeric PP-1:OA complex (dark blue protein and labels, light blue OA) and the wtPP-1:OA complex (red protein and labels, orange OA).

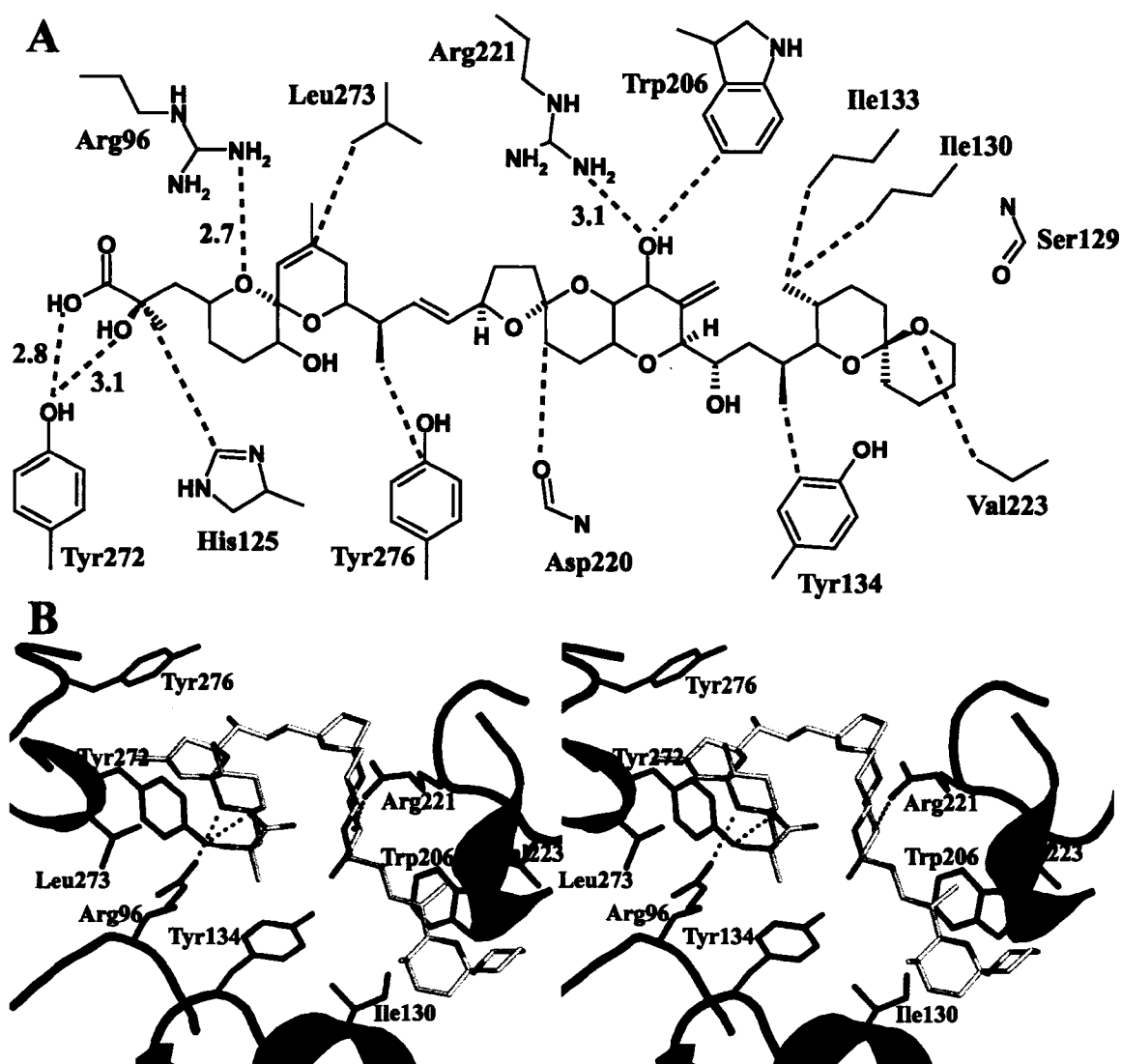


Figure 4.5 Active site contacts between PP-1 and OA as observed in the X-ray crystallographic complex. (A) Chemical representation of all PP-1 residues within 4.0 Å of the OA molecule. The closest interaction for each residue is shown as a dashed line and if this is a putative hydrogen bond, the distance is given. (B) Representation of the active site of the PP-1-CAN chimera:OA complex showing important residues as sticks and the remaining protein as a backbone trace including the secondary structure. OA is shown as sticks and all hydrogen-bonds are shown with dashed lines.

chimeric PP-1 was ~4-fold less sensitive to OA, ~6-fold less sensitive to MCLR and ~3-fold less sensitive to inhibitor-2. These results are consistent with the β 12- β 13/L7 loop being important in inhibitor function and recognition. Within this loop region, there are a few candidate residues that could confer inhibitor specificity. The residue with the greatest potential impact is Tyr272 that has intimate interactions with MCLR, calyculin, OA and was shown mutationally to be important (Table 4.1).^{37,42,46,89} Since no other residue is able to mimic Tyr in both hydrogen-bonding ability and size, any mutation of Tyr272 reduces the inhibitory capacity of all the natural product toxins (Table 4.1). However, this residue is conserved between the two proteins. To determine the contribution toward inhibitor specificity of the remaining residues, we systematically mutated each of the remaining β 12- β 13 residues to their counterpart in the L7 loop.

Using okadaic acid as the inhibitor, the PP-1 mutants Gly274Asp, Glu275Val, Phe276Thr and Asp277Asn all exhibited inhibitory profiles that were very similar to the wild-type PP-1 (Fig. 4.7). A single point mutant, Cys273Leu, showed a significant change in its inhibitor profile. This mutant showed a ~4-fold decrease in its sensitivity to OA, with an IC_{50} (120 nM) value very similar to the chimeric enzyme ($IC_{50} = 110$ nM). A similar result was observed with MCLR where the single Cys273Leu mutant had a reduced sensitivity to MCLR, almost identical to the chimeric enzyme ($IC_{50} > 0.6$ nM for both enzymes), but other mutations had no effect (Gly274Asp, Glu275Val, Phe276Thr and Asp277Asn mutants all had similar inhibitory profiles similar to the wild-type enzyme (Fig. 4.8)). When looking at inhibitor-2, a different pattern emerged (Fig. 4.9). In this

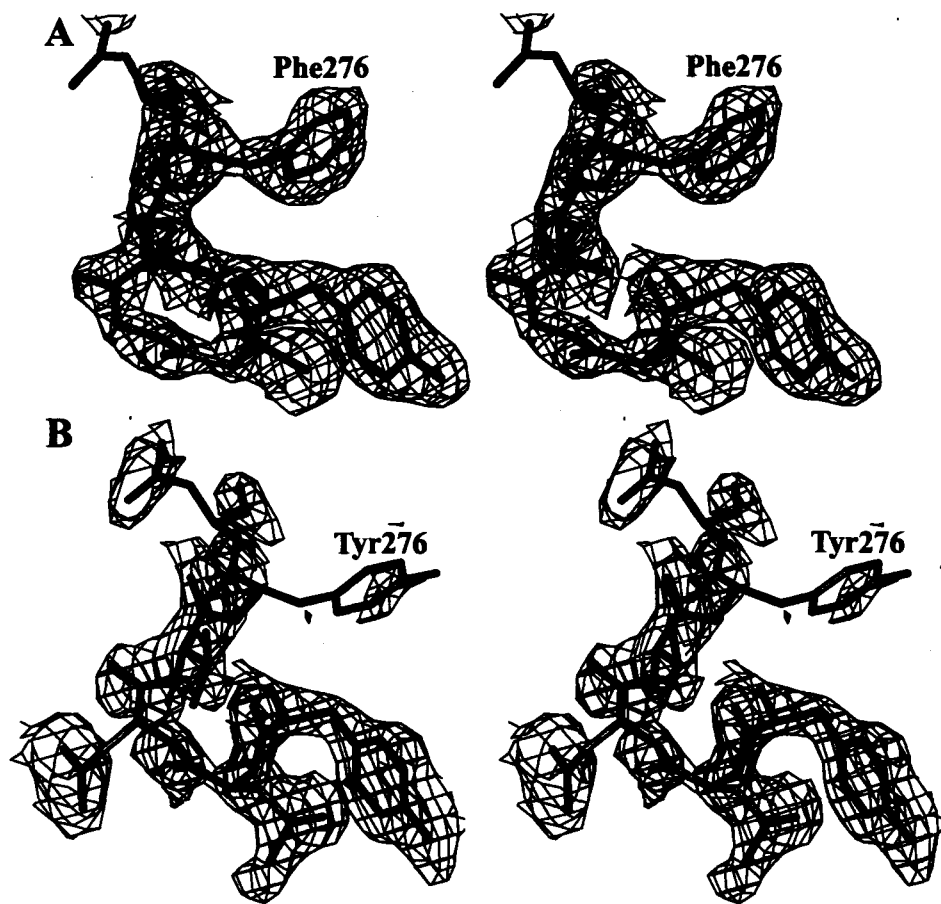


Figure 4.6 Electron density in the β 12- β 13 loop region for the two complexes of (A) wtPP-1 and (B) chimeric PP-1, both with OA bound. The density shown is a σ_A -weighted $2F_o-F_c$ map, contoured at 1σ .

Table 4.3 Kinetic values for inhibition of wtPP-1 and chimeric PP-1 by natural product and endogenous inhibitors				
	Specific Activity (U/mg)	IC ₅₀ (nM)		
		MCLR	OA	Inhibitor-2
wtPP-1	11	0.1 ± 0.01	32 ± 2	1.8 ± 0.5
chimeric PP-1	4	> 0.6	97 ± 5	5.4 ± 2.3

case, no single point mutant could produce a different inhibitory profile from the wtPP-1 enzyme. A change in the enzyme inhibition could only be produced by mutating the entire β 12- β 13 loop, as in the chimeric enzyme. These results suggest that the natural product inhibitors and the endogenous inhibitors may bind differently, the natural product inhibitors relying more on Cys273 for interaction and inhibitor-2 interacting with multiple residues in the loop region.

It was surprising to find that the point Phe276Tyr mutation did not affect the inhibitory profile of the resulting enzyme to a significant degree. The electron density for the Tyr276 residue in the chimeric protein was significantly worse than the corresponding Phe276 in the wtPP-1:OA complex, possibly indicating that the Tyr was an important residue in providing OA insensitivity to CAN (Fig. 4.6). The point mutant did not bear this out kinetically. This residue was shown previously to be important in the mechanism of OA inhibition (Table 4.1). Mutation of Phe276 to a Cys, as is present in PP-2A, increases the sensitivity of the resulting enzyme 40-fold to OA.⁶¹ Obvious interactions that a cysteine would offer over a tyrosine or phenylalanine are not apparent from the X-ray crystallographic structures available. The kinetic results may indicate that a smaller residue can affect binding by facilitating tighter hydrophobic or an increased number of van der Waals interactions. Perhaps the smaller size of the cysteine residue has fewer steric effects than either the phenylalanine or tyrosine residues that are present in PP-1 or CAN respectively.

For the natural product inhibitors, the most sensitive mutation in the series of systematic point mutations that was carried out was replacing Cys273 with a leucine

residue. This suggests that a point mutation, and not an overall change in the conformation of the loop, contributes to disrupting important interactions with the natural product inhibitors OA and MCLR. MacKintosh *et. al.*¹⁰⁰ first revealed the covalent inhibition that occurred between MCLR and Cys273 of PP-1 and that abolition of the covalent binding by mutation of Cys273 to Ala, Ser or Leu increased the IC₅₀ by 5- to 20- fold. This is consistent with the mutational data presented here. Previously, it was shown that this covalent reaction occurs slowly over several hours and only after the enzyme is fully inhibited.^{62,115} Taken together, these data show that Cys273 plays both a vital role in the initial inhibition of PP-1 by MCLR and an important role temporally distant when it forms a covalent reaction with the inhibitor.

Consistent with its importance in toxin interactions, Cys273 is conserved in nearly all known PP-1 sequences. An exception to this is the PP-1 from the social amoeba *Dictyostelium discoideum*, where the equivalent residue is Phe269.¹²⁶ The sensitivity of this enzyme to microcystins was ~2-fold less than a point mutant with the substitution Phe269Cys. These assays were carried out on unpurified cell extracts from *E. coli* and should be verified with purified protein. PP-1 from various plants including *Brassica napus*, *Arabidopsis thaliana* TOPP 8 and *Phaseolus vulgaris* possess a glycine at the equivalent position to Cys273.¹²⁷⁻¹²⁹ Crude extracts from *B. napus* were reported to be as sensitive to natural product inhibitors as the mammalian enzymes but no studies are available using the purified enzymes.^{97,130}

A previous chimeric protein was produced by Conner *et. al.*¹²², who substituted the C-terminus of PP-1 (residues 274 to the C-terminus), with the

equivalent residues of PP-2A. The resulting protein was not inhibited by NIPP-1 or thiophosphorylated inhibitor-1, neither of which normally inhibit PP-2A. It was, however, inhibited by both fostriecin and tautomycin, suggesting that the residues in the second half of the loop region (residues 274 to 277) are unlikely to be important for interactions with these inhibitors (since binding did not change even though the residues were substituted). In contrast, the residues in the C-terminus were vital to endogenous inhibitor binding (NIPP-1 or inhibitor-1). This is partially consistent with our results for the endogenous inhibitors since mutation of Cys273 did affect inhibitor-2 binding but mutations farther towards the C-terminus in the loop also affected binding. Clearly, the endogenous inhibitors have a very complicated and potentially diverse mechanism of binding that make extrapolation from this data difficult.

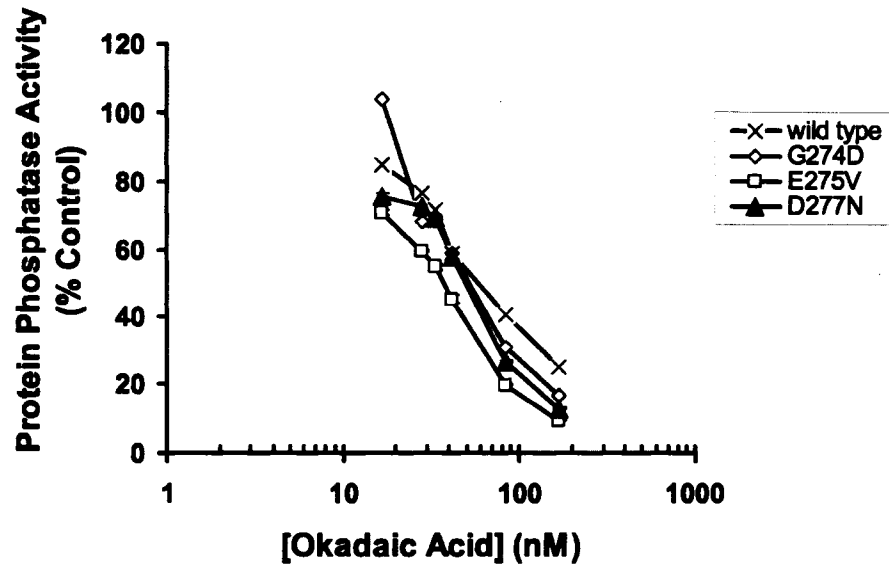
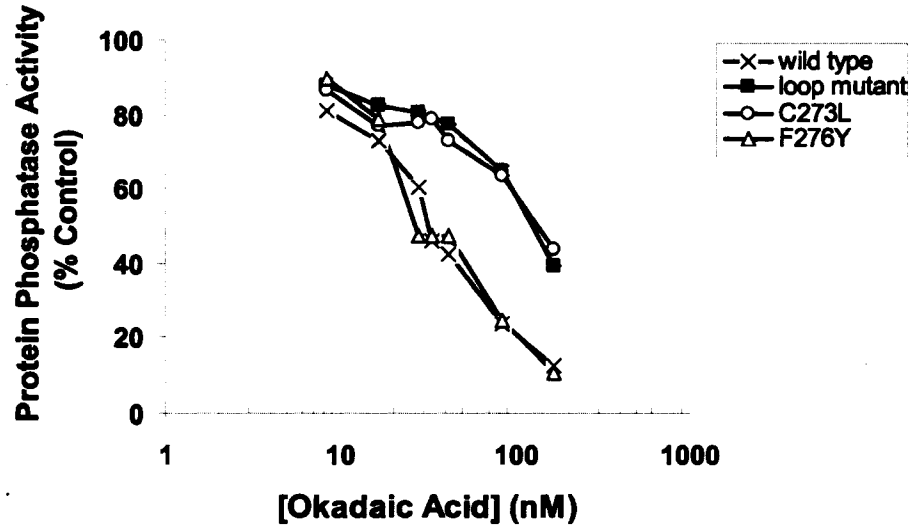


Figure 4.7 Inhibitory profiles of wild-type, chimeric (loop mutant) and point mutants of PP-1 with OA. The substrate for the assays was ^{32}P -phosphorylase *a*.

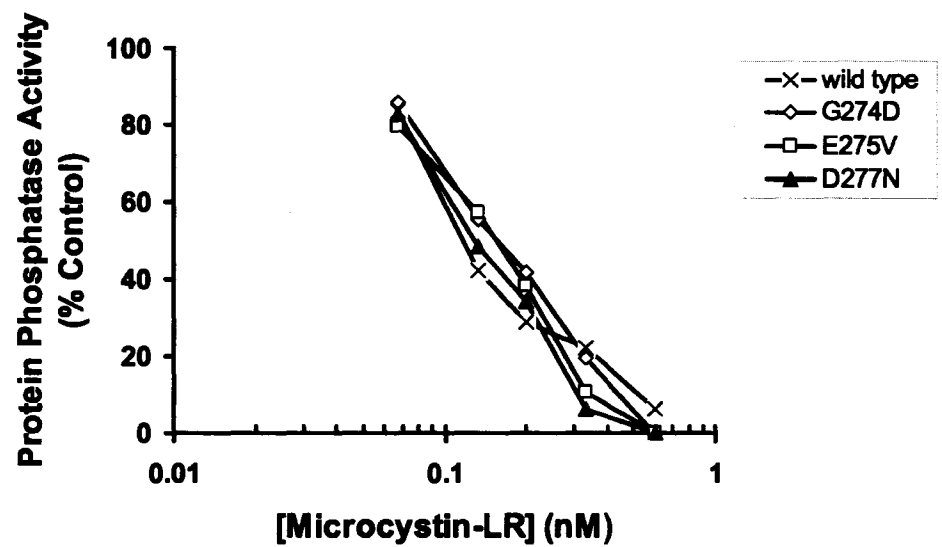
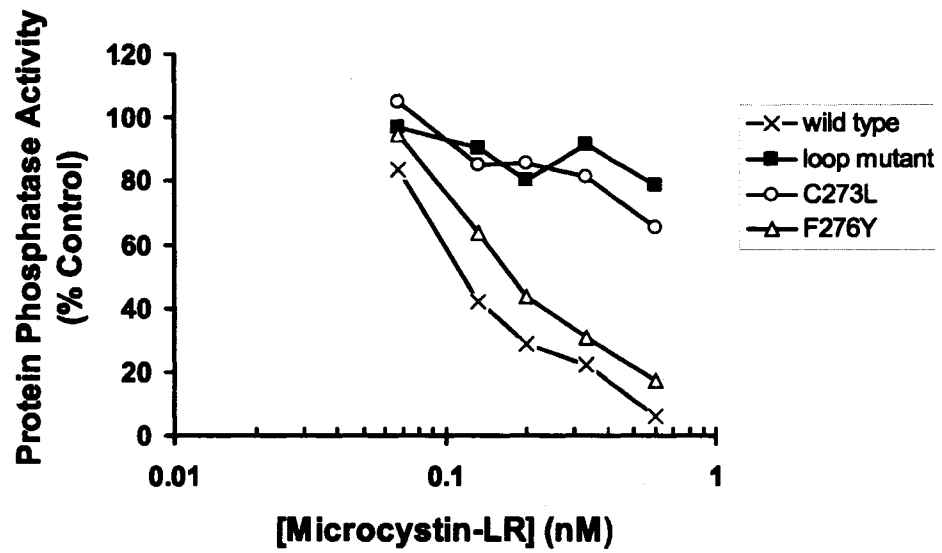


Figure 4.8 Inhibitory profiles of wild-type, chimeric (loop mutant) and point mutants of PP-1 with MCLR. The substrate for the assays was ^{32}P -phosphorylase *a*.

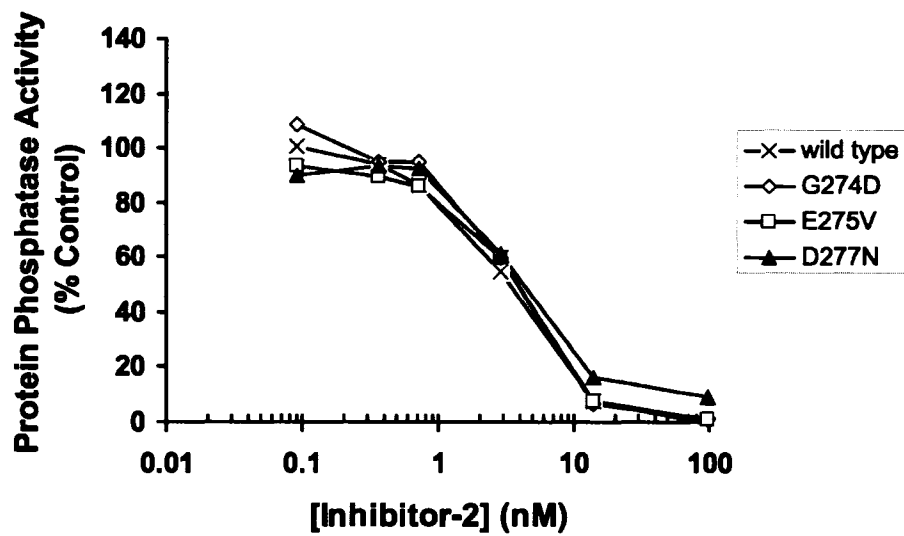
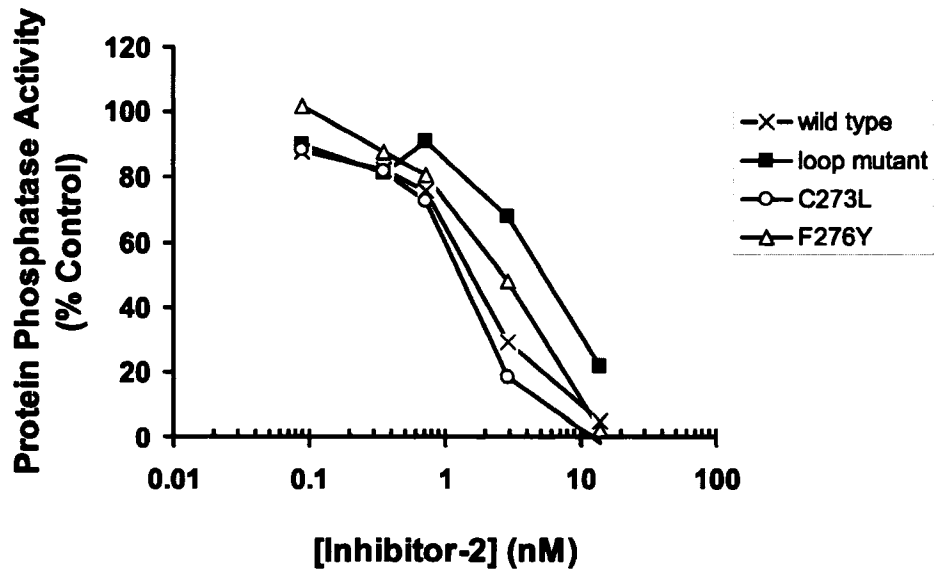


Figure 4.9 Inhibitory profiles of wild-type, chimeric (loop mutant) and point mutants of PP-1 with inhibitor-2. The substrate for the assays was ^{32}P -phosphorylase *a*.

D. Conclusions

The structural and kinetic studies outlined here help to elucidate the role of the β 12- β 13 loop in inhibitor specificity. The crystal structure of the chimeric mutant in complex with OA was determined to directly observe the differences in the β 12- β 13 loop structure. This was examined in the context of the large structural changes observed in the previous PP-1:MCLR structure when compared to the PP-1:OA and PP-1:calyculin structures, indicating that structural rearrangements may be crucial to the mechanism of inhibitor binding. The structural similarity observed between the OA-, calyculin- and tungstate-bound structures and the chimeric PP-1:OA complex indicates that structural changes most likely do not play a large role in the inhibitor mechanism. Not only are the overall structural features very similar among the complexes, but the active site configurations are virtually identical. This also holds when comparing the PP-1 structures to the available structures of CAN. This supports the conclusion that the changes in the loop region in the PP-1:MCLR complex are secondary to the covalent reaction that occurs between the enzyme and the inhibitor and are not crucial to the inhibitory mechanism of MCLR. It also supports the conclusion that amino acid sequence in the β 12- β 13 loop determines inhibitor specificity between members of the PPP family.

The most surprising result of these studies was the importance of the Cys273 for natural product inhibition. The previously available X-ray crystal structures of PP-1 bound to natural product toxins in a non-covalent manner (OA, calyculin) did not indicate a strong role for Cys273 in inhibitor binding. A previous study of site-directed mutants showed that the mutation Cys273Ala did not affect OA, calyculin

or nodularin binding.⁴⁶ The difference in the chemical properties between a leucine and an alanine residue that would create this discrepancy in the kinetic data is not apparent. The possibility exists that a leucine at position 273 in the loop allows for tighter hydrophobic or van der Waals interactions with a generally hydrophobic segment of the natural product inhibitor. This effect might not been seen with a Cys273Ala mutation if the alanine side chain is too small to create the correct environment. The importance of the hydrophobic interactions with this same region of the β 12- β 13 loop is echoed by the mutation of Tyr272, where abolition of the hydrogen-bonding capacity minimally affects toxin binding but removal of the hydrophobic bulk of the residue dramatically affects the efficacy of the toxins (Table 4.1). The dramatic effects of the Cys273Leu mutation cannot be fully rationalized by the X-ray crystal structure presented here.

While Cys273 appears to be vital for natural product inhibition (possibly being a second area of hydrophobic interaction outside of the hydrophobic groove), mutation of this residue did not affect inhibitor-2 binding. This observation is difficult to interpret in the absence of any structural data on the binding mode of inhibitor-2 to PP-1. The inhibitory potential of inhibitor-2 towards CAN is significantly less than either wtPP-1 or the chimeric protein, indicating that interactions and primary sequence changes outside the β 12- β 13/L7 loop region are important in mediating inhibitor-2 action. This is consistent with current models of inhibitor-2 binding.²¹

The importance of the β 12- β 13 loop region was emphasized in a recent X-ray crystal structure of the complex between PP-1 and the myosin phosphatase targeting

subunit (MYPT-1).³⁰ The complex showed some minor active site remodeling with targeting subunit binding but left the loop region in an exposed and prominent position to influence enzyme activity and inhibition. MYPT-1 contains ankyrin repeat motifs that wrap around the β 12- β 13 loop, creating an acidic surface (with the loop region in the middle) that dramatically alters the electrostatic potential in the region adjacent to the active site. The ankyrin repeats, in addition to the N-terminus of the targeting subunit that wraps around the phosphatase and interacts with the hydrophobic groove region, are required for the full activity of MYPT-1. The exact significance of either functional domain is not known. While the β 12- β 13 loop has not been implicated in substrate binding, the exposure of the loop in this first PP-1:targeting subunit X-ray crystal structure indicates that it most likely plays a predominant role in the physiological activity of the phosphatase, in addition to natural product binding.

The studies presented here have revealed the importance of the β 12- β 13 loop region in natural product and endogenous inhibitor binding. In particular, the role of the β 12- β 13 loop region in determining inhibitor specificity among the similar members of the PPP family was investigated. Elucidation of the residue specific role of the β 12- β 13 loop should now allow for the rational creation of a CAN that is sensitive to natural product toxins.

Chapter 5

Summary

A. Natural product inhibitor binding to the PPP family members is not dependant on protein structural changes

It was postulated, prior to starting this work, that variations in three-dimensional structure were potentially responsible for the observed differences in natural product inhibitory profiles of the PPP family members. This conclusion was based on two available PP-1 X-ray crystallographic structures (PP-1 in complexes with MCLR and tungstate) which showed differences in the active site region, namely in the β 12- β 13 loop. The structures presented here show conclusively that this is not the case. We have solved the X-ray crystallographic structures of two novel natural product inhibitors, motuporin and okadaic acid, bound to PP-1. Both of these structures, while having significant interactions with the β 12- β 13 loop region (primarily Tyr272), do not cause structural rearrangements of the loop, or of any part of the protein. When comparing these two structures to the PP-1:tungstate complex and the later determined PP-1:calyculin complex, there are no significant structural changes (largest C_{α} RMSD is 0.7 Å between any two structures). These structures also have very similar conformations to the determined CAN structures.

To confirm these results, we determined the X-ray crystallographic structure of a modified microcystin, dihydromicrocystin-LA, bound to PP-1. This microcystin cannot form a covalent bond with Cys273 of the β 12- β 13 loop but should otherwise behave identically to MCLR in PP-1 inhibition. This structure again showed no structural realignment with natural product binding. Interestingly,

MCLA-2H did bind in an almost identical manner to that observed with MCLR, perhaps indicating an inherent flexibility in the loop region that would allow MCLR to bind despite a covalent tethering. These results, in agreement with those mentioned above, show conclusively that natural product binding to the PPP family members is not dependant on protein structural changes and the affinity of the natural products for the PPP family members cannot be explained by structural changes.

B. The primary sequence of PPP family members determines inhibitor binding affinity

If structural changes are not responsible for natural product inhibitor binding, then the observed differences in affinity for the PPP family members should be due to sequence dissimilarities. To investigate this possibility, we relied on previous mutational data showing that residues in the β 12- β 13 loop were important for inhibitor binding and mutated the residues from the loop region in PP-1 to the equivalent residues in CAN. We subsequently solved the X-ray crystallographic structure of this chimeric protein complexed with OA. This structure showed nearly identical binding of OA to the chimeric protein compared to our previously determined structure of wild-type PP-1 complexed to OA. This was surprising since the enzyme kinetics for this mutant showed a decreased sensitivity to OA over wild-type PP-1. However, the chimeric enzyme was not as insensitive to OA as calcineurin. In comparing the two OA complex structures, the one area of dissimilarity that was evident was residue 276 in the loop, the wild-type enzyme having a Phe residue and the chimeric protein having a Tyr residue. While both

residues occupied similar positions, the disorder (manifested by higher thermal coefficients and poor electron density) for the chimeric protein's Tyr276 suggested that it may be playing a more significant role than that revealed by the X-ray crystallographic structure. In order to determine the role of the tyrosine residue, we individually mutated each residue in the β 12- β 13 loop to the corresponding residue in the CAN L7 loop and determined the inhibition kinetics. Surprisingly, the Phe276Tyr point mutant had very little change in inhibition constants (with MCLR and OA) over the wild-type PP-1 but the Cys273Leu point mutant displayed almost identical kinetics to the chimeric protein. This indicates that the latter mutation was most responsible for the reduced inhibition of the natural product toxins in the chimeric protein. This was contradictory to previous mutagenesis data where mutation of Cys273 (to Ala) had very little effect on the inhibitory values, although the Cys273Leu mutation has never been attempted. The characteristics of the cysteine residue that are amenable to natural product binding over the leucine residue is not immediately apparent and the X-ray crystal structure of the chimeric protein bound to OA does not provide any clues, other than relatively close van der Waals and hydrophobic interactions. These types of interaction would not be expected to change significantly by changing from a cysteine to a leucine residue. The chimeric protein does not display inhibitory kinetics that are identical to CAN, meaning that there are other areas of primary structure changes that affect natural product binding.

(there are other sequence differences between PP-1 and CAN in the active site region). None of these have been verified to be important in determining the

different inhibitory binding constants of the natural product inhibitors to the PPP family.

C. The natural product inhibitors utilize similar functional groups to interact with the PPP family but rely on different sources of binding energy

The structures of OA, MOT and MCLA-2H bound to PP-1 show that the natural products utilize similar functional groups to bind to PP-1, creating a pharmacophore of important interactions for the natural product inhibitors. The important interactions that are required for natural product inhibition include: (1) the interaction of an acidic group with active site waters that are anchored by the catalytic metal ions, (2) a primarily hydrophobic region interacting with the similarly characterized hydrophobic groove of PP-1 and (3) important interactions with the β 12- β 13 loop residues including hydrogen-bonding interactions with Tyr272 and an interaction with Cys273. The interaction with Cys273 is not vital for natural product binding but may largely effect the binding efficacy. The exact nature of this interaction remains a question to be answered. A macrocycle was not included in this pharmacophore because the calyculins/clavosines have proven that a macrocycle does not need to be present to bind the PPP family effectively, although most natural products do have it. This may be a case of divergent, rather than convergent evolution of the small molecule inhibitors.

While the natural product inhibitors all follow the described binding mode, they rely on different elements to make their binding energetically favourable.

The natural product inhibitors, which possess two acid groups or a phosphate (providing them with a larger number of potential hydrogen-binding elements), rely more on binding the active site residues and hydrogen-bonding interactions. This includes the microcystins and the nodularins/motuporin. Others, like okadaic acid, have relatively few interactions with the active site and rely on hydrophobic binding energy and on the decreased entropic cost of having similar bound and unbound structures. These different contributions to binding energy do not seem to drastically affect how the natural product inhibitors bind to different members of the PPP family since all of the pertinent protein binding areas are conserved between family members.

The endogenous inhibitors do not follow the same binding scheme as the natural product inhibitors, relying on a different binding mode that does depend to some degree on the β 12- β 13 loop residues, although mutations in the loop region do not abolish inhibition. The endogenous inhibitors most likely do not interact to a significant degree with the hydrophobic groove but the carboxylic acid/phosphate on most of the inhibitors most likely does bind active site waters and/or Arg96/221. Most of the endogenous inhibitors also contain an RVXF motif, signifying likely binding into the targeting groove on the opposite face of the enzyme from the active site.

The work presented here lays the groundwork for future studies directed at the development of inhibitors of the PPP family. The structures and enzyme kinetics presented reveal a portion of the details of how inhibitors can be selective for different members of the PPP family. The information provided

here should allow for the creation of phosphatase-specific inhibitors. These inhibitors may be in the form of active-site directed compounds, similar to the natural product inhibitors, or may involve small molecules binding into a region adjacent to the active site which disrupt the interaction of the catalytic domain with its targeting subunits. This method may impart more specificity in targeting members of the PPP family.

References

1. Barford, D., Das, A. K. & Egloff, M. P. (1998). The structure and mechanism of protein phosphatases: Insights into catalysis and regulation. *Annual Review of Biophysics and Biomolecular Structure* 27, 133-164.
2. Lerin, C., Montell, E., Nolasco, T., Clark, C., Brady, M. J., Newgard, C. B. & Gomez-Foix, A. M. (2003). Regulation and function of the muscle glycogen-targeting subunit of protein phosphatase 1 (G(M)) in human muscle cells depends on the COOH-terminal region and glycogen content. *Diabetes* 52, 2221-2226.
3. Brady, M. J. & Saltiel, A. R. (2001). The role of protein phosphatase-1 in insulin action. In *Recent Progress in Hormone Research, Vol 56*, Vol. 56, pp. 157-173.
4. Hansen, L., Reneland, R., Berglund, L., Rasmussen, S. K., Hansen, T., Lithell, H. & Pedersen, O. (2000). Polymorphism in the glycogen-associated regulatory subunit of type 1 protein phosphatase (PPP1R3) gene and insulin sensitivity. *Diabetes* 49, 298-301.
5. Allen, P. B., Hvalby, O., Jensen, V., Errington, M. L., Ramsay, M., Chaudhry, F. A., Bliss, T. V. P., Storm-Mathisen, J., Morris, R. G. M., Andersen, P. & Greengard, P. (2000). Protein phosphatase-1 regulation in the induction of long-term potentiation: Heterogeneous molecular mechanisms. *Journal of Neuroscience* 20, 3537-3543.

6. McCluskey, A., Sim, A. T. R. & Sakoff, J. A. (2002). Serine-threonine protein phosphatase inhibitors: Development of potential therapeutic strategies. *J Med Chem* 45, 1151-1175.
7. Notredame, C., Higgins, D. G. & Heringa, J. (2000). T-Coffee: A novel method for fast and accurate multiple sequence alignment. *Journal of Molecular Biology* 302, 205-217.
8. Rusnak, F. & Mertz, P. (2000). Calcineurin: Form and function. *Physiological Reviews* 80, 1483-1521.
9. Dawson, T. M., Dawson, V. L. & Snyder, S. H. (1992). A Novel Neuronal Messenger Molecule in Brain - the Free-Radical, Nitric-Oxide. *Annals of Neurology* 32, 297-311.
10. Moncada, S., Palmer, R. M. J. & Higgs, E. A. (1991). Nitric-Oxide - Physiology, Pathophysiology, and Pharmacology. *Pharmacological Reviews* 43, 109-142.
11. Garthwaite, J. (1991). Glutamate, Nitric-Oxide and Cell Cell Signaling in the Nervous-System. *Trends in Neurosciences* 14, 60-67.
12. Lopez, O. L., Martinez, A. J. & Torre-Cisneros, J. (1991). Neuropathologic findings in liver transplantation: a comparative study of cyclosporine and FK 506. *Transplant Proc.* 23, 3181-2.
13. Martinez-Martinez, S. & Redondo, J. M. (2004). Inhibitors of the calcineurin/NFAT pathway. *Current Medicinal Chemistry* 11, 997-1007.
14. Beullens, M., Van Eynde, A., Vulsteke, V., Connor, J., Shenolikar, S., Stalmans, W. & Bollen, M. (1999). Molecular determinants of nuclear

- protein phosphatase-1 regulation by NIPP-1. *Journal of Biological Chemistry* 274, 14053-14061.
15. Endo, S., Zhou, X. Z., Connor, J., Wang, B. & Shenolikar, S. (1996). Multiple structural elements define the specificity of recombinant human inhibitor-1 as a protein phosphatase-1 inhibitor. *Biochemistry* 35, 5220-5228.
 16. Huang, K. X. & Paudel, H. K. (2000). Ser(67)-phosphorylated inhibitor 1 is a potent protein phosphatase 1 inhibitor. *Proceedings of the National Academy of Sciences of the United States of America* 97, 5824-5829.
 17. Endo, S., Connor, J. H., Forney, B., Zhang, L., Ingebritsen, T. S., Lee, E. Y. C. & Shenolikar, S. (1997). Conversion of protein phosphatase 1 catalytic subunit to a Mn²⁺-dependent enzyme impairs its regulation by inhibitor 1. *Biochemistry* 36, 6986-6992.
 18. Weiser, D. C., Sikes, S., Li, S. & Shenolikar, S. (2004). The inhibitor-1 C terminus facilitates hormonal regulation of cellular protein phosphatase-1 - Functional implications for inhibitor-1 isoforms. *Journal of Biological Chemistry* 279, 48904-48914.
 19. Liu, H. T., Lin, T. H., Kuo, H. C., Chen, Y. C., Tsay, H. J., Jeng, H. H., Tsai, P. C., Shie, F. K., Chen, J. H. & Huang, H. B. (2002). Identification of the alternative splice products encoded by the human protein phosphatase inhibitor-1 gene. *Biochemical and Biophysical Research Communications* 291, 1293-1296.
 20. Connor, J. H., Frederick, D., Huang, H. B., Yang, J., Helps, N. R., Cohen, P. T. W., Nairn, A. C., DePaoli-Roach, A., Tatchell, K. & Shenolikar, S.

- (2000). Cellular mechanisms regulating protein phosphatase-1 - A key functional interaction between inhibitor-2 and the type 1 protein phosphatase catalytic subunit. *Journal of Biological Chemistry* 275, 18670-18675.
21. Yang, J., Hurley, T. D. & DePaoli-Roach, A. A. (2000). Interaction of inhibitor-2 with the catalytic subunit of type 1 protein phosphatase. Identification of a sequence analogous to the consensus type 1 protein phosphatase-binding motif. *J Biol Chem* 275, 22635-44.
22. Lin, T. H., Chen, Y. C., Chyan, C. L., Tsay, L. H., Tang, T. C., Jeng, H. H., Lin, F. M. & Huang, H. B. (2003). Phosphorylation by glycogen synthase kinase of inhibitor-2 does not change its structure in free state. *Febs Letters* 554, 253-256.
23. Wakula, P., Beullens, M., Ceulemans, H., Stalmans, W. & Bollen, M. (2003). Degeneracy and function of the ubiquitous RVXF motif that mediates binding to protein phosphatase-1. *Journal of Biological Chemistry* 278, 18817-18823.
24. Huang, H. B., Horiuchi, A., Watanabe, T., Shih, S. R., Tsay, H. J., Li, H. C., Greengard, P. & Nairn, A. C. (1999). Characterization of the inhibition of protein phosphatase-1 by DARPP-32 and inhibitor-2. *Journal of Biological Chemistry* 274, 7870-7878.
25. Shirato, H., Shima, H., Sakashita, G., Nakano, T., Ito, M., Lee, E. Y. C. & Kikuchi, K. (2000). Identification and characterization of a novel protein inhibitor of type 1 protein phosphatase. *Biochemistry* 39, 13848-13855.

26. Kwon, Y. G., Huang, H. B., Desdouits, F., Girault, J. A., Greengard, P. & Nairn, A. C. (1997). Characterization of the interaction between DARPP-32 and protein phosphatase 1 (PP-1): DARPP-32 peptides antagonize the interaction of PP-1 with binding proteins. *Proceedings of the National Academy of Sciences of the United States of America* 94, 3536-3541.
27. Desdouits, F., Cohen, D., Nairn, A. C., Greengard, P. & Girault, J. A. (1995). Phosphorylation of Darpp-32, a Dopamine-Regulated and Camp-Regulated Phosphoprotein, by Casein Kinase-I in-Vitro and in-Vivo. *Journal of Biological Chemistry* 270, 8772-8778.
28. Desdouits, F., Siciliano, J. C., Greengard, P. & Girault, J. A. (1995). Dopamine-Regulated and Camp-Regulated Phosphoprotein Darpp-32 - Phosphorylation of Ser-137 by Casein Kinase-I Inhibits Dephosphorylation of Thr-34 by Calcineurin. *Proceedings of the National Academy of Sciences of the United States of America* 92, 2682-2685.
29. Kim, Y. M., Watanabe, T., Allen, P. B., Lee, S. J., Greengard, P., Nairn, A. C. & Kwon, Y. G. (2003). PNUTS, a protein phosphatase 1 (PP1) nuclear targeting subunit. *Journal of Biological Chemistry* 278, 13819-13828.
30. Terrak, M., Kerff, F., Langsetmo, K., Tao, T. & Dominguez, R. (2004). Structural basis of protein phosphatase 1 regulation. *Nature* 429, 780-4.
31. Carmody, L. C., Bauman, P. A., Bass, M. A., Mavila, N., DePaoli-Roach, A. A. & Colbran, R. J. (2004). A protein phosphatase-1 gamma 1 isoform selectivity determinant in dendritic spine-associated neurabin. *Journal of Biological Chemistry* 279, 21714-21723.

32. McAvoy, T., Allen, P. B., Obaishi, H., Nakanishi, H., Takai, Y., Greengard, P., Nairn, A. C. & Hemmings, H. C. (1999). Regulation of neurabin I interaction with protein phosphatase 1 by phosphorylation. *Biochemistry* 38, 12943-12949.
33. Eto, M., Karginov, A. & Brautigan, D. L. (1999). A novel phosphoprotein inhibitor of protein type-1 phosphatase holoenzymes. *Biochemistry* 38, 16952-16957.
34. Eto, M., Elliott, E., Prickett, T. D. & Brautigan, D. L. (2002). Inhibitor-2 regulates protein phosphatase-1 complexed with NimA-related kinase to induce centrosome separation. *Journal of Biological Chemistry* 277, 44013-44020.
35. Egloff, M. P., Cohen, P. T., Reinemer, P. & Barford, D. (1995). Crystal structure of the catalytic subunit of human protein phosphatase 1 and its complex with tungstate. *J Mol Biol* 254, 942-59.
36. Egloff, M. P., Johnson, D. F., Moorhead, G., Cohen, P. T., Cohen, P. & Barford, D. (1997). Structural basis for the recognition of regulatory subunits by the catalytic subunit of protein phosphatase 1. *Embo J* 16, 1876-87.
37. Goldberg, J., Huang, H. B., Kwon, Y. G., Greengard, P., Nairn, A. C. & Kuriyan, J. (1995). Three-dimensional structure of the catalytic subunit of protein serine/threonine phosphatase-1. *Nature* 376, 745-53.
38. Griffith, J. P., Kim, J. L., Kim, E. E., Sintchak, M. D., Thomson, J. A., Fitzgibbon, M. J., Fleming, M. A., Caron, P. R., Hsiao, K. & Navia, M. A.

- (1995). X-ray structure of calcineurin inhibited by the immunophilin-immunosuppressant FKBP12-FK506 complex. *Cell* 82, 507-22.
39. Kissinger, C. R., Parge, H. E., Knighton, D. R., Lewis, C. T., Pelletier, L. A., Tempczyk, A., Kalish, V. J., Tucker, K. D., Showalter, R. E., Moomaw, E. W. & et al. (1995). Crystal structures of human calcineurin and the human FKBP12-FK506-calcineurin complex. *Nature* 378, 641-4.
40. Jin, L., Harrison, S. C., Huai, Q., Kim, H. Y., Liu, Y., Zhao, Y., Mondragon, A., Liu, J. O. & Ke, H. (2002). Crystal structure of human calcineurin complexed with cyclosporin A and human cyclophilin:Crystal structure of calcineurin-cyclophilin-cyclosporin shows common but distinct recognition of immunophilin-drug complexes. *Proc Natl Acad Sci U S A* 99, 13522-6. Epub 2002 Sep 30.
41. Huai, Q., Kim, H. Y., Liu, Y., Zhao, Y., Mondragon, A., Liu, J. O. & Ke, H. (2002). Crystal structure of calcineurin-cyclophilin-cyclosporin shows common but distinct recognition of immunophilin-drug complexes. *Proc Natl Acad Sci U S A* 99, 12037-42. Epub 2002 Sep 6.
42. Kita, A., Matsunaga, S., Takai, A., Kataiwa, H., Wakimoto, T., Fusetani, N., Isobe, M. & Miki, K. (2002). Crystal Structure of the Complex between Calyculin A and the Catalytic Subunit of Protein Phosphatase 1. *Structure* 10, 715-24.
43. Yu, L., Haddy, A. & Rusnak, F. (1995). Evidence That Calcineurin Accommodates an Active-Site Binuclear Metal Center. *Journal of the American Chemical Society* 117, 10147-10148.

44. King, M. M. & Huang, C. Y. (1984). The Calmodulin-Dependent Activation and Deactivation of the Phosphoprotein Phosphatase, Calcineurin, and the Effect of Nucleotides, Pyrophosphate, and Divalent Metal-Ions - Identification of Calcineurin as a Zn and Fe Metalloenzyme. *Journal of Biological Chemistry* 259, 8847-8856.
45. Huang, H. B., Horiuchi, A., Goldberg, J., Greengard, P. & Nairn, A. C. (1997). Site-directed mutagenesis of amino acid residues of protein phosphatase 1 involved in catalysis and inhibitor binding. *Proc Natl Acad Sci USA* 94, 3530-5.
46. Zhang, L., Zhang, Z., Long, F. & Lee, E. Y. (1996). Tyrosine-272 is involved in the inhibition of protein phosphatase-1 by multiple toxins. *Biochemistry* 35, 1606-11.
47. Lee, E. Y., Zhang, L., Zhao, S., Wei, Q., Zhang, J., Qi, Z. Q. & Belmonte, E. R. (1999). Phosphorylase phosphatase: new horizons for an old enzyme. *Front Biosci.* 4, D270-85.
48. McCready, T. L., Islam, B. F., Schmitz, F. J., Luu, H. A., Dawson, J. F. & Holmes, C. F. (2000). Inhibition of protein phosphatase-1 by clavosines A and B. Novel members of the calyculin family of toxins. *J Biol Chem* 275, 4192-8.
49. Tachibana, K., Scheuer, P. J., Tsukitani, Y., Kikuchi, H., Vanengen, D., Clardy, J., Gopichand, Y. & Schmitz, F. J. (1981). Okadaic Acid, a Cytotoxic Polyether from 2 Marine Sponges of the Genus Halichondria. *J Am Chem Soc* 103, 2469-2471.

50. Bagu, J. R., Sonnichsen, F. D., Williams, D., Andersen, R. J., Sykes, B. D. & Holmes, C. F. B. (1995). Comparison of the Solution Structures of Microcystin-LR and Motuporin. *Nat Struct Biol* 2, 114-116.
51. Annala, A., Lehtimäki, J., Mattila, K., Eriksson, J. E., Sivonen, K., Rantala, T. T. & Drakenberg, T. (1996). Solution structure of nodularin. An inhibitor of serine/threonine-specific protein phosphatases. *J Biol Chem* 271, 16695-702.
52. Bagu, J. R., Sykes, B. D., Craig, M. M. & Holmes, C. F. B. (1997). A molecular basis for different interactions of marine toxins with protein phosphatase-1 - Molecular models for bound motuporin, microcystins, okadaic acid, and calyculin A. *Journal of Biological Chemistry* 272, 5087-5097.
53. Cameron, A. M., Steiner, J. P., Roskams, A. J., Ali, S. M., Ronnett, G. V. & Snyder, S. H. (1995). Calcineurin Associated with the Inositol 1,4,5-Trisphosphate Receptor-Fkbp12 Complex Modulates Ca²⁺ Flux. *Cell* 83, 463-472.
54. Liu, C. W. Y., Wang, R. H., Dohadwala, M., Schonthal, A. H., Villa-Moruzzi, E. & Berndt, N. (1999). Inhibitory phosphorylation of PP1 alpha catalytic subunit during the G(1)/S transition. *Journal of Biological Chemistry* 274, 29470-29475.
55. Meraldi, P. & Nigg, E. A. (2001). Centrosome cohesion is regulated by a balance of kinase and phosphatase activities. *Journal of Cell Science* 114, 3749-3757.

56. Chen, J., Martin, B. L. & Brautigam, D. L. (1992). Regulation of Protein Serine-Threonine Phosphatase Type-2a by Tyrosine Phosphorylation. *Science* 257, 1261-1264.
57. Faux, M. C. & Scott, J. D. (1996). More on target with protein phosphorylation: Conferring specificity by location. *Trends in Biochemical Sciences* 21, 312-315.
58. Bollen, M. (2001). Combinatorial control of protein phosphatase-1. *Trends in Biochemical Sciences* 26, 426-431.
59. Jones, J. A. & Hannun, Y. A. (2002). Tight binding inhibition of protein phosphatase-1 by phosphatidic acid - Specificity of inhibition by the phospholipid. *Journal of Biological Chemistry* 277, 15530-15538.
60. Zhang, L. & Lee, E. Y. (1997). Mutational analysis of substrate recognition by protein phosphatase 1. *Biochemistry*. 36, 8209-14.
61. Zhang, Z., Zhao, S., Long, F., Zhang, L., Bai, G., Shima, H., Nagao, M. & Lee, E. Y. (1994). A mutant of protein phosphatase-1 that exhibits altered toxin sensitivity. *J Biol Chem* 269, 16997-7000.
62. Craig, M., Luu, H. A., McCready, T. L., Williams, D., Andersen, R. J. & Holmes, C. F. B. (1996). Molecular mechanisms underlying the interaction of motuporin and microcystins with type-1 and type-2A protein phosphatases. *Biochem Cell Biol* 74, 569-78.
63. Yang, J., Roe, S. M., Cliff, M. J., Williams, M. A., Ladbury, J. E., Cohen, P. T. & Barford, D. (2005). Molecular basis for TPR domain-mediated regulation of protein phosphatase 5. *Embo J*. 24, 1-10. Epub 2004 Dec 2.

64. Ali, A., Zhang, J., Bao, S. D., Liu, I., Otterness, D., Dean, N. M., Abraham, R. T. & Wang, X. F. (2004). Requirement of protein phosphatase 5 in DNA-damage-induced ATM activation. *Genes & Development* 18, 249-254.
65. Wechsler, T., Chen, B. P. C., Harper, R., Morotomi-Yano, K., Huang, B. C. B., Meek, K., Cleaver, J. E., Chen, D. J. & Wabl, M. (2004). DNA-PKcs function regulated specifically by protein phosphatase 5. *Proceedings of the National Academy of Sciences of the United States of America* 101, 1247-1252.
66. Klee, C. B., Ren, H. & Wang, X. T. (1998). Regulation of the calmodulin-stimulated protein phosphatase, calcineurin. *Journal of Biological Chemistry* 273, 13367-13370.
67. Kennedy, M. T., Brockman, H. & Rusnak, F. (1996). Contributions of myristoylation to calcineurin structure/function. *Journal of Biological Chemistry* 271, 26517-26521.
68. Zhu, D. H., Cardenas, M. E. & Heitman, J. (1995). Myristoylation of Calcineurin-B Is Not Required for Function or Interaction with Immunophilin-Immunosuppressant Complexes in the Yeast *Saccharomyces Cerevisiae*. *Journal of Biological Chemistry* 270, 24831-24838.
69. Fernandez, J. J., Cardenas, M. L., Souto, M. L., Trujillo, M. M. & Norte, M. (2002). Okadaic acid, useful tool for studying cellular processes. *Current Medicinal Chemistry* 9, 229-262.
70. Suganuma, M., Fujiki, H., Suguri, H., Yoshizawa, S., Hirota, M., Nakayasu, M., Ojika, M., Wakamatsu, K., Yamada, K. & Sugimura, T. (1988). Okadaic

Acid - an Additional Non-Phorbol-12-Tetradecanoate-13-Acetate-Type Tumor Promoter. *Proceedings of the National Academy of Sciences of the United States of America* 85, 1768-1771.

71. Fujiki, H., Suganuma, M., Suguri, H., Yoshizawa, S., Ojika, M., Wakamatsu, K., Yamada, K. & Sugimura, T. (1987). Induction of Ornithine Decarboxylase Activity in Mouse Skin by a Possible Tumor Promoter, Okadaic Acid. *Proceedings of the Japan Academy Series B-Physical and Biological Sciences* 63, 51-53.
72. Hescheler, J., Mieskes, G., Ruegg, J. C., Takai, A. & Trautwein, W. (1988). Effects of a Protein Phosphatase Inhibitor, Okadaic Acid, on Membrane Currents of Isolated Guinea-Pig Cardiac Myocytes. *Pflugers Archiv-European Journal of Physiology* 412, 248-252.
73. Nishiwaki, S., Fujiki, H., Suganuma, M., Furuyasuguri, H., Matsushima, R., Iida, Y., Ojika, M., Yamada, K., Uemura, D., Yasumoto, T., Schmitz, F. J. & Sugimura, T. (1990). Structure Activity Relationship within a Series of Okadaic Acid-Derivatives. *Carcinogenesis* 11, 1837-1841.
74. Takai, A., Bialojan, C., Troschka, M. & Ruegg, J. C. (1987). Smooth-Muscle Myosin Phosphatase Inhibition and Force Enhancement by Black Sponge Toxin. *FEBS Letters* 217, 81-84.
75. Takai, A., Murata, M., Torigoe, K., Isobe, M., Mieskes, G. & Yasumoto, T. (1992). Inhibitory Effect of Okadaic Acid-Derivatives on Protein Phosphatases - a Study on Structure Affinity Relationship. *Biochemical Journal* 284, 539-544.

76. Sasaki, K., Murata, M., Yasumoto, T., Mieskes, G. & Takai, A. (1994). Affinity of Okadaic Acid to Type-1 and Type-2a Protein Phosphatases Is Markedly Reduced by Oxidation of Its 27-Hydroxyl Group. *Biochemical Journal* 298, 259-262.
77. Fujiki, H. & Suganuma, M. (1993). Tumor Promotion by Inhibitors of Protein Phosphatase-1 and Phosphatase-2a - the Okadaic Acid Class of Compounds. In *Advances in Cancer Research, Vol 61*, Vol. 61, pp. 143-194.
78. Quinn, R. J., Taylor, C., Suganuma, M. & Fujiki, H. (1993). The Conserved Acid-Binding Domain Model of Inhibitors of Protein Phosphatase-1 and Phosphatase-2a - Molecular Modeling Aspects. *Bioorganic & Medicinal Chemistry Letters* 3, 1029-1034.
79. Gupta, V., Ogawa, A. K., Du, X. H., Houk, K. N. & Armstrong, R. W. (1997). A model for binding of structurally diverse natural product inhibitors of protein phosphatases PP1 and PP2A. *Journal of Medicinal Chemistry* 40, 3199-3206.
80. Bialojan, C. & Takai, A. (1988). Inhibitory effect of a marine-sponge toxin, okadaic acid, on protein phosphatases. Specificity and kinetics. *Biochem J* 256, 283-90.
81. Gauss, C. M., Shepeck, J. E., Nairn, A. C. & Chamberlin, R. (1997). A molecular modeling analysis of the binding interactions between the okadaic acid class of natural product inhibitors and the Ser-Thr phosphatases, PP1 and PP2A. *Bioorganic & Medicinal Chemistry* 5, 1751-1773.
82. Otwinowski, M. & Minor, W. (1997). *Methods Enzymol* 276, 307-326.

83. Navaza, J. & Saludjian, P. (1997). AMoRe: An automated molecular replacement program package. In *Macromolecular Crystallography, Pt A*, Vol. 276, pp. 581-594.
84. Tachibana, K., Scheuer, P. J., Tsukitani, Y., Kikuchi, H., Vanengen, D., Clardy, J., Gopichand, Y. & Schmitz, F. J. (1981). Okadaic Acid, a Cytotoxic Polyether from 2 Marine Sponges of the Genus *Halichondria*. *Journal of the American Chemical Society* 103, 2469-2471.
85. Brunger, A. T., Adams, P. D., Clore, G. M., Gros, P., Grosse-Kunstleve, R. W., Jiang, J.-S., Kuszewski, J., Nilges, M., Pannu, N. S., Read, R. J., Rice, L. M., Simonson, T. & Warren, G. L. (1998). Crystallography & NMR system: A new software suite for macromolecular structure determination. *Acta Crystallographica Section D-Biological Crystallography* 54, 905-921.
86. McRee, D. E. (1999). XtalView Xfit - A versatile program for manipulating atomic coordinates and electron density. *J Struct Biol* 125, 156-165.
87. Hooft, R. W., Vriend, G., Sander, C. & Abola, E. E. (1996). Errors in protein structures. *Nature* 381, 272.
88. Laskowski, R. A., Moss, D. S. & Thornton, J. M. (1993). Main-chain bond lengths and bond angles in protein structures. *J Mol Biol* 231, 1049-67.
89. Maynes, J. T., Bateman, K. S., Cherney, M. M., Das, A. K., Luu, H. A., Holmes, C. F. B. & James, M. N. G. (2001). Crystal structure of the tumor-promoter okadaic acid bound to protein phosphatase-1. *J Biol Chem* 276, 44078-82.

90. Lindvall, M. K., Pihko, P. M. & Koskinen, A. M. (1997). The binding mode of calyculin A to protein phosphatase-1. A novel spiroketal vector model. *J Biol Chem* 272, 23312-6.
91. Kleywegt, G. J. (2005). LSQMAN 050920 edit.
92. Dawson, J. F. & Holmes, C. F. B. (1999). Molecular mechanisms underlying inhibition of protein phosphatases by marine toxins. *Front Biosci* 4, D646-58.
93. Carmichael, W. W. (1994). Toxins of Cyanobacteria. *Scientific American* 270, 78-86.
94. Honkanen, R. E., Zwiller, J., Moore, R. E., Daily, S. L., Khatra, B. S., Dukelow, M. & Boynton, A. L. (1990). Characterization of Microcystin-LR, a Potent Inhibitor of Type-1 and Type-2a Protein Phosphatases. *J Biol Chem* 265, 19401-19404.
95. Yoshizawa, S., Matsushima, R., Watanabe, M. F., Harada, K., Ichihara, A., Carmichael, W. W. & Fujiki, H. (1990). Inhibition of Protein Phosphatases by Microcystis and Nodularin Associated with Hepatotoxicity. *J Cancer Res Clin Oncol* 116, 609-614.
96. Nishiwakimatsushima, R., Nishiwaki, S., Ohta, T., Yoshizawa, S., Suganuma, M., Harada, K., Watanabe, M. F. & Fujiki, H. (1991). Structure-Function-Relationships of Microcystins, Liver-Tumor Promoters, in Interaction with Protein Phosphatase. *Jpn J Cancer Res* 82, 993-996.
97. MacKintosh, C., Beattie, K. A., Klumpp, S., Cohen, P. & Codd, G. A. (1990). Cyanobacterial microcystin-LR is a potent and specific inhibitor of

- protein phosphatases 1 and 2A from both mammals and higher plants. *FEBS Lett* 264, 187-92.
98. Holmes, C. F. B. & Boland, M. P. (1993). Inhibitors of Protein Phosphatase-1 and Phosphatase-2a - Two of the Major Serine Threonine Protein Phosphatases Involved in Cellular-Regulation. *Curr Opin Struct Biol* 3, 934-943.
99. Ohta, T., Nishiwaki, R., Suganuma, M., Yatsunami, J., Komori, A., Okabe, S., Tatematsu, M. & Fujiki, H. (1993). Significance of the Cyanobacterial Cyclic Peptide Toxins, the Microcystins and Nodularin, in Liver-Cancer. *Mutat Res* 292, 286-287.
100. MacKintosh, R. W., Dalby, K. N., Campbell, D. G., Cohen, P. T., Cohen, P. & MacKintosh, C. (1995). The cyanobacterial toxin microcystin binds covalently to cysteine-273 on protein phosphatase 1. *FEBS Lett* 371, 236-40.
101. Desilva, E. D., Williams, D. E., Andersen, R. J., Klix, H., Holmes, C. F. B. & Allen, T. M. (1992). Motuporin, a Potent Protein Phosphatase Inhibitor Isolated from the Papua-New-Guinea Sponge Theonella-Swinhoei Gray. *Tetrahedron Letters* 33, 1561-1564.
102. Powell, H. R. (1999). The Rossmann Fourier autoindexing algorithm in MOSFLM. *Acta Crystallogr D Biol Crystallogr* 55, 1690-1695.
103. Bailey, S. (1994). The Ccp4 Suite - Programs for Protein Crystallography. *Acta Crystallogr D Biol Crystallogr* 50, 760-763.

104. Murshudov, G. N., Vagin, A. A. & Dodson, E. J. (1997). Refinement of macromolecular structures by the maximum-likelihood method. *Acta Crystallogr D Biol Crystallogr* 53, 240-255.
105. Maynes, J. T., Luu, H. A., Cherney, M. M., Andersen, R. J., Williams, D., Holmes, C. F. & James, M. N. (2006). Crystal Structures of Protein Phosphatase-1 Bound to Motuporin and Dihydromicrocystin-LA: Elucidation of the Mechanism of Enzyme Inhibition by Cyanobacterial Toxins. *J Mol Biol*. 356, 111-20. Epub 2005 Nov 22.
106. Lins, L. & Brasseur, R. (1995). The hydrophobic effect in protein folding. *Faseb J*. 9, 535-40.
107. Burgi, H. B., Dunitz, J. D. & Shefter, E. (1973). Geometrical Reaction Coordinates .2. Nucleophilic Addition to a Carbonyl Group. *J Am Chem Soc* 95, 5065-5067.
108. Runnegar, M., Berndt, N., Kong, S. M., Lee, E. Y. C. & Zhang, L. F. (1995). In-Vivo and in-Vitro Binding of Microcystin to Protein Phosphatase-1 and Phosphatase-2a. *Biochem Biophys Res Commun* 216, 162-169.
109. Drahl, C., Cravatt, B. F. & Sorensen, E. J. (2005). Protein-reactive natural products. *Angew Chem Int Ed Engl* 44, 5788-809.
110. Moorhead, G., MacKintosh, R. W., Morrice, N., Gallagher, T. & MacKintosh, C. (1994). Purification of type 1 protein (serine/threonine) phosphatases by microcystin-Sepharose affinity chromatography. *FEBS Lett* 356, 46-50.

111. Kondo, F., Ikai, Y., Oka, H., Okumura, M., Ishikawa, N., Harada, K., Matsuura, K., Murata, H. & Suzuki, M. (1992). Formation, characterization, and toxicity of the glutathione and cysteine conjugates of toxic heptapeptide microcystins. *Chem Res Toxicol* 5, 591-6.
112. Rinehart, K. L., Harada, K., Namikoshi, M., Chen, C., Harvis, C. A., Munro, M. H. G., Blunt, J. W., Mulligan, P. E., Beasley, V. R., Dahlem, A. M. & Carmichael, W. W. (1988). Nodularin, Microcystin, and the Configuration of Adda. *J Am Chem Soc* 110, 8557-8558.
113. Hastie, C. J., Borthwick, E. B., Morrison, L. F., Codd, G. A. & Cohen, P. T. (2005). Inhibition of several protein phosphatases by a non-covalently interacting microcystin and a novel cyanobacterial peptide, nostocyclin. *Biochim Biophys Acta* 18, 18.
114. Maynes, J. T., Perreault, K. R., Cherney, M. M., Luu, H. A., James, M. N. G. & Holmes, C. F. B. (2004). Crystal structure and mutagenesis of a protein phosphatase-1 : calcineurin hybrid elucidate the role of the beta 12-beta 13 loop in inhibitor binding. *J Biol Chem* 279, 43198-43206.
115. Holmes, C. F. B., Maynes, J. T., Perreault, K. R., Dawson, J. F. & James, M. N. G. (2002). Molecular enzymology underlying regulation of protein phosphatase-1 by natural toxins. *Curr Med Chem* 9, 1981-9.
116. Williams, D. E., Craig, M., Dawe, S. C., Kent, M. L., Holmes, C. F. B. & Andersen, R. J. (1997). Evidence for a covalently bound form of microcystin-LR in salmon liver and dungeness crab larvae. *Chem Res Toxicol* 10, 1293-1293.

117. Williams, D. E., Dawe, S. C., Kent, M. L., Andersen, R. J., Craig, M. & Holmes, C. F. (1997). Bioaccumulation and clearance of microcystins from salt water mussels, *Mytilus edulis*, and in vivo evidence for covalently bound microcystins in mussel tissues. *Toxicon* 35, 1617-25.
118. Fischer, W. J., Hitzfeld, B. C., Tencalla, F., Eriksson, J. E., Mikhailov, A. & Dietrich, D. R. (2000). Microcystin-LR toxicodynamics, induced pathology, and immunohistochemical localization in livers of blue-green algae exposed rainbow trout (*Oncorhynchus mykiss*). *Toxicol Sci* 54, 365-73.
119. Shepbeck, J. E., 2nd, Gauss, C. M. & Chamberlin, A. R. (1997). Inhibition of the Ser-Thr phosphatases PP1 and PP2A by naturally occurring toxins. *Bioorg Med Chem* 5, 1739-50.
120. MacKintosh, C. & MacKintosh, R. W. (1994). Inhibitors of protein kinases and phosphatases. *Trends Biochem Sci* 19, 444-8.
121. Watanabe, T., Huang, H. B., Horiuchi, A., da Cruze Silva, E. F., Hsieh-Wilson, L., Allen, P. B., Shenolikar, S., Greengard, P. & Nairn, A. C. (2001). Protein phosphatase 1 regulation by inhibitors and targeting subunits. *Proc Natl Acad Sci U S A* 98, 3080-5.
122. Connor, J. H., Kleeman, T., Barik, S., Honkanen, R. E. & Shenolikar, S. (1999). Importance of the beta12-beta13 loop in protein phosphatase-1 catalytic subunit for inhibition by toxins and mammalian protein inhibitors. *J Biol Chem* 274, 22366-72.
123. Shima, H., Tohda, H., Aonuma, S., Nakayasu, M., DePaoli-Roach, A. A., Sugimura, T. & Nagao, M. (1994). Characterization of the PP2A alpha gene

- mutation in okadaic acid- resistant variants of CHO-K1 cells. *Proc Natl Acad Sci U S A* 91, 9267-71.
124. Wei, Q. & Lee, E. Y. (1997). Mutagenesis of the L7 loop connecting beta strands 12 and 13 of calcineurin: evidence for a structural role in activity changes. *Biochemistry* 36, 7418-24.
125. Dawson, J. F., Luu, H. A., Bagu, J. R. & Holmes, C. F. (2000). Mutation of the toxin binding site of PP-1c: comparison with PP-2B. *Biochem Biophys Res Commun* 270, 543-9.
126. Andrioli, L. P., Zaini, P. A., Viviani, W. & Da Silva, A. M. (2003). Dictyostelium discoideum protein phosphatase-1 catalytic subunit exhibits distinct biochemical properties. *Biochem J* 373, 703-11.
127. MacKintosh, R. W., Haycox, G., Hardie, D. G. & Cohen, P. T. (1990). Identification by molecular cloning of two cDNA sequences from the plant *Brassica napus* which are very similar to mammalian protein phosphatases-1 and -2A. *FEBS Lett* 276, 156-60.
128. Lin, Q., Li, J., Smith, R. D. & Walker, J. C. (1998). Molecular cloning and chromosomal mapping of type one serine/threonine protein phosphatases in *Arabidopsis thaliana*. *Plant Molecular Biology* 37, 471-481.
129. Zimmerlin, A., Jupe, S. C. & Bolwell, G. P. (1995). Molecular-Cloning of the Cdna-Encoding a Stress-Inducible Protein Phosphatase-1 (Pp1) Catalytic Subunit from French Bean (*Phaseolus-Vulgaris* L). *Plant Molecular Biology* 28, 363-368.

130. MacKintosh, C. & Cohen, P. (1989). Identification of high levels of type 1 and type 2A protein phosphatases in higher plants. *Biochem J* 262, 335-9.
131. Liu, P., Huang, C., Wang, H. L., Zhou, K., Xiao, F. X. & Qun, W. (2004). The importance of Loop 7 for the activity of calcineurin. *FEBS Lett.* 577, 205-8.